



Project Evaluation REPORT 2019 – 2020

Name of the Programme : **M.E - Thermal and Fluid Engineering**
Year of study and Batch : **II & B2**
Name of the Supervisor : **Dr.A.ADINARAYANAN**
Title of the Project :

**THERMAL AND VISCO-THERMAL ANALYSIS OF
SHOREA ROBUSTA WITH JUTE REINFORCED BIO
FILLER BASED POLYMER MATERIALS**

Nature of the Project : **Individual**

Reg No of Students who are with this Project:

KAMESHWARAN R (AMTF18006)



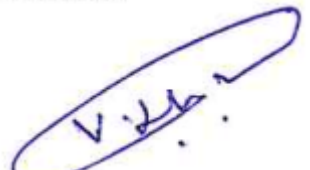
Project Evaluation REPORT 2019 – 2020

Name of the Department: **Mechanical Engineering**

Name of the Student	KAMESHWARAN R
Register No	AMTF18006
Programme of study	M.E - Thermal and Fluid Engineering
Year and Batch	II and 2 (2019 – 2020)
Semester	IV
Title of the Project	THERMAL AND VISCO-THERMAL ANALYSIS OF SHOREA ROBUSTA WITH JUTE REINFORCED BIO FILLER BASED POLYMER MATERIALS
Duration of Project	3 Months
Mentor of the Student	Dr.A.Adinarayanan

Evaluation by the Department

Sl No.	Criterion	Max. Marks	Marks Allotted
1	Idea / Techique Idnetification	5	5
2	Conceptualisation of idea / techique	5	5
3	Thought process /clarity of idea	5	5
4	Methodology to solve the problem	5	4
5	Project Scheduling	5	5
6	Preparing the equipment/ component list	5	5
7	Literature Review	5	5
8	Design work	5	5
9	Conference Presentation/ Publication	10	10
10	Problem statement and scope of the project	10	8
11	Analysis and modern Tool usage in problem solving	10	9
12	Project report	10	8
13	Originality score	10	10
14	Written or Video Presentation or Demo	5	4
15	Viva-Voce	5	4
Total		100	92

Signature of the Mentor 	Signature of the Internal Examiner 	Signature of HoD/Programme Head 
--	---	--

**THERMAL AND VISCO-THERMAL ANALYSIS
OF SHOREA ROBUSTA WITH JUTE
REINFORCED BIO FILLER BASED POLYMER
MATERIALS**

A PROJECT REPORT

Submitted by

KAMESHWARAN R AMTF18006

in partial fulfillment for the award

of the degree of

MASTER OF ENGINEERING

in

THERMAL AND FLUID ENGINEERING



AMET: CHENNAI 603112

JUNE 2020

AMET: CHENNAI 603112

BONAFIDE CERTIFICATE

Certified that this project report “**THERMAL AND VISCO-THERMAL ANALYSIS OF SHOREA ROBUSTA WITH JUTE REINFORCED BIO FILLER BASED POLYMER MATERIALS**” is the bonafide work of “**KAMESHWARAN R –AMTF18006**” who carried out the project work under my supervision.



SIGNATURE

Dr.R.RAJAVEL,
HEAD OF THE DEPARTMENT,
PROFESSOR AND HOD,
DEPT OF MECHANICAL ENGG.
AMET, CHENNAI.



SIGNATURE

DR. A. ADINARAYANAN
SUPERVISOR,
ASSOCIATE PROFESSOR,
DEPT OF MECHANICAL ENGG.
AMET, CHENNAI.

Project Viva-Voice examination held on.....

INTERNAL EXAMINER

EXTERNAL EXAMINER

ABSTRACT

Now-a-days, the natural fibres from renewable natural resources offer the potential to act as a reinforcing material for polymer composites alternative to the use of glass, carbon and other man-made fibres. Among various fibres, jute is most promising reinforcement material due to its high content of cellulose and widely used natural fibre due to its advantages like easy availability, low density, low production cost. *shora robusta* seed oil available in india. Which can be used as bio polymer. It has better adhesion properties. Hence it is chosen as matrix material. Composites are prepared by mixing polyester resin and shora robusta seed oil. Composites were fabricated at different volume fraction of jute fibre, polyester, shora robusta seed oil. Density was evaluated for bio resin and thermogravimetric analysis (TGA) was performed for pure polyester and hybrid matrix and damping factor, glass transition temperature was found by dynamic mechanical analysis.

Key words: Composite, Polymer, Shorea robusta, Thermal Analysis

ACKNOWLEDGEMENT

We thank **Col. Dr. G. THIRUVASAGAM**, Vice Chancellor of **AMET** for extending his generous hand in providing the best of the resources in the academy of maritime education and training.

We are honored to express our thanks to our beloved head of the department **Prof. DR.R.RAJAVEL**, who always served as a source of inspiration and encouraged us throughout the project and also contributed his valuable suggestion, instruction and encouragement in doing this project.

We have no words to express our thanks to our project supervisor **Dr. A. ADINARAYANAN**, Associate professor and faculty advisor **MR.A.R. SIVARAM**, Assistant Professor for his keen interest, guidance, inspiration and valuable suggestion during the course of our project.

We our special thanks to all the faculty members in department of mechanical engineering for their timely help and assistance in the lab that has helped us to carry out this project.

TABLE OF CONTENTS

Chapter No	Description	PageNo
	ABSTRACT	iii
	LIST OF TABLES	viii
	LIST OF FIGURES	ix
1	INTRODUCTION	1
	1.1 Composite	1
	1.2 Classification of composite	1
	1.2.1 Major classification of composite	1
	1.2.2 Classification based on matrix material	2
	1.2.2.1 Polymer matrix composites	2
	1.2.2.2 Metal matrix materials composites	4
	1.2.2.3 Ceramic matrix materials composites	4
	1.2.2.4 Carbon and graphic matrix composites	5
	1.2.3 Composite based on reinforcement	5
	1.3 Types of fibre	6
	1.3.1 Natural fibre	6
	1.4 Bio composites	
	1.4.1 Characteristics of biocomposites	8
	1.5 Application of composites	8
	1.6 Advantages of composites	9
	1.7 Disadvantages of composites	9

2	LITERATURE SURVEY	10
3	OBJECTIVE AND METHODOLOGY	16
4	MATERIALS AND METHODS	18
	4.1 Materials	18
	4.1.1 Polyester resin	18
	4.1.2 Jute fibre	20
	4.1.3 Shorea robusta seed oil	21
	4.2 Sample preparation	22
	4.1.3 Hand lay method	22
	4.3 Thermogravimetric analysis (TGA)	24
	4.3.1 Working principle of TGA	25
	4.4 Dynamic mechanical analyzer	26
	3.4.1 DMA-DMS 6100	27
5	RESULT AND DISCUSSION	28
	5.1 Density of bioresin	28
	5.1.1 density calculation	29
	5.1 Thermal stability of polyester and biocomposites	29
	5.1.2 Tga Curve For Pure Polyester ,Pure Bio Rein And Hybrid Composites	33
	5.1.3 Thermal Properties Of Polyester, Bio	

	5.1 Dynamic Analysis OfPolyester AndBioComposites	35
	5.1.1 dynamic analysis ofcompositematerial	38
	5.1.2 Reinforcement Result ForCompositeMaterial	38
	5.1.3 Thermal Stability OfReinforcement Composite Material	39
	5.1.1Dynamic Result ForReinforcement Composite Material	39
	5.5 Thermal Stability And Dynamic Result For Reinforcement Material	40
6	CONCLUSION	39
7	REFERENCE	40

LIST OF FIGURES

FIGURE NO	DESCRIPTION	PAGE NO
1.1	Typesofmatrices	2
1.2	Typesofthemosets	3
1.3	Typesofthermoplastics	4
1.4	Typesofreinforcement	6
1.5	Source of fibresfromnature	7
3.1	Jutefibre	20
3.2	shoera robusta see oil inpowderform	21
3.3	Hand layprocesssheet	23
3.4	Samplepreparation	23
3.5	Thermogravimetricanalyzer	24
3.6	Sample of TGAtesting	25
3.7	Samplepan	25
3.8	Sample pan ontothetray	25
3.9	Dynamic mechanicalanalyzer	27
4.1	Measurementofdensity	28
4.2	Thermal stability ofbioresin	29
4.3	Thermal stabilityofpolyester	30
4.1	thermal stability of 10% ofbioresin	30
4.2	thermal stability of 20% ofbioresin	31

4.3	thermal stability of 30% of bioresin	31
4.4	thermal stability of 40% of bioresin	32
4.5	thermal stability of 50% of bioresin	32
4.6	Tga Curve For Pure Polyester, Pure Bio Rein And Hybrid Composites.	32
4.7	dynamic analysis of polyester	35
4.8	dynamic analysis of 10% bioresin	35
4.9	dynamic analysis of 20% bioresin	36
4.10	dynamic analysis of 30% bioresin	36
4.11	dynamic analysis of 40% bioresin	37
4.12	dynamic analysis of 50% bioresin	37
4.13	thermal stability of reinforcement material	39
4.14	dynamic result for reinforcement material	39

LIST OF TABLES

Tableno	Description	Page No
3.1	Properties of jute fibre	21
3.2	Materials used	23
3.3	Types of samples	23
3.4	Parameters of TGA	24
4.1	Density calculation	29
4.2	Thermal Properties Of Polyester, Bio Resin And Hybrid Composites	34
4.3	Dynamic Analysis Of Composite Material	38
4.4	Thermal Stability And Dynamic Result For Reinforcement Material	40

CHAPTER 1

INTRODUCTION

1.1 COMPOSITE:

A composite material is made by combining two or more materials often ones that have very different properties. The two materials work together to give the composite unique properties.

A composite is a structural material that consists of two or more combined constituents that are combined at a macroscopic level and are not soluble in each other. One constituent is called reinforcing phase and one in which it is embedded is called the matrix.

1.2 CLASSIFICATION OF COMPOSITES:

1.2.1 MAJOR CLASSIFICATION OF COMPOSITE

There are two major types of composite materials based on raw materials used. They are,

1. Synthetic composite
2. Natural composite

Synthetic composites are made from synthesized polymers or small molecules. Synthetic fibres do not depend either on an agricultural crop or animal farming. And basically synthetic fibre composite properties are stronger than natural composite but synthetic fibres burn more readily than natural and cost of making materials would be more. Some of the synthetic composites are carbon/graphite, boron, Kevlar and ceramic composite.

Natural composites are made from fibres which are available naturally from plant and animals. It is also called as green composite due to environmental friendliness. We have to prefer natural composite instead of synthetic composite.

1.2.2 CLASSIFICATION BASED ON MATRIX MATERIAL

Composites cannot be made from constituents with divergent linear expansion characteristics. The interface is the area of contact between the reinforcement and the matrix materials. In some cases, the region is a distinct added phase. Whenever there is interphase, there has to be two interphases between each side of the interphase and its adjacent constituent. Some composites provide interphases when surfaces dissimilar constituents interact with each other. Choice of fabrication method depends on matrix properties and the effect of matrix on properties of reinforcements. One of the prime considerations in the selection and fabrication of composites is that the constituents should be chemically inert non-reactive.

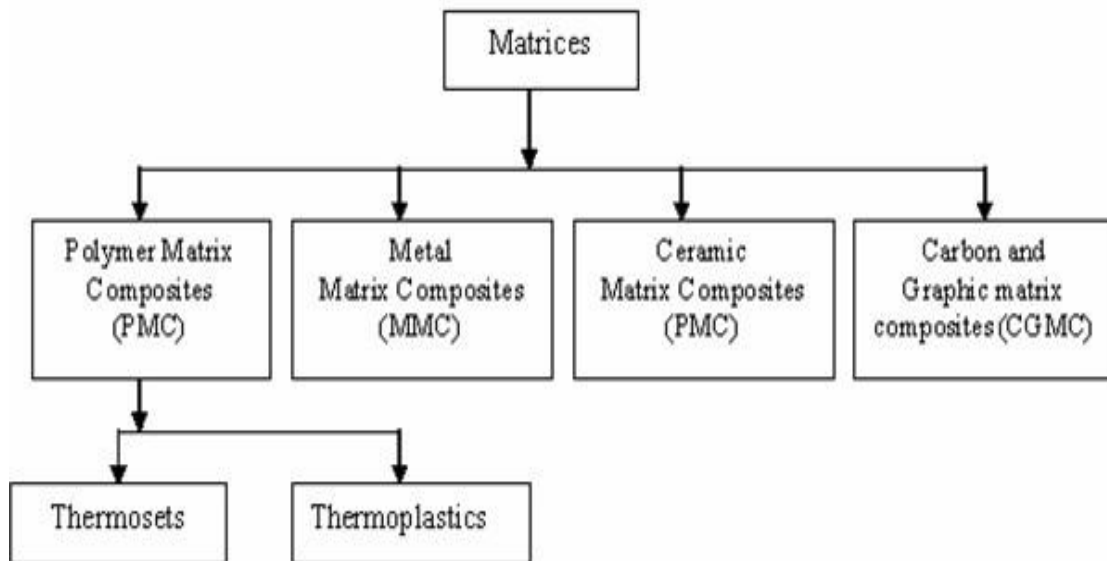


Fig 1.1 Types of Matrices

1.2.2.1 POLYMER MATRIX COMPOSITES(PMCs)

The most common advanced composites are polymer matrix composites. These composites consist of a polymer thermoplastic or thermosetting reinforced by fiber (natural carbon or boron). These materials can be

fashioned into a variety of shapes and sizes. They provide great strength and stiffness along with resistance to corrosion. The reason for these being most common is their low cost, high strength and simple manufacturing principles.

Two main kinds of polymers are thermosets and thermoplastics. Thermosets have qualities such as a well-bonded three-dimensional molecular structure after curing. Thermosets find wide ranging applications in the chopped fibre composites form particularly when a premixed or molding compound with fibres' of specific quality and aspect ratio happens to be starting material as in epoxy, polymer and phenol polyamide resins.

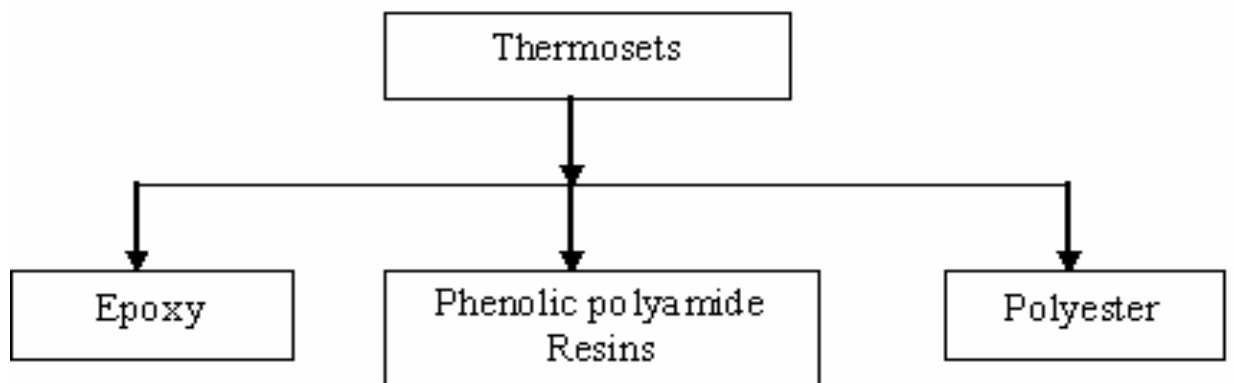


Fig 1.2 Types of Thermosets

Thermoplastics have one- or two-dimensional molecular structure and they tend to at an elevated temperature and show exaggerated melting point. Another advantage is that the process of softening at elevated temperatures can be reversed to regain its properties during cooling, facilitating applications of conventional compress techniques to mould the compounds.

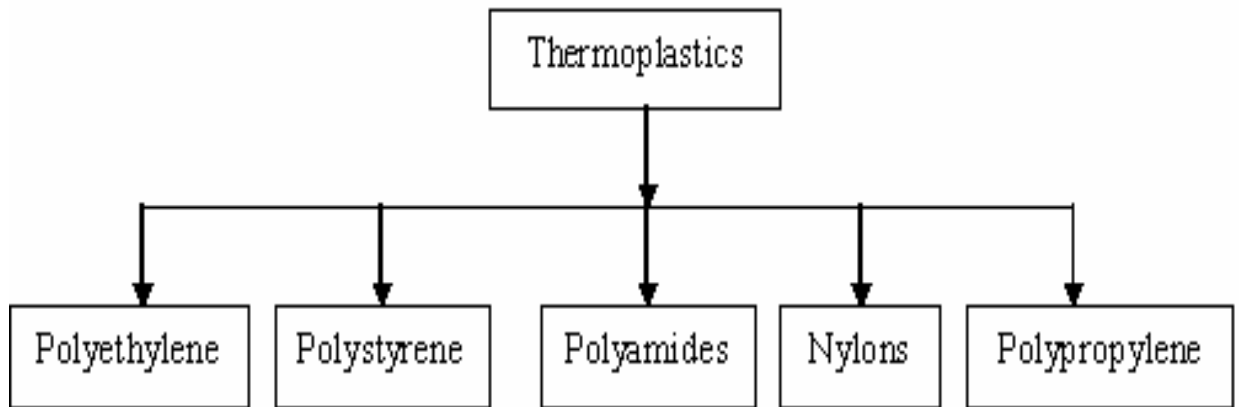


Fig 1.3 Types of Thermoplastics

1.2.2.2 METAL MATRIX MATERIALS COMPOSITES(MMC)

Metal matrix composites, as the name implies, have a metal matrix. Examples of matrices in such composites include aluminum, magnesium and titanium. The typical fiber includes carbon and silicon carbide. Metals are mainly reinforced to suit the needs of design. For example, the elastic stiffness and strength of metals can be increased, while large coefficient of thermal expansion, and thermal and electrical conductivities of metals can be reduced by the addition of fibers such as silicon carbide.

1.2.2.3 CERAMICS MATRIX COMPOSITES(CMC)

Ceramic matrix composites have ceramic matrix such as alumina, calcium, aluminosilicate reinforced by silicon carbide. The advantages of CMC include high strength, hardness, high service temperature limits for ceramics, chemical inertness and low density. Naturally resistant to high temperature, ceramic materials have a tendency to become brittle and to fracture. Composites successfully made with ceramic matrices are reinforced with silicon carbide fibers.

1.2.2.4 CARBON AND GRAPHIC MATRIX COMPOSITES(CGMC)

Ceramic matrix composites (CMCs) are a subgroup of composite materials as well as a subgroup of technical ceramics they consist of ceramic fiber embedded in a ceramic matrix, thus forming a ceramic fiber reinforced ceramic (CFRC) material. The matrix and fibers can consist of any ceramic material, whereby carbon and carbon fibers can also be considered a ceramic material.

The motivation to develop CMCs was to overcome the problems associated with the conventional technical ceramics like alumina, silicon carbide, aluminum nitride, silicon nitride or zirconium – they fracture easily under mechanical or thermo-mechanical loads because of cracks initiated by small defects or scratches

1.2.3 COMPOSITE BASED ON REINFORCEMENT

Reinforcements for the composites can be fibers, fabrics particles or whiskers. Fibers are essentially characterized by one very long axis with other two axes either often circular or near circular. Particles have no preferred orientation and so does their shape. Whiskers have a preferred shape but are small both in diameter and length as compared to fibers types of reinforce fiber-reinforced composite (FRC) is a composite building material that consists of three components: (i) the fibers as the discontinuous or dispersed phase, (ii) the matrix as the continuous phase, and (iii) the fine interphase region, also known as the interface. This is a type of advanced composite group. Compounding natural fibers from cellulosic waste streams to form a high-strength fiber composite material in a polymer matrix.

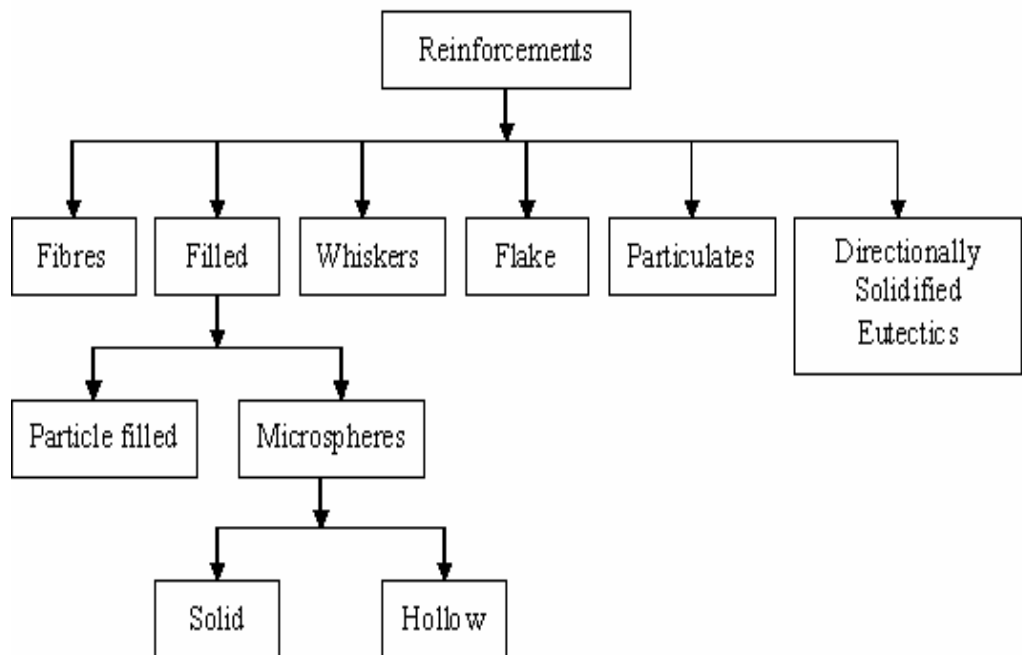


Fig 1.4 Types of Reinforcement

1.3 TYPES OFFIBRE

1.3.1 Naturalfibres

1.3.2 synthetic fibres

1.3.1 NATURALFIBRE

The interest in natural fibre-reinforced polymer composite materials is rapidly growing both in terms of their industrial applications and fundamental research. They are renewable, cheap, completely or partially recyclable, and biodegradable. Plants, such as flax, cotton, hemp, jute, sisal, kenaf, pineapple, ramie, bamboo, banana, etc.,

The natural fibre-containing composites are more environmentally friendly, and are used in transportation (automobiles, railway coaches, aerospace), military

applications, building and construction industries (ceiling paneling, partition boards), packaging, consumer products, etc.

Natural fibres are cheaper, bio-degradable and no health hazard. Furthermore natural fibre reinforced fibres are seen to have good potential in the future as a substitute. Natural fibers are extracted from various part of the plant; they are as shown in figure 1.9

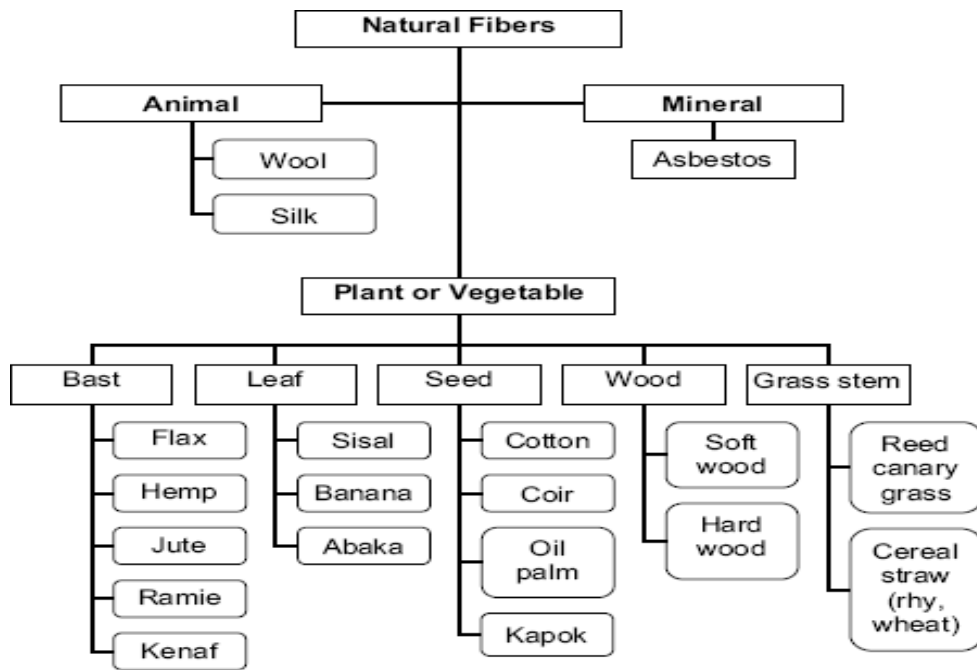


Figure 1.5 Source of fibres from nature

1.3.2 SYNTHETIC FIBRE

Synthetic fibres are man-made fibres. Synthetic fibres are made from different chemicals, hence each kind of synthetic fibres have their own properties. Synthetic fibres are more in length and are long lasting. The only limitation in synthetic fibres is that they are poor absorbents of moisture and they catch fire easily.

- kevlar
- carbon
- glass
- Rayon
- Nylonetc...

1.4 BIO COMPOSTIES

A biocomposite is a material formed by a matrix (resin) and a reinforcement of natural fibers (usually derived from plants or cellulose).

1.4.1 CHARACTERISTICS OF BIO COMPOSITES

- the petrochemical resin is replaced by a vegetable or animal resin,and/or
- the bolsters (fiberglass, carbon fibre.) are replaced by natural fibre (wood fibres, hemp, flax, sisal,jute...)

1.5 APPLICATIONS OF COMPOSITE MATERIALS

Engineeringapplications

Aerospace

Automobile

Pressure vessel and pipes

Other applications

Medical table

Bullet proof shield etc...

1.6 ADVANTAGES OF COMPOSITE MATERIALS

Light weight

High specific stiffness and strength

Easy moldable to complex forms

Easy bondable etc..

1.7 DISADVANTAGES OF COMPOSITE MATERIALS

Cost of materials

Long development time

Difficulty manufacturing

Low ductility

Temperature limit etc..

CHAPTER 2

LITERATURE SURVEY

M. Jawaid et al.,[1] obtained The dynamic mechanical and thermal analysis of oil palm empty fruit bunch (EFB)/woven jute fibre (J w) reinforced epoxy hybrid composites were carried out. The thermal stability curves of hybrid composites as compared to pure epoxy, pure EFB and pure woven composites. It is seen that the initial degradation temperature of epoxy matrix was found to increase from 256°C to 288°C with the reinforcement of fibre in the matrix, due to the bonding of the fibres to the matrix. Thermal stability can be expressed in the terms of parameters like initial decomposition temperature ,final degradation temperature (FDT). Thermal analysis study indicated that thermal stability of pure EFB composite increased by the addition of woven jute fibres. The storage modulus (Eo) was found to decrease with temperature in all cases, and hybrid composites had showed better values of Eo at glass transition temperature (Tg) compared to EFB and epoxy. Loss modulus showed shifts in the Tg of the polymer matrix with the addition of fibre as reinforcing phase, which indicate that fibre plays an important role in case of Tg. The Tan delta peak height was minimum for jute composites and maximum for epoxy matrix. We anticipated that these studies will optimized the use of oil palm EFB fibres and its utilization in development of unique cost effective advanced hybrid composites possessing appropriate stiffness, damping behaviour and thermal stability.

K.Bhanu et al.,[2] carried out to improve the adhesion of jute fibre with polylactide(PLA). For this purpose, surface of the jute fiber was modified by alkali, permanganate, peroxide and silane treatments. The surface modified fibers were characterized by FTIR spectroscopy. Surface treatments resulted in enhancement of tensile and flexural properties and reduction in Izod impact strength. Dynamic mechanical analysis (DMA) results showed that, treated composite s have higher storage modulus and lower tangent delta with respect to untreated composite. The degree of interfacial adhesion between the jute fiber and PLA was estimated using

adhesion parameter obtained through DMA data. The results of thermogravimetric analysis (TGA) showed a higher thermal stability for silane treated composites. Experimental results on abrasive wear tests revealed that the wear resistance of composite is sensitive to fiber/matrix adhesion. Alkali, permanganate and peroxide treated composites exhibited lower thermal stability, whereas silane 1 and silane 2 treated composites showed a higher thermal stability when compared to untreated composites. It is observed that fiber matrix adhesion affected the abrasive wear resistance of the jute fiber reinforced composites. Silane 2 treated jute fiber composite with better fiber matrix adhesion exhibited maximum abrasive wear resistance.

Smita Mohanty et al.,[3] summarized an experimental study on the mechanical and viscoelastic behavior of jute fibre reinforced high density polyethylene (HDPE) composites. Variations in mechanical strength, storage modulus (E'), loss modulus (E'') and damping parameter ($\tan \delta$) with the addition of fibres and coupling agents were investigated. The thermal behavior of the composites was evaluated from TGA/DTG thermograms. The fibre–matrix morphology in the treated composites was confirmed by SEM analysis of the tensile fractured specimens. FTIR spectra of the treated and untreated jute fibres was also studied to ascertain the existence of type of interfacial bonds. The mechanical and dynamic mechanical properties of HDPE : jute fibre composites have been investigated. Composites prepared at 30% fibre loading and 1% MAPE concentration showed optimum mechanical strength. The mechanical findings were corroborated with morphological evidence and DMA studies. Storage modulus vs. temperature plots also showed an increase in the magnitude of the peaks with fibre reinforcement and addition of MAPE. The damping properties of the treated and untreated composites, however, decreased in comparison to the virgin matrix. TGA and DTG thermograms displayed an increase in the thermal stability of HDPE matrix with fibre reinforcement and MAPE treatment. Based on these studies, it can be concluded that jute fibres could effectively reinforce HDPE matrix when used in an optimal concentration of fibres and coupling agents.

H.P.S Abdul khalil et al., [4] carried out effect of layering pattern on the dynamic mechanical properties and thermal degradation of oil palm jute reinforced epoxy hybrid composite .dynamic mechanical thermal stability of oil palm empty fruit bunches/jute fibre reinforced hybrid composites were carried out. The storage modulus of EFB composites is comparable with hybrid composites, and it clear from results that pure woven jute composite show highest storage modulus, hybrid composites values lies between pure EFB and pure J w composites. Hybrid composites show higher value of loss modulus compared to pure EFB and pure epoxy above Tg . The Tg obtained from loss modulus is found to be lower than that from Tan d curves.

The shifts in the Tg of the polymer matrix with the addition of fibre as reinforcing phase indicate that fibre play an important role above Tg. The epoxy matrix has the highest Tan d value indicating that there is a large degree of mobility, thus good damping behaviours. Reinforcement of oil palm or woven jute fibres decreased the damping behaviours of composites as the fibre acted as a barrier to the free movement of molecular chain. A Cole–Cole plot was drawn and it shows an imperfect semicircular shape indicating heterogeneity of the system as well as good fibre/matrix bonding. Thermal analysis study indicated that thermal stability of pure EFB composite increased by the addition of woven jute fibres. Finally, it can be concluded that hybridising of oil palm EFB and jute fibres resulted in better dynamic mechanical and thermal properties.

M.Adrian et al., [5] were used to recycling of fibre reinforced polymeric waste by pyrolysis. The samples under investigation included composites of polyesters, phenolic and epoxy resins, and polypropylene, reinforced with glass and/or carbon fibre. Both the product mass balance and gas composition were dependent on the polymer matrix, pyrolysis temperature and, at the higher temperatures studied, the decomposition of thermally unstable fillers present in several samples, most notably calcium carbonate. The waste samples were also pyrolysed in a thermo-gravimetric analyser. A Shimadzu TGA-50H TGA was employed to study the pyrolysis of the composite samples. The sample (10 mg) was heated at 10 °C min⁻¹ to 900 °C, with

nitrogen passing through the furnace at 50 ml/min. The furnace temperature was then increased by 10°C to trigger the gas supply to change over to air, and held at this temperature for 15 min. The polymer matrix and pyrolysis temperature markedly influenced both the product mass balance and pyrolysis gas composition. At higher pyrolysis temperatures, the decomposition of calcium carbonate filler had a noticeable effect on the product yields and gas composition. The average molecular mass and mass range of the pyrolysis oils and waxes were dependent on the composite matrix. Decomposition of the various polymer matrices was generally a single stag process. However, composites with phenolic and epoxy resin matrices continued to lose mass steadily after polymer decomposition had ended. This may be related to carbonisation of the remainingsolids.

Chandramika Bora et al.,[6] obtained a simple method of preparation of reduced graphene oxide (rGO) based unsaturated polyester (PE) resin nano composite. The synthesized samples were characterized by Fourier trans-form infrared spectroscopy (FTIR), X-ray diffraction (XRD), scanning electron microscopy (SEM), atomic force microscopy (AFM), thermogravimetric analysis (TGA), differential scanning calorimetr y (DSC). Thermal properties of the PE/rGO composite films were evaluated with thermo gravimetric analysis (TGA) and differential scanning calorimetry (DSC). GO shows a major weight loss at the temperature range of 200–320° C which is attributed to the removal of most of the oxygen-containing functional groups. The 60% residual weight of GO indicates that some functional groups existed on GO surface before the thermal treatment. rGO showed around 20% weight loss at the temperature range of 250–500°C, which is due to the removal of most of the oxygen-containing functional groups during the chemical reduction process. rGO exhibited about 70% residual weight at 600°C indicating its excellent thermal stability. In the TGA curve of PE resin, initial weight loss occurs at a temperature of 240°C. The weight loss after 300°C is due to the complete degradation of the polymer. The major degradation temperature of polyester was found to be improved from 245 to 289°C on incorporation of the rGO. The composite exhibited significant improvement in mechanical properties at a lowrGO

loading. The tensile strength and Young's modulus of the composites increased by 123% and 87% respectively at 3 wt.% loading of the rGO. The thermal property of the PE resin was also improved with the incorporation of rGO in the composite.

G. U. Raju et al.,[7] carried out thermal properties of ground nut shell particles reinforced polymer composites. Due to increased environmental consciousness throughout the world the application of natural fibers has drawn much attention in different engineering fields. The make use of natural fibers as reinforcing materials in thermoplastics and thermoset matrix composites provides optimistic environmental profits with regard to ultimate disposability and better use of raw materials. TGA and DSC analyses were also carried out to ascertain the thermal stability of these composites. The results revealed that using groundnut shell particles as reinforcement for polymer matrix could successfully develop beneficial composites and can be used for thermal applications. The confirmation results indicate that the additive models are adequate for determining the optimum thermal properties at 95% confidence interval. The groundnut shell as reinforcing material is an agricultural product; eco-friendly, non-toxic, low cost and easily available material as compared to conventional fibers like glass, kevlar, asbestos etc. Hence, this composite can be used as good alternate for wood in thermal applications such as thermal insulation and coatings. Thermal stability is valuable information required to manufacture more thermally stable composites, possibly with good fire resistance. The composite specimen of 1.5 mm particle, 60-wt% of filler material with vinyl ester resin has the higher thermal stability.

V.s.aigbodion et al.,[8] obtained High density polyethylene (HDPE) composite reinforced with 20wt% orange peels ash particles (OPAp) was prepared by compression moulding. Thermogravimetric analysis (DTA/TGA) (space) was conducted on the HDPE/orange peels ash particle composite to clarify the effect of OPAp on the thermal decomposition behavior of the resultant composite. The thermal stability of the polymer composites plays a crucial role in determining the limit of their working temperature and the environmental conditions for uses, which are related to their thermal decomposition temperature

and decomposition rate. TGA/DTA curves of the thermal decomposition for pure HDPE and the HDPE/OPAp composite exhibit only one dominant decline of the residual weight, indicating random scission of the HDPE main chains as the prevailing decomposition reaction(8). The values of the activation energy for thermal decomposition reflected the improvement of the thermal stability of the HDPE/OPAp composite. This study has established that the orange peels ash particles are beneficial to act as thermal decomposition resistant and reinforcing particles in the HDPE matrix composite.

Betiana A et al.,[9] were conducted the viscoelastic properties of jute/polypropylene nonwoven reinforced composites were investigated using dynamic mechanical analysis. The surface of jute fibers was treated with defined content of alkali solution for improving the adhesion characteristics of fiber–matrix interface in the resultant composites. Nonwovens having 40 and 60 wt% jute content were used as reinforcements in jute/polypropylene composites. The popularity of natural fiber reinforced composites over glass fiber reinforced composites is ever-increasing due to their economic and environmental advantages. The jute/PP nonwoven composite samples were subjected to dynamic mechanical analysis (DMA) in a single-cantilever bending mode using Perkin–Elmer DMA 8000 according to ASTM D4065 standard. The samples were cut in rectangular plates with dimensions of 28*7*3mm³. During the DMA test, the temperature was kept in the range of 20–200 C with a heating rate of 2C/min, under nitrogen flow. The DMA tests were performed using an oscillation frequency of 1 Hz. the results of dynamic mechanical analysis

(DMA) of jute/PP nonwoven composites and neat PP matrix. In general, it has been observed that the peak storage modulus, E₀(at 20 C) increases with an increase in the jute fiber content. a relationship between temperature and storage modulus (E₀) of a typical nonwoven composite stacking sequence. The magnitudes of peak storage modulus and loss modulus of nonwoven composites improved with an increase in the jute fiber content. The influence of stacking sequence of preferentially and non-preferentially aligned nonwovens on viscoelastic properties

of composites was also investigated. The interface adhesion characteristics of composites under dynamic loading conditions were evaluated using adhesion efficiency factor and reinforcement effectiveness coefficient .

Betiana A et al., [10] used to dynamic mechanical behaviour of pp- jute composites. The dynamic mechanical response and the short term creep-recovery behavior of composites made from bi-directional jute fabrics and polypropylene were studied. In order to improve the compatibility of the polar fibers and the non-polar matrix, two alternatives were compared: the addition of coupling agents and the chemical modification of the fibers. In the first case, two commercial maleated polypropylenes and lignin, a natural polymer, were used. In the second approach, the fibers were esterified using a commercial alkenyl succinic anhydride. The degree of interfacial adhesion was inferred from the measured properties and confirmed by the observation of the composite fractured surface. The maleated polypropylenes acted as compatibilizers since they were able to join the fibers to the neat PP ,locating themselves in the interphase region. On the other hand, a clear separation between fibers and matrix could be observed when lignin was used as compatibilizing agent and when the chemically modified fibers were used to prepare the composite. The creep deformation could be directly related to the interfacial properties. Burgers model parameters were calculated from the creep part of the curves ,and the recovery part was modeled using these values. A very good agreement between experimental data and theoretical curves were obtained in the creep region, although small discrepancies were found in the recovery part. The feasibility of the construction of a master curve (using the time–temperature principle) to predict long term creep behavior of the composites was investigated.

Heitor Luiz Ornaghi Jr et al.,[11] evaluated dynamic fragility of an epoxy resin. he performance of epoxy/epoxy cyclohexyl polyhedral oligomeric silsesquioxane nano composites focusing on differential scanning calorimetry and dynamic mechanical

analysis. Nano composites with distinct nano reinforcement contents (1, 2 and 5 wt.%) were studied. Using differential scanning calorimetry and dynamic mechanical analysis. The viscoelastic properties were characterized using an Anton Paar Physica MCR 101 DMTA equipment in the torsion mode and rectangular specimens of 50 mm × 10 mm × 3 mm. The sweep experiments were carried out from the glass transition temperature (determined by non isothermal runs) for each sample at 3 °C intervals after temperature equilibration until 373.15 K. At each temperature the frequency varied. It was observed that the glass transition temperature decreases following the incorporation of epoxy cyclohexyl polyhedral oligomeric silsesquioxane, indicating, in principle, that there is more mobility in the new system formed. However, other calculated parameters) showed no trend as a result of epoxy cyclohexyl polyhedral oligomeric silsesquioxane incorporation.

2.1 SUMMARY OF THE LITERATURE SURVEY

Very few researchers have reported the use of eco-friendly natural fillers on the properties of polymer composites. *S. robusta* is a large tree up to 50-m tall and with a width of 5 m. Under normal conditions, *S. robusta* trees attain a height of about 18–32 m and girths of 1.5–2 m; bole is clean, straight, and cylindrical but often bears epicormic branches; crown is spreading and spherical. *S. robusta* filler materials are extracted from the seed and bark of the tree by three methods: (a) water rendering, (b) rotary milling method, and (c) solvent extraction. In this study, *S. robusta*, which is found in the Indian sub-continent, has been used as filler material in polyester resin. The effect of the mechanical, thermal, biodegradable, and dynamic mechanical behavior of the composite material with different wt% of *S. robusta* filler was analyzed. Morphology study was conducted to understand the filler distribution and adhesion with the matrix using scanning electron micrograph (SEM) images.

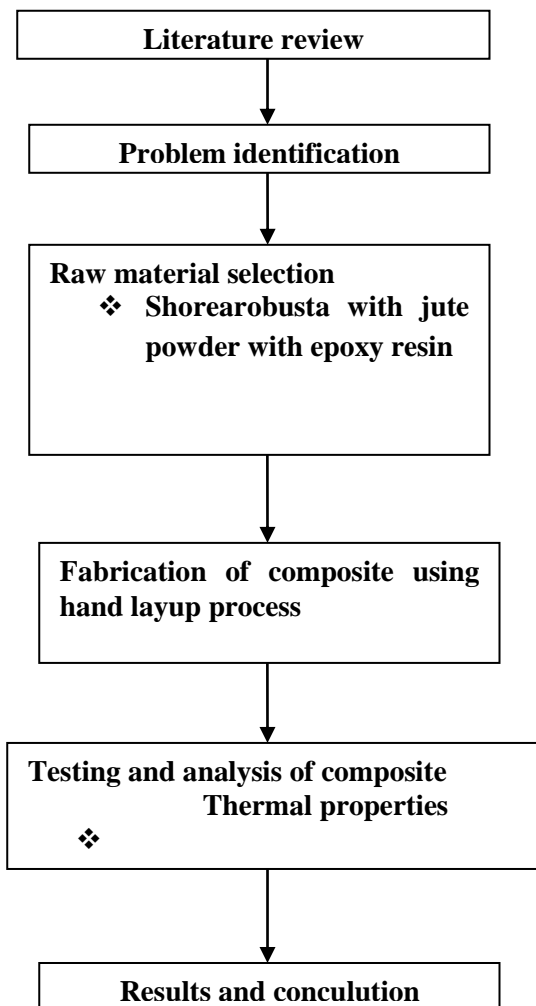
CHAPTER 3

OBJECTIVE AND METHODOLOGY

3.1 OBJECTIVE OF THEWORK

- Project aim is reduce synthetic resin and increase bioresin.
- From the literature it is absorbed that bio resin is not used anywhere for preparing composite materials
- bio resin is shora rubustra seed oil. that type of resin does not used so far. which is mixed with synthetic resin and then reinforcement by jutefibre.
- To study the influence of volume fraction of bio resin on TGA,DMA of behavior onmaterials
- To find thermal stability of the composites by using thermogravimetric analyzer (TGA).
- To find damping factor and glass transition temperature by dynamic mechanical analyzer(DMA).

3.2 Project Methodology



CHAPTER 4

MATERIALS AND METHODS

4.1 MATERIALS

- Synthetic resin – polyesterresin.
- Naturalfiber- jutefiber.
- Bio resin-shora rubustra seedoil

4.1.1 POLYESTERRESIN

Polyesters are one of the least expensive resins available to the FRP boat builder utilizing female tooling in the form of a mold. Polyester has the advantage of being extremely inexpensive when compared with other thermoset resins i.e. vinylesters and epoxies. If the upside is cheap pricing, the down side includes poor adhesions, high water absorption, high shrinkage, and high VOC's. Polyester resins are only compatible with fiberglass fibers. Polyester is best suited for applications insensitive to weight and do not require high adhesion or fracture toughness. For instance if a simple inexpensive solid fiberglass part must be fabricated in open tooling in one operation and requires no secondary bonding. If shape accuracy is not critical, resistance to water is of no concern, and ventilation of the workspace is excellent, then polyester's a great candidate.

Properties of Polyester Resin

Polyester resins are popular and widely used, especially in the marine industry to shape and form hulls and outer layers of ships. Other industries also employ polyester resin thanks to its numerous beneficial properties. They are used in the auto industry, as an adhesive and even as wood filler. The following are some of the properties exhibited by polyester resins.

Color

Polyester resins are, across the board, pale in color. This could be a pale gray color to a dull and diluted white.

Thermosetting

All polyester resins are thermosetting, that is, they are malleable until they are heated, at which time they permanently harden, even when exposed to the same heat a second time.

Resistant

Polyester resins are pretty resistant to both water and to UV rays. This is another reason why they are often employed in the marine industry.

Brittle

Because of the thermosetting nature of polyester resins, they can be fairly brittle because of their resistance to being bent or changed. When enough pressure is applied, they can crack or shatter.

Viscosity

Polyester resins are generally viscous. In order to lessen their viscosity, styrene is added. However, styrene may create fumes that can endanger those who work with polyester resins.

Aesthetics:

The fiber blends well with other fibers and maintains a natural look. polyester can be engineered to be very similar in appearance and hand to wool, linen and silk.

The low absorbency causes the fabric to be very uncomfortable. This can be improved through blending it with other fibers. Static can be controlled through additives and changes in the compound.

Environmental impact:

The impact is very similar to that of nylon. Polyester is extensively recycled, and less pollution is created when the recycled fibers are reengineered than when new ones are created.

4.1.2 JUTE FIBRE

Now-a-days, the natural fibres from renewable natural resources offer the potential to act as a reinforcing material for polymer composites alternative to the use of glass, carbon and other man-made fibres. Among various fibres, jute is most promising reinforcement material due to its high content of cellulose and widely used natural fibre due to its advantages like easy availability, low density, low production cost.



Fig 4.1 jute fibre

Physical and mechanical properties of jute fibre[1]

PROPERTIES	JUTE
Density(g/cm ³)	1.46
Tensile strength	393-773
Young's modulus(Gpa)	26.5
Cellulose content(%)	58-63
Hemicelluloses content(%)	12
Diameter(micro meter)	20-200
Elongation at break(%)	1.5-1.8

Table 4.1

4.1.3 SHOREA ROBUSTA SEEDOIL

Shorea robusta seed oil is an edible oil extracted from the seeds of *Shorea robusta*. *Shorea robusta* is known as the Sal tree in India. Sal is indigenous to India and occurs in two main regions separated by Gangetic plain, namely the northern and central Indian regions. This tree is native to the Indian Subcontinent, ranging south of the Himalaya, from Myanmar in the east to Nepal. *Shorea robusta* is a large, deciduous tree up to 50 m tall, having a trunk circumference up to 5 m. It has melting point of 45-55 C.



Fig 4.2 shorea robusta seed oil in powder form

4.2 SAMPLE PREPARATION

4.2.1 HAND LAY-UP PROCESS

Hand lay-up technique is the simplest method of composite processing. The infrastructural requirement for this method is also minimal. The processing steps are quite simple. First of all, a release gel is sprayed on the mold surface to avoid the sticking of polymer to the surface.

Thin plastic sheets are used at the top and bottom of the mold plate to get good surface finish of the product. Reinforcement in the form of jute fibres are cut as per the mold size and placed at the surface of mold after perspex sheet. Then thermosetting polymer in liquid form is mixed thoroughly in suitable proportion with a prescribed hardner (curing agent) and poured onto the surface of jute fibre already placed in the mold.

The polymer is uniformly spread with the help of brush. Second layer of jute is then placed on the polymer surface and a roller is moved with a mild pressure on the mat-polymer layer to remove any air trapped as well as the excess polymer present. The process is repeated for each layer of polymer and mat, till the required layers are stacked. After placing the plastic sheet, release gel is sprayed on the inner surface of the top mold plate which is then kept on the stacked layers and the pressure is applied. After curing either at room temperature or at some specific temperature, mold is opened and the developed composite part is taken out and further processed.

The schematic of hand lay-up is shown in figure 4.1. The time of curing depends on type of polymer used for composite processing. For example, for epoxy based system, normal curing time at room temperature is 24-48 hours. This method is mainly suitable for thermosetting polymer based composites. Capital and infrastructural requirement is less as compared to other methods. Production rate is less and high volume fraction of reinforcement is difficult to achieve in the processed composites. Hand lay-up method finds application in many areas like

aircraft components, automotive parts, boat hulls, diase board, deck etc. Generally, the materials used to develop composites through hand lay-up method are given in table 4.2.

Raw materials used in hand lay-up method

Materials used

Matrix	Polyester, shora rubustra seed oil
Reinforcement	Jute fibre

Table 4.2

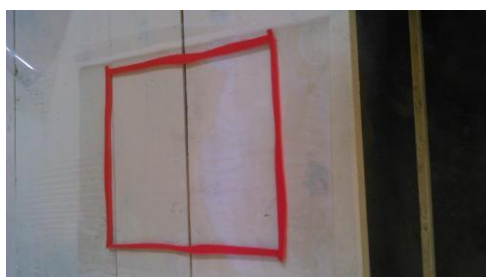


Fig 4.3 hand layprocesssheet



Fig 4.4 samplepreparation

TYPES OF SAMPLES

BIO RESIN(%)	SYNTHETIC RESIN(%)
10	90
20	80
30	70
40	60
50	50

Table 4.3

4.3 THERMOGRAVIMETRIC ANALYSIS(TGA)

4.3.1 Thermogravimetric analysis is a technique that uses heat to drive reactions and physical changes in materials providing quantitative measurements of any mass change in the polymer or material associated with a transition or thermaldegradation.

4.3.2 Mass change due to decomposition, oxidation or degradation of a polymer with time and temperature can be directly recorded from theTGA.

4.3.3 TGA is mainly used to characterize the decomposition and thermal stability of materials under differentconditions.

4.3.4 A Thermal gravimetric analyzer TG/DTA 6200 (SEIKO MODEL) is used to investigate the thermal stability of thecomposites.

4.3.1 PARAMETER OFTGA

NAME	WEIGHT	TEMPERATURE	HEATING RATE	ATMOSPHERE
TG/DTA6200 Seiko model	5-7mg	20-800 C	20 C/min	Nitrogen

Table 3.4

4.3.2 TG/DTA 6200 (SEIKOMODEL)



Fig 4.5 Thermo gravimetric analyzer

4.3.3 WORKING PRINCIPLE OF TGA

Thermogravimetric analysis (TGA) is an analytical technique used to determine a material's thermal stability by monitoring the weight change that occurs as a specimen is heated. The measurement is normally carried out in air or in an inert atmosphere, such as nitrogen, and the weight is recorded as a function of increasing temperature.

In addition to weight changes, some instruments also record the temperature difference between the specimen and one or more reference pans (differential thermal analysis, or DTA) finally result in the form of graph which is obtained by monitor



Fig 4.6 sample of TGA testing



Fig 4.7 samplepan



Fig 4.8 sample pan onto the tray

4.4 DYNAMIC MECHANICAL ANALYSIS

4.4.1 Dynamic mechanical analysis (DMA) is a powerful technique for the characterization of the viscoelastic properties of materials. DMA measures the modulus (stiffness) and damping (energy dissipation) properties of materials as they are deformed under periodic stress.

4.4.2 The technique can be used to evaluate a wide variety of materials such as thermoplastics, composites, thermosets, elastomers, films, fibers, coatings and adhesives.

VISCOELASTIC BEHAVIOR

4.4.3 Polymeric materials exhibit viscoelastic behavior which means that they simultaneously possess both solid-like as well as liquid-like characteristics. The degree to which the polymer exhibits more solid-like or liquid-like properties is dependent upon temperature as well as time or frequency.

PHASE ANGLE

The sample strain response lags behind the input stress wave with respect to time and this lag is known as the phase angle, δ . Damping = $\tan \delta = E''/E'$

COMPLEX MODULUS, E^* ,

4.4.4 The ratio of the dynamic stress to the dynamic strain yields the complex modulus, E^* , which can be further broken down to yield the storage modulus, E' , and the loss modulus, E''

STORAGE MODULUS, E'

4.4.5 The storage modulus refers to the ability of a material to store energy and it is related to the stiffness of the material.

LOSS MODULUS, E''

4.4.6 The loss modulus represents the heat dissipated by the sample as a result of the material's given molecular motions and this reflects the damping

characteristics of the polymer. Because of the viscoelastic nature of many

materials, which includes all polymers, these mechanical properties are functions of temperature as well as time (frequency).

4.4.1 DYNAMIC MECHANICAL ANALYZER (DMA) – DMS 6100

DMA is used for the evaluation of storage modulus , loss modulus , damping factor.the heating rate 5 c/min and frequency 1Hz and temperature Range from 20-800 and sample size of dma is 50*40*3-4mm



Fig 4.9 Dynamic mechanical analyzer

CHAPTER 5

RESULTS AND DISCUSSION

5.1.1 DENSITY OF BIORESIN



fig 5.1 Measurement of density

In this method a beaker of 50ml has been taken in which a 20-25ml water was poured and also a bio resin was added into it with considerable amount which has been weighed before, once adding bio resin into the beaker the water amount comes up in the beaker and which was noted and then again same amount of bio resin was added into the beaker by which the water level comes up and the procedure was repeated for three to four times and then the average was taken by the formula

5.1.1 DENSITY CALCULATION

S.NO	VOLUME OF WATER(ml)	PAN WEIGHT(gm)	CHANGE IN VOLUME(cc ³)	CHANGE IN MASS (g)	DENSITY (kg/m ³)
1	23	124	–	–	–
2	34	136	11	12	1.09
3	38	140	15	16	1.06
4	43	145	20	21	1.05
5	50	151	27	27	1.00
AVERAGE OF DENSITY					1.05

Table 5.1

Density = mass/volume

Finally density of the bio resin = 1.05 g/cm³

5.1 THERMAL STABILITY OF POLYESTER AND BIOCOSCOMPOSITES

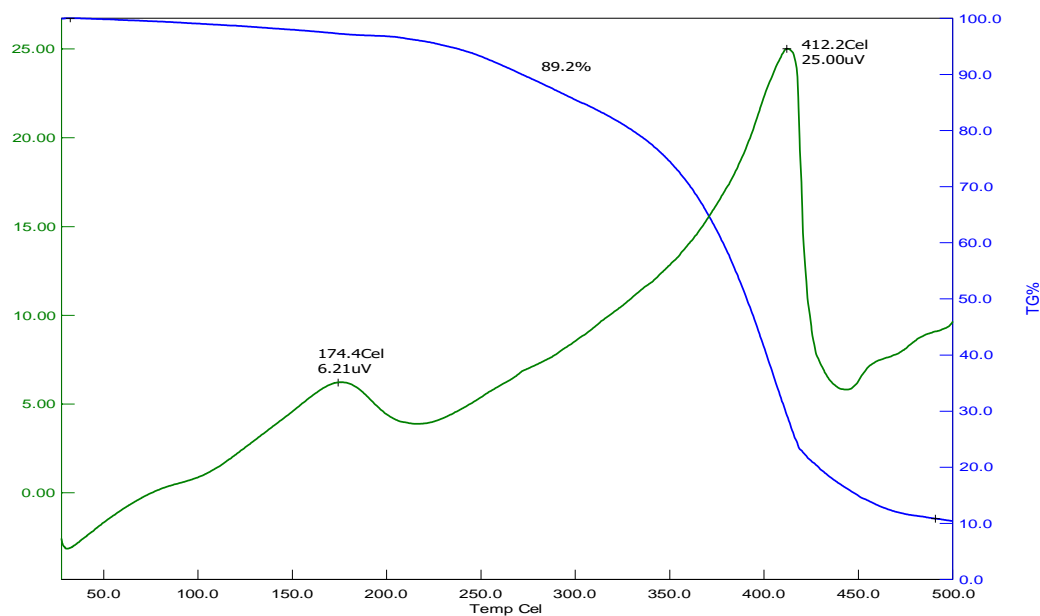


fig 5.2 thermal stability of pure bio resin

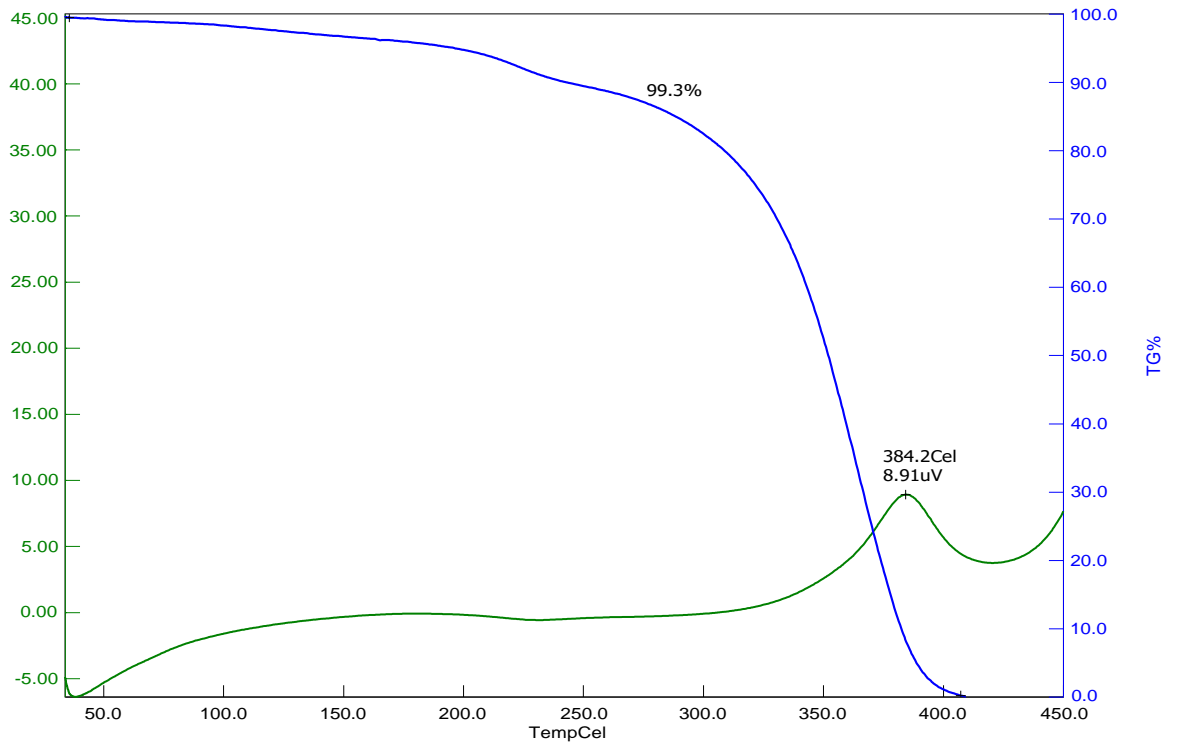


fig 5.3 thermal stability of pure polyester

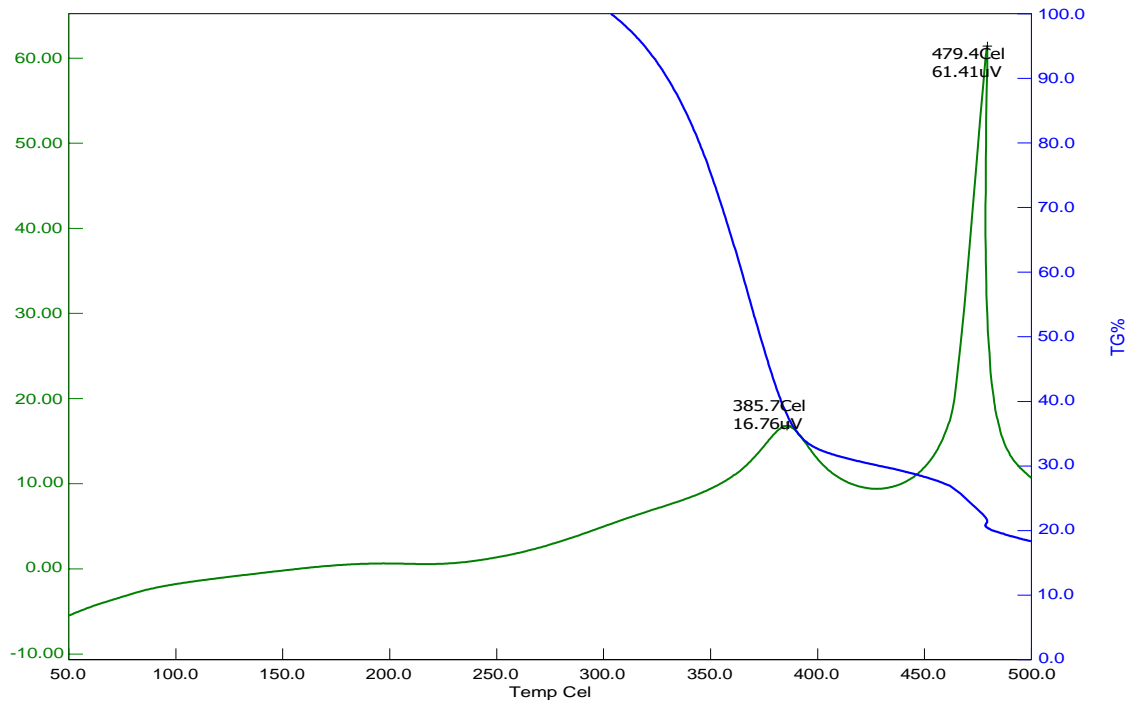


fig 5.4 thermal stability of 10% of bio resin

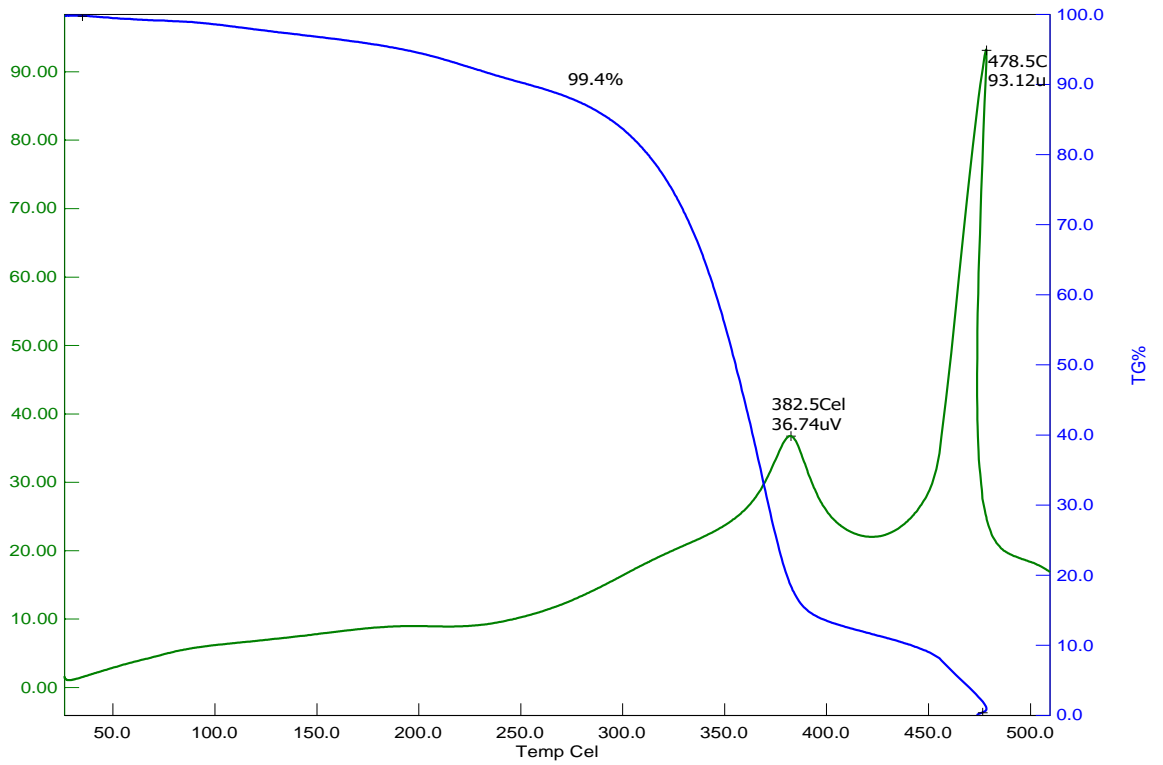


fig 5.5 thermal stability of 20% of bio resin

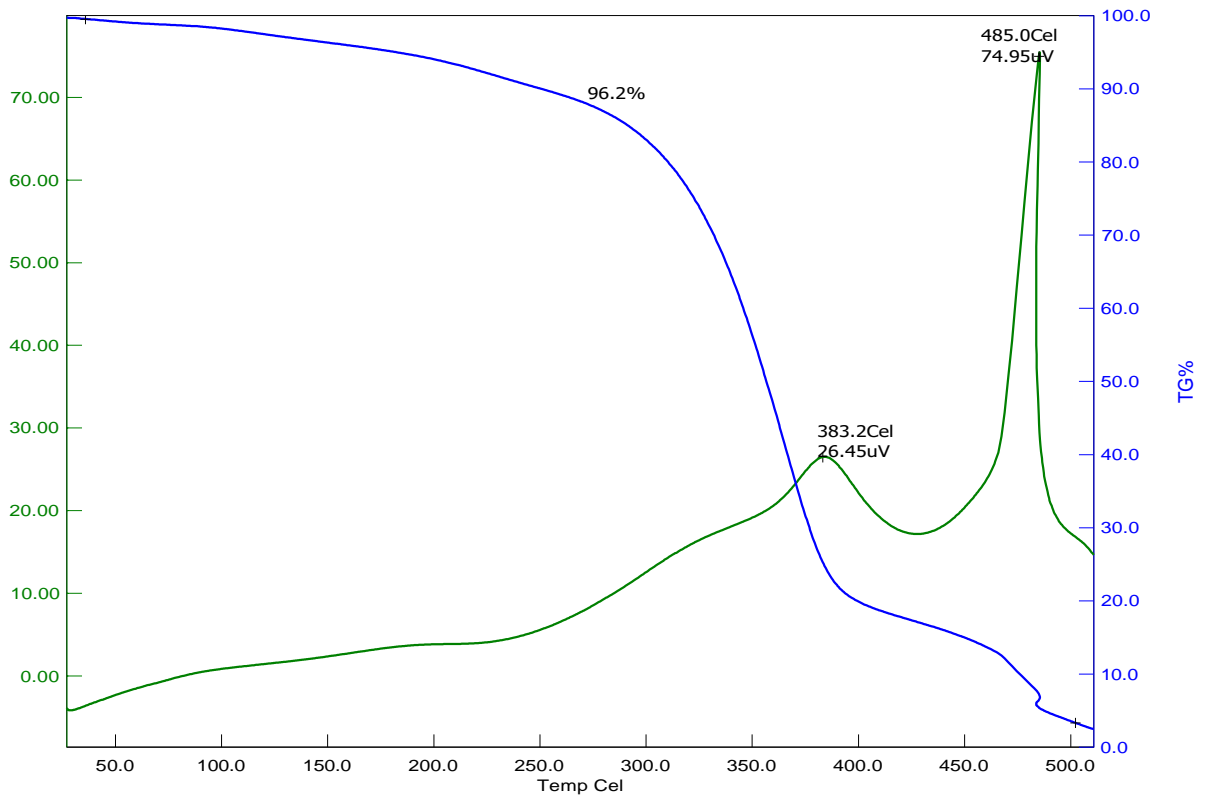


fig 5.6 thermal stability of 30% of bio resin

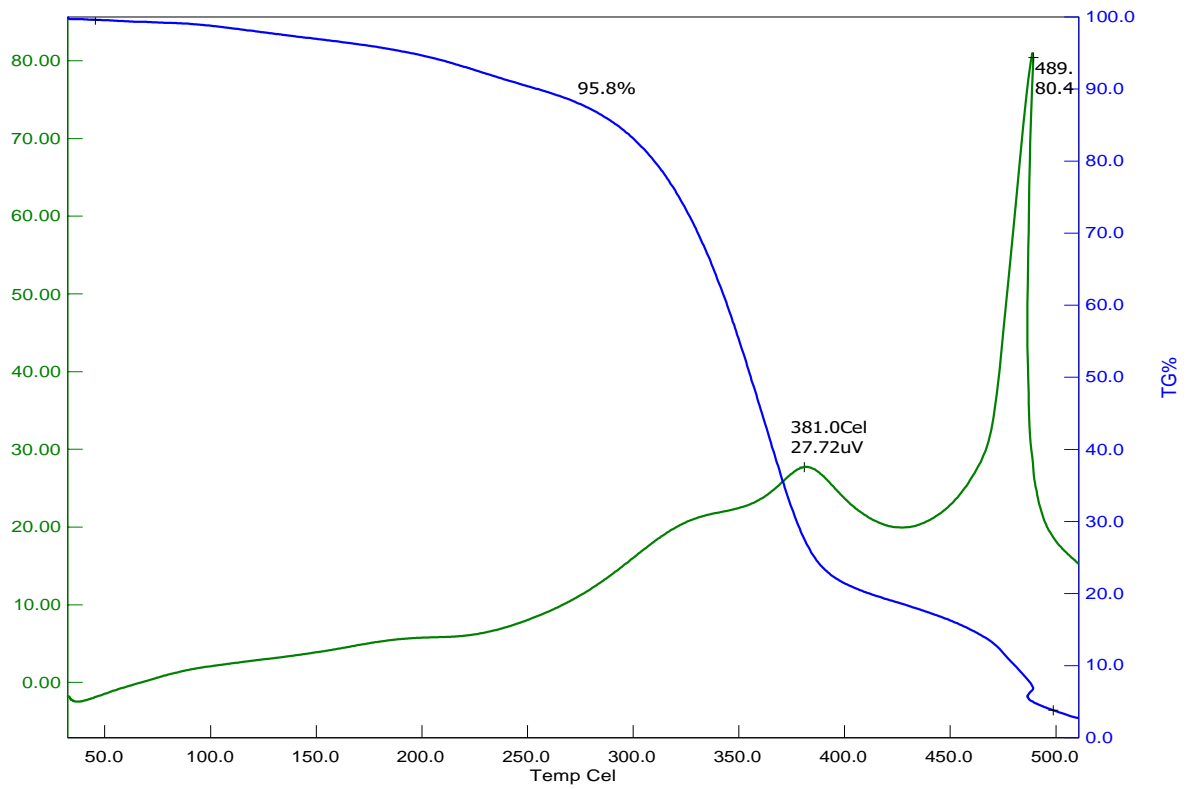


fig 5.7 thermal stability of 40% of bio resin

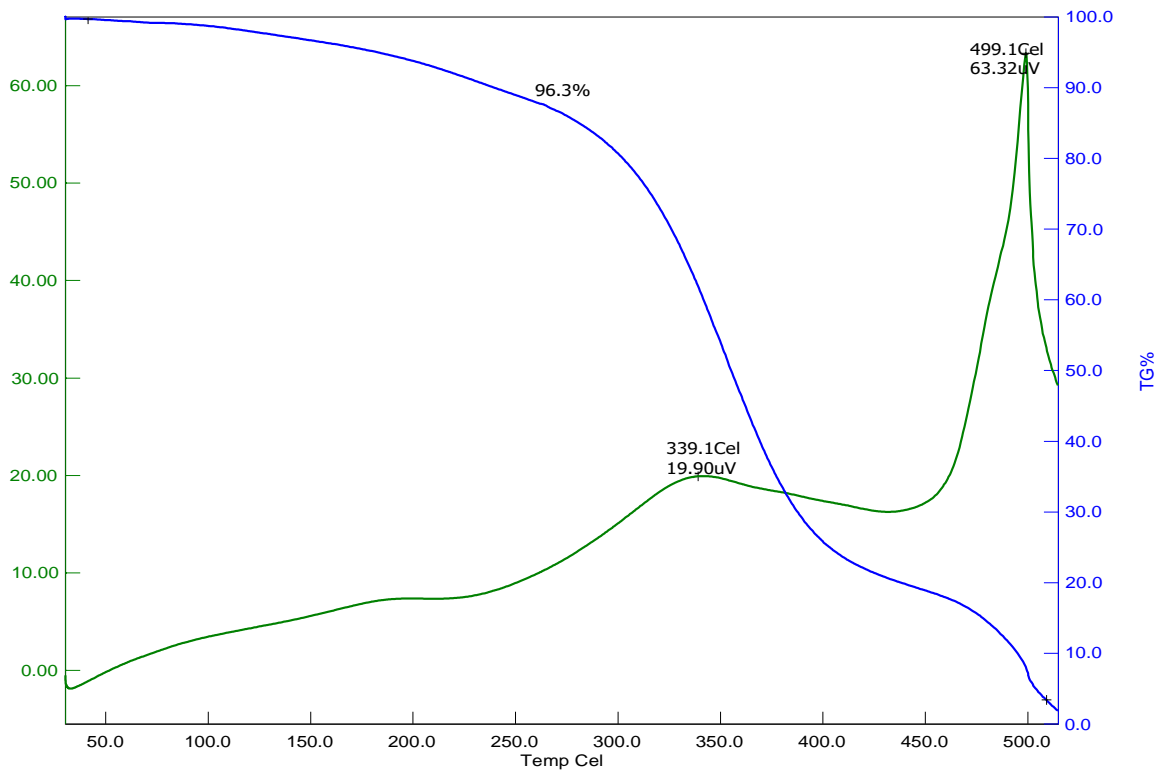


fig 5.8 thermal stability of 50% of bio resin

5.1.2 TGA CURVE FOR PURE POLYESTER, PURE BIO REIN AND HYBRID COMPOSITES.

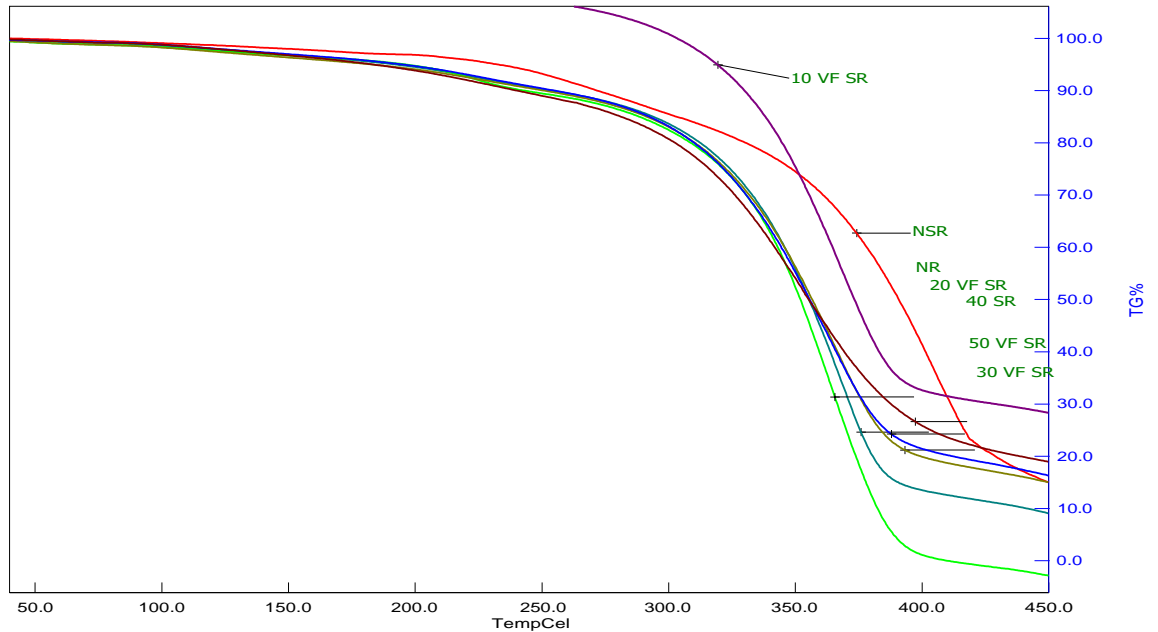


fig 4.10 Tga Curve For Pure Polyester ,Pure Bio Rein And Hybrid Composites.

5.1.3 THERMAL PROPERTIES OF POLYESTER, BIO RESIN AND HYBRID COMPOSITES

The thermal stability curves of hybrid composites as compared to pure polyester and pure bio resin are shown in fig. thermal stability can be expressed in the terms of parameters like initial decomposition temperature, final decomposition temperature. it is seen that the initial degradation temperature of pure polyester was found to 302°C. which is reinforcement by jute fibre. and also that the initial decomposition temperature of bio resin was found to 312°C and all other composition of matrix decomposition values are given from the table. The final degradation temperature of the pure polyester and bio resin was 391°C, 423°C respectively. from the graph composition of matrix had slightly improved the thermal stability of the composites and also bio resin had a better thermal stability compare to pure polyester. finally by adding the bio resin with synthetic rein, the thermal stability does not changed.

Composites	Degradation temperature (°C)			Residue(%)
	IDT	MDT(at 50°C)	FDT	
Polyester	302	352	391	0.7
Bio resin	312	391	423	10.8
10 VF SR	301	373.4	397	19
20 VF SR	302	355.4	396	0.6
30 VF SR	300	355.6	398	3.8
40 VF SR	301	355.7	397	4.2
50 VF SR	301	355.4	401	3.7

Table 5.2

Where,

VF- volume of fraction

SR- bio resin

NR- neat resin(Polyester)

NSR-neat bio resin

IDT-initial decomposition temperature

MDT- middle decomposition temperature

FDT- final decomposition temperature

5.1 DYNAMIC ANALYSIS OF POLYESTER AND BIOCOMPOSITES

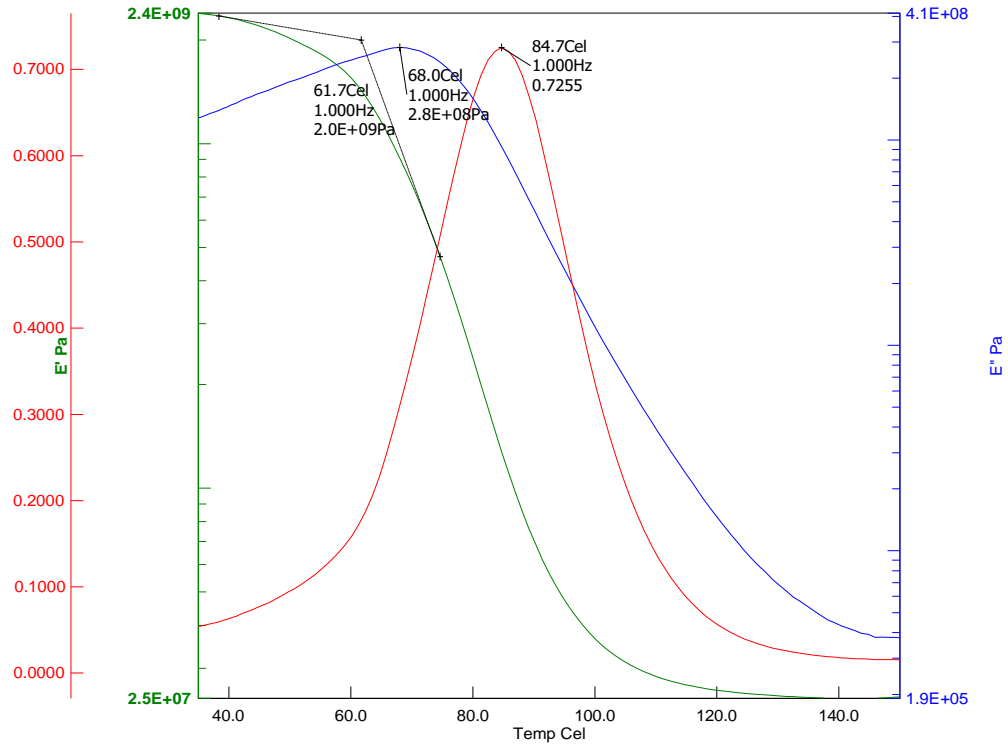


fig 5.10 dynamic analysis of polyester

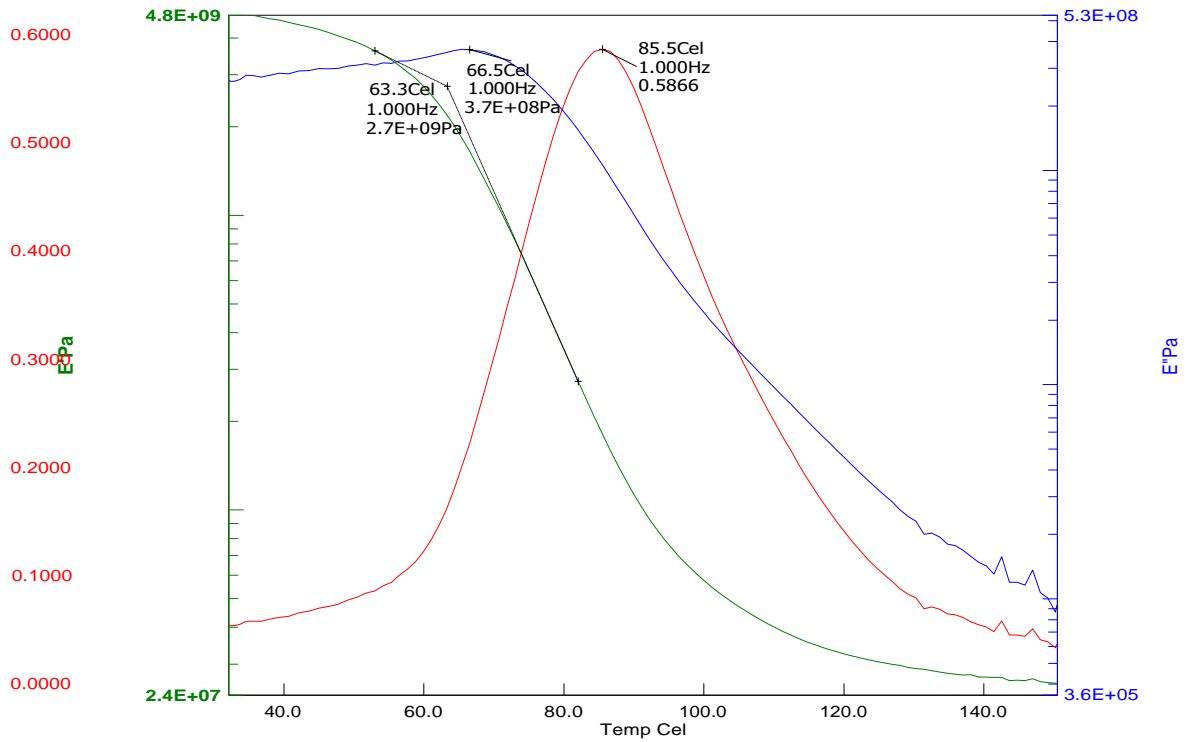


fig 5.11 dynamic analysis of 10% of bio resin

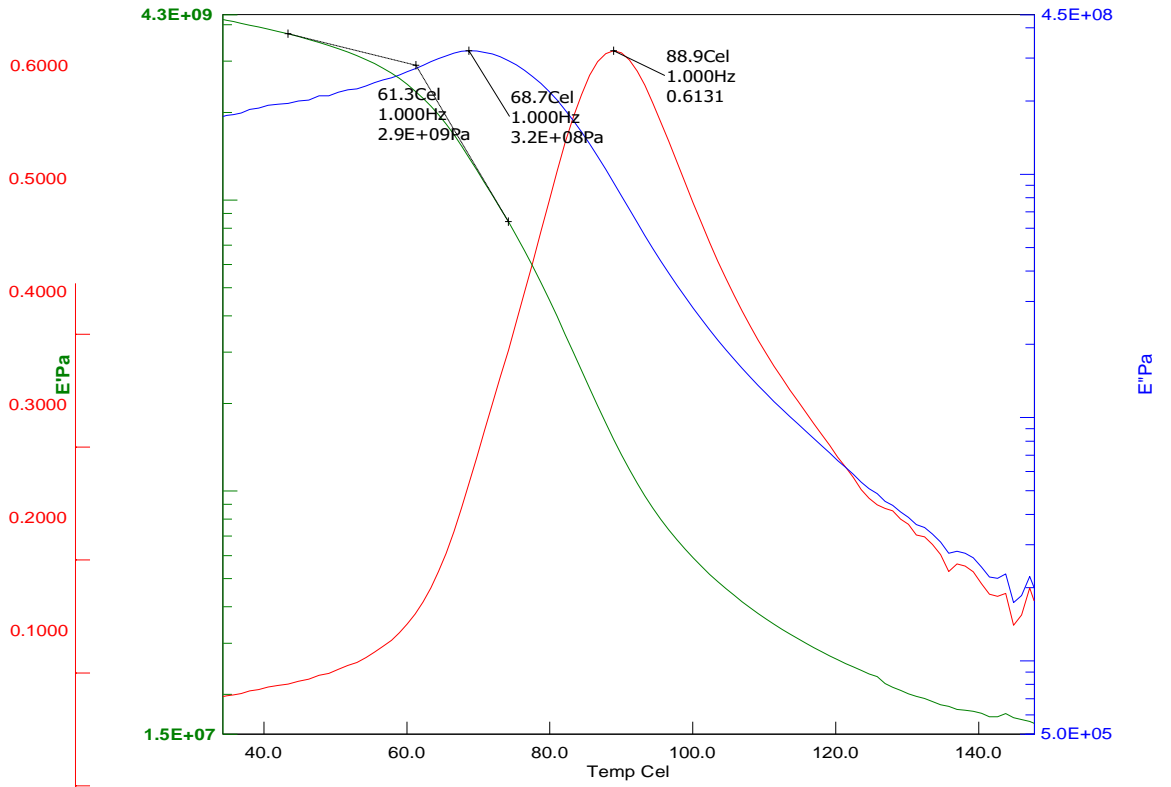


fig 5.12 dynamic analysis of 20% of bio resin

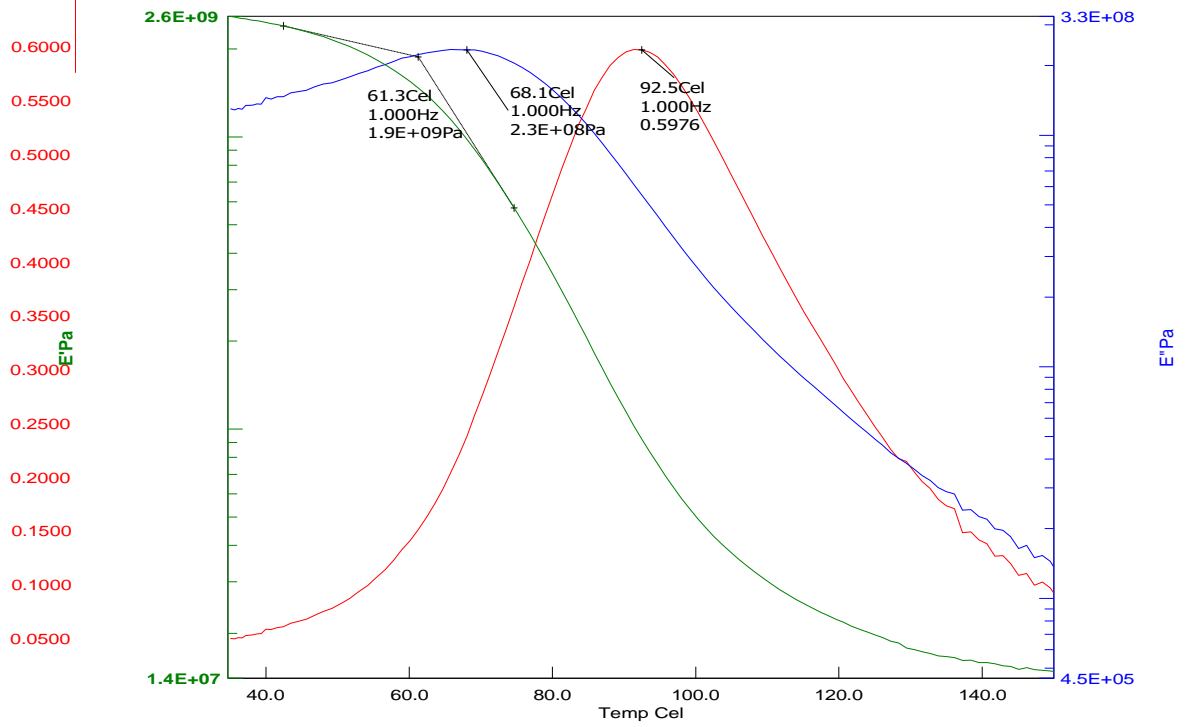


fig 5.13 dynamic analysis of 30% of bio resin

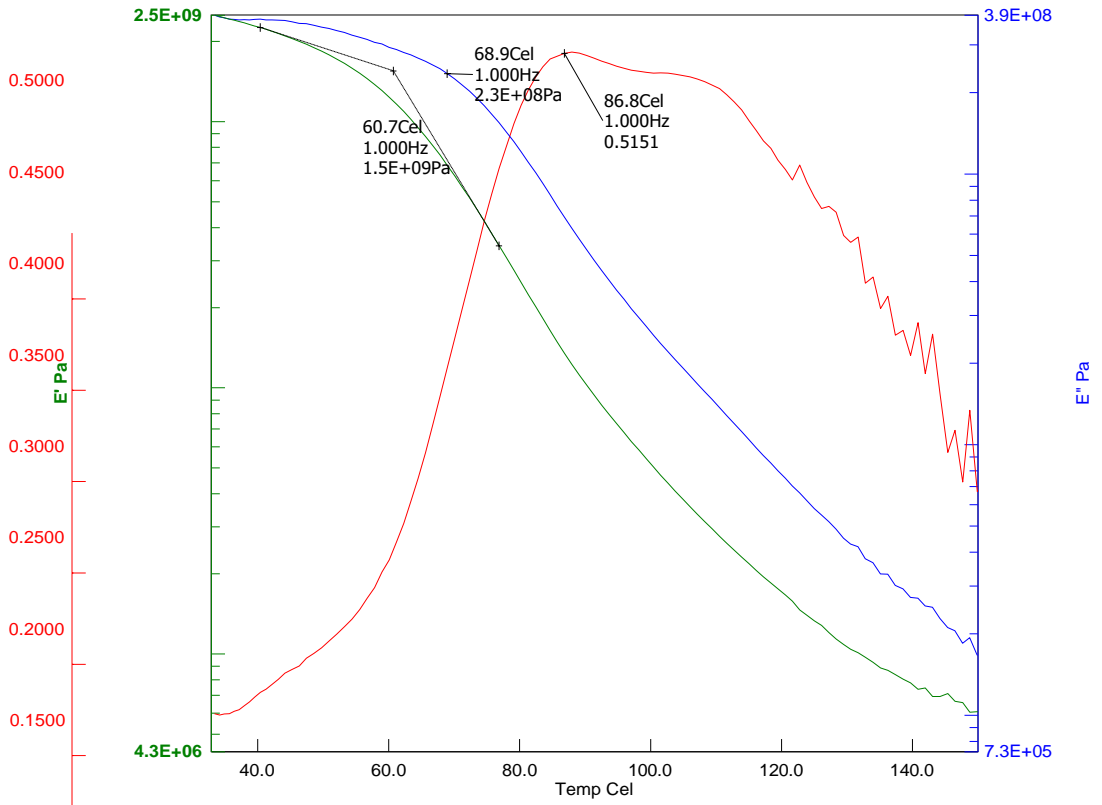


fig 5.14 dynamic analysis of 40% of bio resin

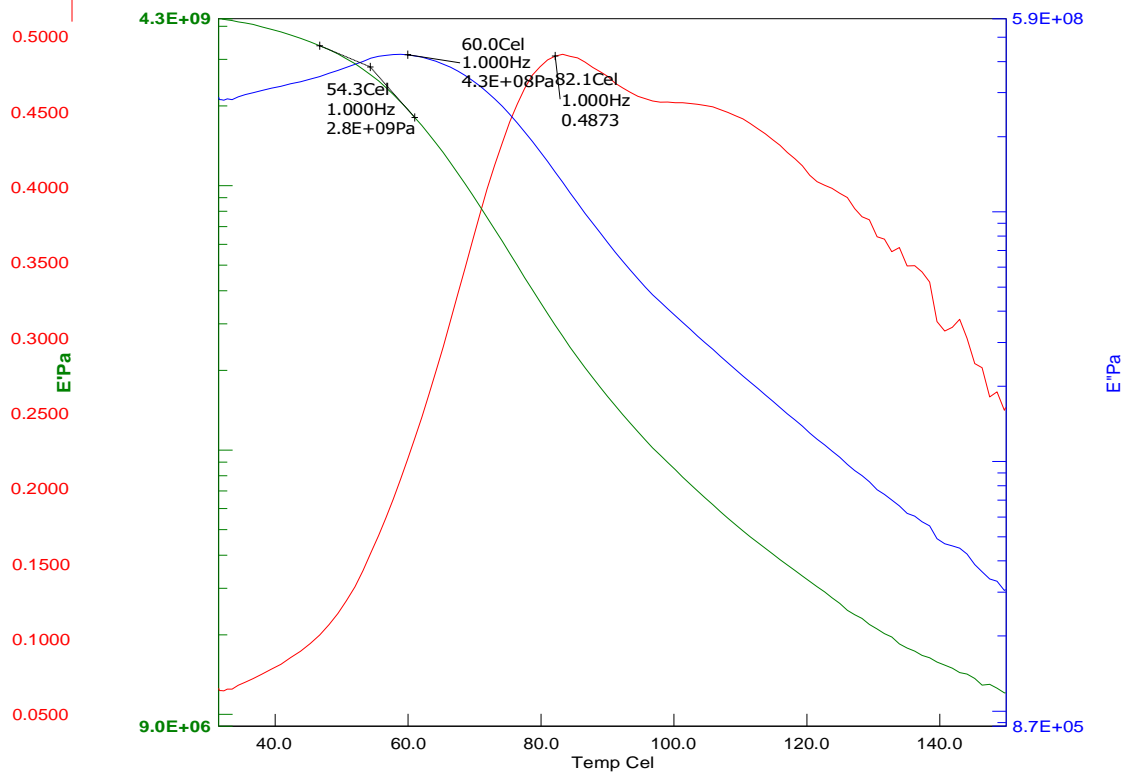


fig 5.15 dynamic analysis of 50% of bio resin

5.1.1 DYNAMIC ANALYSIS OF COMPOSITE MATERIAL

composites	Storage modulus	Loss modulus	Glass transition temperature	Damping factor
NR	2.0E+09 Pa	2.8E+08 Pa	84.7	0.7255
10 VF NR	2.7E+09 Pa	3.7E+08 Pa	85.5	0.5866
20 VF NR	2.9E+09 Pa	3.2E+08 Pa	88.9	0.6131
30 VF NR	1.9E+09 Pa	2.3E+08 Pa	92.5	0.5976
40 VF NR	1.5E+09 Pa	2.3E+08 Pa	86.8	0.5151
50 VF NR	2.8E+09 Pa	8.4E+08 Pa	82.1	0.4873

Table 5.3

Where,

VF- volume of fraction

NR- neat resin(Polyester)

5.2 REINFORCEMENT RESULT FOR COMPOSITE MATERIAL

Thermal stability and dynamic results like storage modulus, loss modulus, glass transition temperature, damping factor for Reinforcement of composite material has done by thermogravimetric analyzer and dynamic mechanical analyzer. the result indicates that the reinforcement material has more thermal stability and damping factor than other composites .

REINFORCEMENT SAMPLE PREPARATION

Jute fibre –10%

Shora robusta seed oil – 20%

Polyester –70%

5.2.1 THERMAL STABILITY OF REINFORCEMENT COMPOSITE MATERIAL

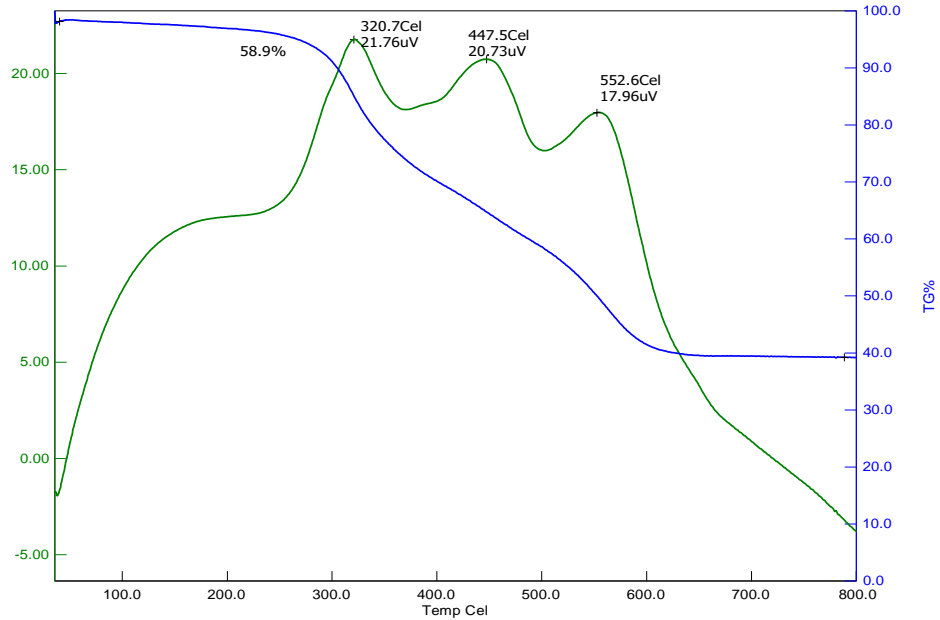


Fig 5.16 thermal stability of reinforcement material

5.4.2 DYNAMIC RESULT FOR REINFORCEMENT COMPOSITE MATERIAL

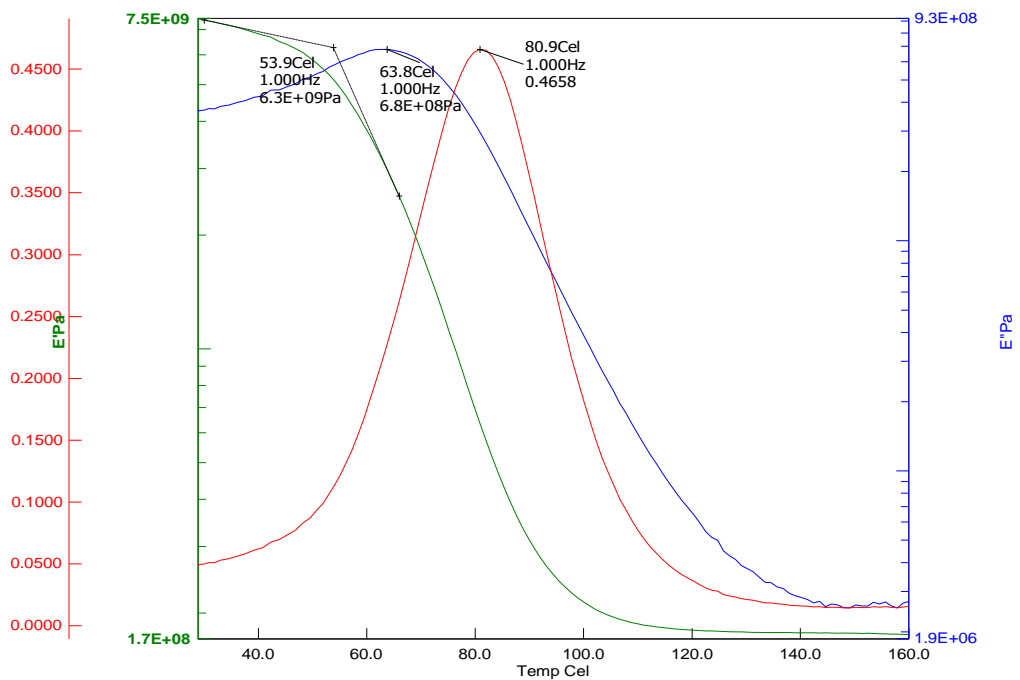


Fig 5.16 Dynamic result for reinforcement material

5.3 THERMAL STABILITY AND DYNAMIC RESULT FOR REINFORCEMENT MATERIAL

composites	Degradation temperature (°C)			Residue(%)
	IDT	MDT(at 50°C)	FDT	
Polyester	288	520	780	58.9

composites	Storage modulus	Loss modulus	Glass transition temperature	Damping factor
reinforcement	6.3E+09 Pa	6.8E+08 Pa	80.9	0.4658

Table 5.4

The result indicates that the reinforcement material has more thermal stability and more dynamic result than the all other composite materials. Thermal stability of reinforcement material is around 780 C with remaining residue of 58.9 % . then the dynamic result shows that the storage modulus of the reinforcement material has more than the other composites material and damping factor result gives low damping factor which shows the material is better than the other composites. hence jute fibre is one of the best reinforcement material.

CHAPTER
6 CONCLUSIO

N

A composite sample was prepared by using synthetic resin and bio resin. The fabricated composite is subjected to thermogravimetric analysis and dynamic mechanical analysis

- The result indicates that the composites material shows thermal stability of the hybrid matrix which was compared with pure polyester. which indicates that the thermal stability of the hybrid matrix is higher higher than pure polyester
- Density of bio resin was found out
- The result indicates that the composites material shows storage modulus, loss modulus, glass transition temperature of the hybrid matrix is more than the polyester.
- the result indicates that the reinforcement material has more thermal stability and damping factor than other composites

REFERENCES

- [1] Adrian M. Cunliffe, Nicola Jones, Paul T. Williams : Recycling of fibre-reinforced polymeric waste by pyrolysis: thermo-gravimetric and bench-scale investigations. *J.anal.appl.pyrolysis*2003;70:315-338
- [2] aigbodion v.s , s.b.hassan , c.ucatuanya : effect of orange peels ash on thermal properties of high density polyethylene. *j.mater. environ .sci.* 3(6)(2012)1027-1036.
- [3] Bhanu K. Goriparthi , K.N.S. Suman , Nalluri Mohan Rao : Effect of fiber surface treatments on mechanical and abrasive wear performance of polylactide/jute composites. *.compos part A:appl sci Manuf*2012;43:1800-1808.
- [4] Betiana A. Acha, Mari'a M. Reboredo, Norma E. Marcovich : Creep and dynamic mechanical behavior of PP–jute composites: Effect of the interfacial adhesion. *compos part A:appl sci Manuf*2007;38:1507-1516..
- [5] Chandramika Bora , Pranjal Bharali , Silpi Baglari , Swapan K. Dolui , Bolin K. Konwar : Strong and conductive reduced graphene oxide/polyester resin composite films with improved mechanical strength, thermal stability and its antibacterial activity. *Composites and technology*2013;87:1-7.
- [6] Heitor Luiz Ornaghi Jr , Vinicios Pistor , Ademir José Zattera: Effect of the epoxy cyclohexyl polyhedral oligomeric silsesquioxane content on the dynamic fragility of an epoxy resin. *journal of non-crystalline solids*2012;358:427-432.
- [7]. M. Jawaid, Abdul Khalil H.P.S , Omar S. Alattas : Woven hybrid biocomposites: Dynamic mechanical and thermal properties. *compos part A:appl sci Manuf* 2012;43:288-293
- [8] M.jawaid , H.P.S Abdul khalil , Rudi Dungani , A.Hadiyane: effect of jute fibre loading on tensile and dynamic mechanical properties of oil palm epoxy composites. *compos part B:appl sci Manuf*2013;45:619-624.
- [9] Y. Karaduman , M.M.A. Sayeed , L. Onal , A. Rawal : Viscoelastic properties of surface modified jute fiber/polypropylene nonwoven composites. *compos part B:appl sci Manuf*2014;67:111-118.
- [10] Ray D, Sarkar BK, Das S, Rana AK. Dynamic mechanical & thermal analysis of vinyl ester–resin–matrix composites reinforced with untreated & alkali-treated jute fibres. *Compos Sci Technol*2002;62(2):911–7.
- [11] Woo EM, Seferis JC. Viscoelastic characterization of high performance epoxy matrix composites. *Polym Compos*1991;12(4):273–80.
- [12] Kuburi, LS, Dauda, M, Obada, DO, Umaru, S, Doodoo-Arhin, D, Iliyasu, I & Mustapha, S 2017, 'Effects of Coir Fiber Loading on the Physio-mechanical and

Morphological Properties of Coconut Shell Powder Filled Low Density Polyethylene Composites', *Procedia Manufacturing*, vol. 7, pp. 138-144.

[13]Kumar, CS, Arumugam, V, Sajith, S, Dhakal, HN & John, R 2015, 'Acoustic emission characterisation of failure modes in hemp/epoxy and glass/epoxy composite laminates', *Journal of Nondestructive Evaluation*, vol. 34, no. 4, p. 31.

[14]Kuzak, SG & Shanmugam, A 1999, 'Dynamic mechanical analysis of fiber reinforced phenolics', *J. Appl. Polym. Sci.*, vol. 73, no. 5, pp. 649-658.

[15]Li, X, Panigrahi, SA, Tabil, LG & Crerar, WJ 2004, 'Flax fiber-reinforced composites and the effect of chemical treatments on their properties', In North central ASAE/CSAE Conference.

[16]Li, X, Tabil, LG & Panigrahi, S 2007, 'Chemical treatments of natural fiber for use in natural fiber-reinforced composites: a review', *Journal of Polymers and the Environment*, vol. 15, no. 1, pp. 25-33.

[17]Malviya, S, Rawat, S, Kharia, A & Verma, M 2011, 'Medicinal attributes of *Acacia Nilotica* Linn.-A comprehensive review on ethnopharmacological claims', *International Journal of Pharmacy & Life Sciences*, vol. 2, no. 6.

[18]Mathews, FL & Rawlings, RD 1999, 'Composite Materials: Engineering and Science', Taylor and Francis, USA.

[19]Maurya, HO, Gupta, M, Srivastava, R & Singh, H 2015, 'Studied on the mechanical properties of epoxy composite using short sisal fiber', *Mater. Today: Proc.*, vol. 2, pp. 1347-1355.

[20]Meena, PD, Kaushik, P, Shukla, S, Soni, AK, Kumar, M & Kumar, A 2006, 'Anticancer and antimutagenic properties of *Acacia Nilotica* (Linn.) on 7, 12-dimethylbenz (a) anthracene-induced skin papillomagenesis in Swiss albino mice', *Asian Pac. J. Cancer Prev.*, vol. 7, no. 4, pp. 627-632.

[21]Mishra, S, Naik, JB & Patil, YP 2001, 'The compatibilising effect of maleic anhydride on swelling and mechanical properties of plant-fiber-reinforced novolac composites', *Composites Science and Technology*, vol. 60, no. 9, pp. 1729-1735.

[22]Mohan, TP & Kanny, K 2011, 'Studied the water barrier properties of nanoclay filled sisal fiber reinforced epoxy composites', *Composites Part A: Applied Science and Manufacturing*, vol. 42, no. 4, pp. 385-393.

[23]Mohan, TP, Kumar, MR & Velmurugan, R 2006, 'Thermal, mechanical and vibration characteristics of epoxy-clay nanocomposites', *Journal of materials science*, vol. 41, no. 18, pp. 5915-5925.

[24]Mohanty, AK, Misra, M & Drzal, LT 2001, 'Surface modifications of natural

fibers and performance of the resulting biocomposites: an overview', *Composite interfaces*, vol. 8, no. 5, pp. 313-343.

[25]Mohanty, AK, Misra, M & Drzal, LT 2002, 'Sustainable bio-composites from renewable resources: opportunities and challenges in the green materials world', *Journal of Polymers and the Environment*, vol. 10, no. 1-2, pp. 19-26.

[26]Muthukumar, S & Lingadurai, K, 'Global Journal of Engineering Science and Researches'.Nair, KM, Thomas, S & Groeninckx, G 2001, 'Thermal and dynamic mechanical analysis of polystyrene composites reinforced with short sisal fibers', *Composites Science and Technology*, vol. 61, no. 16, pp. 2519-2529.

[27]Olumuyiwa Agunsoye, J, Talabi, S & Isaac, SO 2012, 'Study of mechanical behaviour of coconut shell reinforced polymer matrix composite', *J. Miner. Mater. Charact. Eng.*, vol. 11, no. 11, pp. 774–779.

[28]Omar, F, Bledzki, AK, Fink, HP & Sain, M 2014, 'Progress Report on Natural Fiber Reinforced Composites', *Macromol. Mater. Eng.*, vol. 299, pp. 9–26.

[29]Onuegbu, GC & Igwe, IO 2011, 'The effects of filler contents and particle sizes on the mechanical and end-use properties of snail shell powder filled polypropylene', *Materials Sciences and Applications*, vol. 2, no. 07, p. 810.

[30]Palanikumar, K, Ramesh, M & Hemachandra Reddy, K 2016, 'Conducted the experimental investigation on the mechanical properties of green hybrid sisal and glass fiber reinforced polymer composites', *J. Nat. Fibers*, vol. 13, pp. 321–331.



Project Evaluation REPORT 2019 – 2020

Name of the Programme : **M.E - Thermal and Fluid Engineering**
Year of study and Batch : **II & 2**
Name of the Supervisor : **Mr.A.R.Sivaram**
Title of the Project :

**MODELLING AND ANALYSIS OF ATURBO CHARGER WITH
VARIOUS ANGLES**

Nature of the Project : **Individual**

Reg No of Students who are with this Project:

SARAVANA SHAASTHA S (AMTF18002)



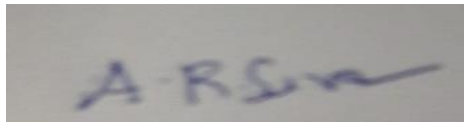
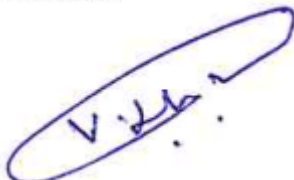
Project Evaluation REPORT 2019 – 2020

Name of the Department: **Mechanical Engineering**

Name of the Student	SARAVANA SHAASTHA S
Register No	AMTF18002
Programme of study	M.E - Thermal and Fluid Engineering
Year and Batch	II and 2 (2019 – 2020)
Semester	IV
Title of the Project	MODELLING AND ANALYSIS OF ATURBO CHARGER WITH VARIOUS ANGLES
Duration of Project	3 Months
Mentor of the Student	Mr.A.R.Sivaram

Evaluation by the Department

Sl No.	Criterion	Max. Marks	Marks Allotted
1	Idea / Techique Idnetification	5	5
2	Conceptualisation of idea / techique	5	5
3	Thought process /clarity of idea	5	5
4	Methodology to solve the problem	5	4
5	Project Scheduling	5	5
6	Preparing the equipment/ component list	5	5
7	Literature Review	5	5
8	Design work	5	5
9	Conference Presentation/ Publication	10	10
10	Problem statement and scope of the project	10	9
11	Analysis and modern Tool usage in problem solving	10	9
12	Project report	10	9
13	Originality score	10	10
14	Written or Video Presentation or Demo	5	5
15	Viva-Voce	5	5
Total		100	96

Signature of the Mentor 	Signature of the Internal Examiner 	Signature of HoD/Programme Head 
--	---	--

MODELLING AND ANALYSIS OF ATURBO CHARGER WITH VARIOUS ANGLES

A PROJECT REPORT

Submitted by

SARAVANA SHAASTHA S (AMTF18002)

In partial fulfillment for the award of the

degree of

MASTER OF ENGINEERING

In

**THERMAL AND FLUID
ENGINEERING**

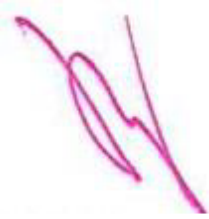


AMET UNIVERSITY: CHENNAI 603112

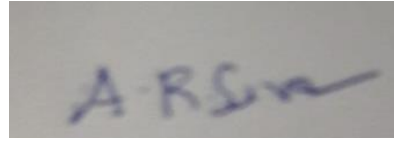
JUNE 2020

BONAFIDE CERTIFICATE

Certified that this project report “**MODELLING AND ANALYSIS OF A TURBO CHARGER WITH VARIOUS ANGLES**” is the bonafide work of “**SARAVANA SHAASTHA S (AMTF18002)**” who carried out the projectwork under my supervision.



Dr.R.RAJAVEL



Mr.A.R.SIVARAM

HEAD OF THE DEPARTMENT

AND PROFESSOR

DEPARTMENT OF MECHANICAL
ENGINEERING,

AMET, CHENNAI 603112

ASSISTANT PROFESSOR

DEPARTMENT OF

MECHANICAL ENGINEERING,

AMET, CHENNAI 603112

Project Viva-voce examination held on.....

INTERNAL EXAMINER

EXTERNAL EXAMINER

ACKNOWLEDGEMENT

Inspiration to achieve, encouragement when things go against your expectations and proper guidance in the right directions are indispensable for the success of any project and we are not an exception to that we have received these in excess from all corners from various people. We are indebted to submit our gratitude to them.

We thank **Col. Dr. G. THIRUVASAGAM**, Vice-Chancellor of AMET (Deemed to be University) for extending his generous hand in providing the best of their sources in the AMET..

We are honoured to express our thanks to our beloved Head of the Department Prof. **Dr. R. RAJAVEL**, who always served as a source of inspiration and encouraged us throughout the project and also contributed his valuable suggestions, instruction and encouragement in doing this project.

We have no words to express our thanks to our supervisor **Mr.A.R.SIVARAM**, Assistant Professor for his keen interest, guidance, inspiration and valuable suggestion during the course of our project.

We specially thank all staff of department of mechanical engineering for their support and assistance.

ABSTRACT

A turbocharger, (or turbo), is a turbine-driven forced induction device that increases an internal combustion engine's efficiency and power output by forcing extra air into the combustion chamber. This improvement over a naturally aspirated engine's power output is due to the fact that the compressor can force more air and proportionately more fuel into the combustion chamber than atmospheric pressure alone. A turbocharger may also be used to increase fuel efficiency without increasing power. This is achieved by recovering waste energy in the exhaust and feeding it back into the engine intake. By using this otherwise wasted energy to increase the mass of air, it becomes easier to ensure that all fuel is burned before being vented at the start of the exhaust stage.

Key words: Turbo , Turbocharger , Stages , Vanes, power , Efficiency , Atmospheric.

TABLE OF CONTENTS

CHAPTER NO.	TITLE	PAGE NO.
	ABSTRACT	i
	LIST OF FIGURES	iii
	LIST OF TABLES	iv
	LIST OF CHARTS	iv
1.	INTRODUCTION	
	1.1 TURBOCHARGER	1
	1.2 KEY COMPONENT	6
	1.2.1 Turbine	7
	1.2.2 Compressor	8
	1.2.3 Centre Housing / HUB Rotating Assembly	9
	1.2.4 Inter Cooling	17
2.	LITERATURE SURVEY	23
3.	OBJECTIVE & METHODOLOGY	47
	SIMULATION WORK	
4.	SOLIDWORKS	
	4.1. INTRODUCTION TO SOLIDWORKS	49
	4.2. COMMONLY USING TOOLS FOR MODELLING IN SOLIDWORKS	50
	VELOCITY CALCULATION FOR COMPRESSOR	
	4.3. FOR BLADE ANGLE 15°	51
	4.4. FOR BLADE ANGLE 18°	51
	4.5. FOR BLADE ANGLE 20°	52

ANALYSING TOOL

5.	ANALYSIS OF TURBOCHARGER COMPRESSOR	53
	5.1. FOR BLADE ANGLE 15°	53
	5.2. FOR BLADE ANGLE 18°	54
	5.3. FOR BLADE ANGLE 20°	
6.	RESULTS AND DISCUSION	56
	6.1. COMPARISON OF ANALYSIS RESULTS	
7.	CONCLUSION	64
	REFERENCE	

LIST OF FIGURES

FIGURE NO.	NAME OF THE FIGURE	PAGE NO.
1.1	Section of the Turbo charger	2
1.2	Side view of turbo charger	3
1.3	Compressor impeller side with the cover removed	4
1.4	Turbine side housing removed	5
1.5	Pivoting vane (left) and moving wall (right) variable geometry turbochargers	12
1.6	Comparison of fixed geometry (BorgWarner KP39) and variable geometry (BorgWarner BV40) mass flow vs. pressure ratio	13
1.7	Effect of variable geometry turbine nozzle opening and blade speed ratio on turbine efficiency	16
1.8	Illustration of typical component layout in a production turbocharged petrol engine	17
1.9	Illustration of inter-cooler location	17
1.10	A recirculating type anti-surge valve	20
4.1	Design and modelling of compressor	49
4.2	Isometric view of compressor	49
5.1	Mesh model of compressor	51
5.2	Velocity distribution	51
5.3	Pressure distribution at out casing	52
5.4	Iterations	52
5.5	Pressure distribution at blades	53
5.7	Mesh model of compressor	53
5.8	Iterations	54
5.9	Temperature distribution	54

5.10	Velocity distribution	55
5.11	Pressure distribution at blades	55
5.12	Pressure distribution at out casing	56
5.13	Temperature distribution	56
5.14	Meshed model of compressor	57
5.15	Velocity distribution	57
5.17	Iterations	58
5.18	Pressure distribution at out casing	58
6.1	Velocity comparison	59
6.2	Pressure distribution comparison	59
6.3	Comparison of Temperature distribution	60

LIST OF TABLES

TABLE NO.	NAME OF THE TABLE	PAGE NO.
4.1	Speed of the compressor for respective angle	43
6.1	Comparison of velocity	59
6.2	Comparison of Pressure distribution	59
6.3	Comparison of Temperature distribution	60

CHAPTER 1

INTRODUCTION

1.1. TURBOCHARGER

A turbocharger, or colloquially turbo, is a turbine-driven forced induction device that increases an internal combustion engine's efficiency and power output by forcing extra air into the combustion chamber. This improvement over a naturally aspirated engine's power output is due to the fact that the compressor can force more air—and proportionately more fuel— into the combustion chamber than atmospheric pressure (and for that matter, ram air intakes) alone.

Turbochargers were originally known as turbo superchargers when all forced induction devices were classified as superchargers. Today the term "supercharger" is typically applied only to mechanically driven forced induction devices. The key difference between a turbocharger and a conventional supercharger is that a supercharger is mechanically driven by the engine, often through a belt connected to the crankshaft, whereas a turbocharger is powered by a turbine driven by the engine's exhaust gas. Compared with a mechanically driven supercharger, turbochargers tend to be more efficient, but less responsive. Twin charger refers to an engine with both a supercharger and a turbocharger.

Turbochargers are commonly used on truck, car, train, aircraft, and construction equipment engines. They are most often used with Otto cycle and Diesel cycle internal combustion engines. They have also been found useful in automotive fuel cells.

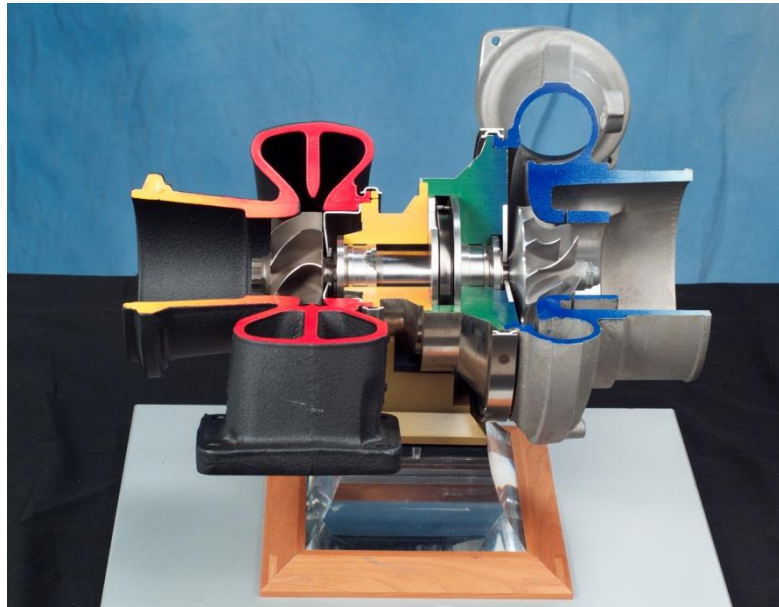


Fig.1.1 Section of the Turbo charger

Nowadays the greater importance is being placed on improving the efficiency and fuel consumption of automobiles due to the global move to reduce CO₂ emissions. An engine ideally should deliver simultaneously a high power density at low fuel consumption. High pressure Turbocharging is very much essential to improve the fuel consumption of an engine by enabling downsizing. Therefore, it necessitates developing an optimum turbo charging system to suit the engine specification.

Computational fluid dynamics (CFD) is the analysis of systems involving fluid flow, heat transfer and associated phenomena by means of computer-based simulations. The advent of high speed digital computers combined with the development of accurate numerical algorithms for solving physical problems on these computers has made it possible to use CFD as a research tool and design tool. In the present study CFD simulation on a Turbocharger Radial Turbine was conducted to obtain the characteristics of flow through Turbine using commercially available CFD tool ANSYS 16.0 . Compressed air (or air/gas mixture in case of gas engine) flow results in a larger quantity of mixture being forced into the engine, creating more power.

The energy used to drive the turbo compressor is extracted from waste exhaust gases. As exhaust gasses leave the engine they are directed through a turbine wheel placed in the exhaust flow. The gases drive the turbine wheel around, which is directly connected via a shaft, to the compressor wheel.

Increased exhaust gas flow increases the inlet pressure which thereby drives the turbine wheel faster, this provides the engine more air or air/gas mixture, producing more power. A limit is reached once a pre-determined boost pressure is achieved.

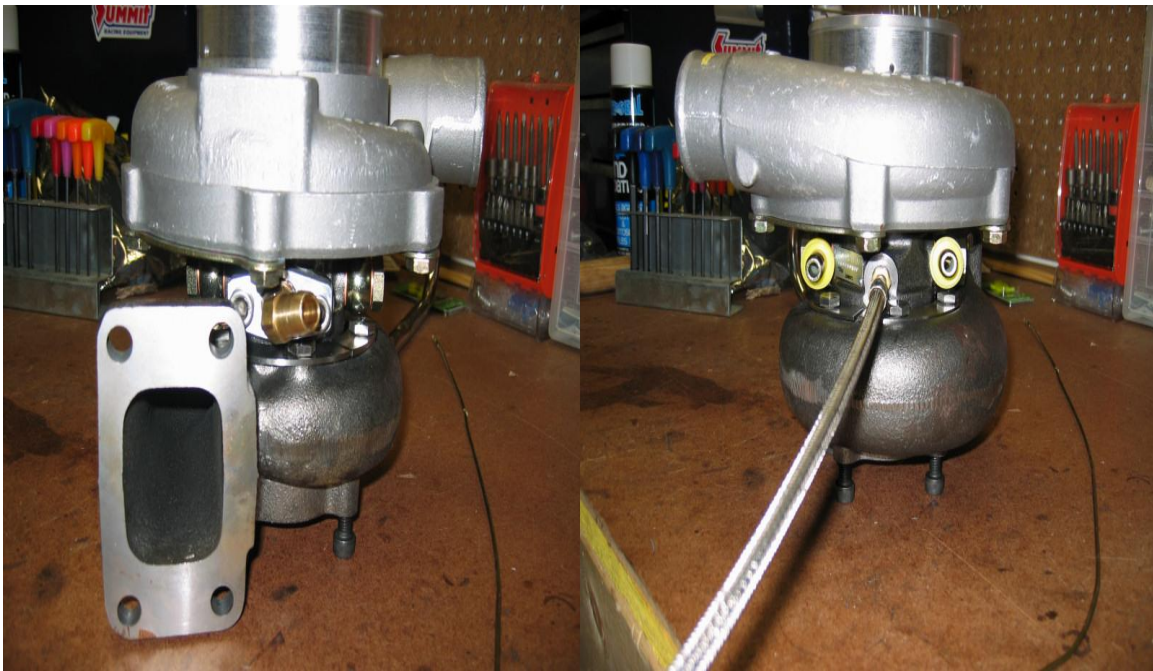


Fig 1.2 Side view of turbo charger

At this point the exhaust gas is redirected away from the turbine wheel, thus slowing it down and limiting the maximum boost pressure. This redirection valve is known as the waste gate. This extraction of energy, from exhaust gas, to improve engine efficiency is the device known as the Turbocharger.

The advantages of using a turbo engine include improved fuel efficiency and reduced exhaust emissions. In order to handle speeds up to 150,000 rpm, the turbine shaft has to be supported very carefully. Most bearings would explode at speeds like this, so most turbochargers use a fluid bearing. This type of bearing supports the shaft on a thin layer of oil that is constantly pumped around the shaft. It cools the shaft and some of the other turbocharger parts, and it allows the shaft

to spin without much friction. When intake air (or air/gas mixture) is compressed by a turbocharger it is also heated. Hot intake air (or air/gas mixture) is not good for power and will increase the chance of detonation.

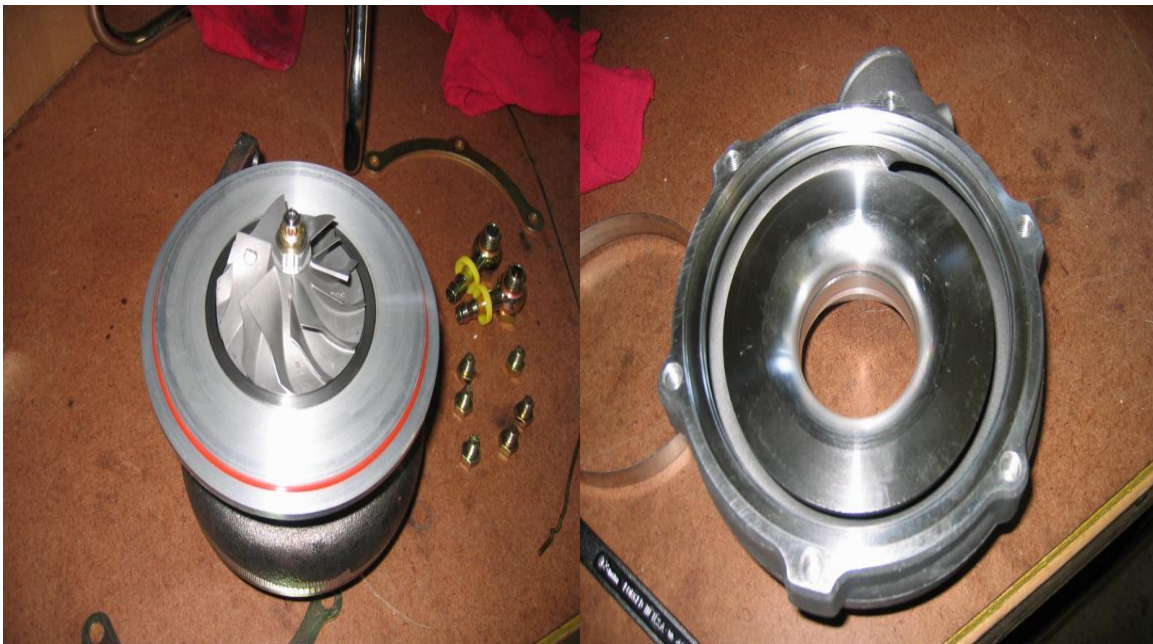


Fig 1.3 Compressor impeller side with the cover removed.

In petrol engine turbocharger applications, boost pressure is limited to keep the entire engine system, including the turbocharger, inside its thermal and mechanical design operating range. Over-boosting an engine frequently causes damage to the engine in a variety of ways including pre-ignition, overheating, and over-stressing the engine's internal hardware. For example, to avoid engine knocking (also known as detonation) and the related physical damage to the engine, the intake manifold pressure must not get too high, thus the pressure at the intake manifold of the engine must be controlled by some means. Opening the waste gate allows the excess energy destined for the turbine to bypass it and pass directly to the exhaust pipe, thus reducing boost pressure. The wastegate can be either controlled manually (frequently seen in aircraft) or by an actuator (in automotive applications, it is often controlled by the engine control unit).

A turbocharger may also be used to increase fuel efficiency without increasing power. This is achieved by diverting exhaust waste energy, from the combustion process, and feeding it back into the turbo's "hot" intake side that spins the turbine.

As the hot turbine side is being driven by the exhaust energy, the cold intake turbine (the other side of the turbo) compresses fresh intake air and drives it into the engine's intake. By using this otherwise wasted energy to increase the mass of air, it becomes easier to ensure that all fuel is burned before being vented at the start of the exhaust stage. The increased temperature from the higher pressure gives a higher Carnot efficiency.



Fig 1.4 Turbine side housing removed.

A reduced density of intake air is caused by the loss of atmospheric density seen with elevated altitudes. Thus, a natural use of the turbocharger is with aircraft engines. As an aircraft climbs to higher altitudes, the pressure of the surrounding air quickly falls off. At 18,000 feet (5,500 m), the air is at half the pressure of sea level, which means that the engine produces less than half-power at this altitude. In aircraft engines, turbocharging is commonly used to maintain manifold pressure as altitude increases (i.e. to compensate for lower-density air at higher altitudes). Since atmospheric pressure reduces as the aircraft climbs, power drops as a function of altitude in normally aspirated engines. Systems that use a turbocharger to maintain an engine's sea-level power output are called turbo-normalized systems. Generally, a turbo-normalized system attempts to maintain a manifold pressure of 29.5 inHg (100 kPa).

1.2 KEYCOMPONENT

- Turbine
- Compressor
- Center housing / hub rotating assembly
- Intercooler

1.2.1 TURBINE

Energy provided for the turbine work is converted from the enthalpy and kinetic energy of the gas. The turbine housings direct the gas flow through the turbine as it spins at up to 250,000 rpm. The size and shape can dictate some performance characteristics of the overall turbocharger. Often the same basic turbocharger assembly is available from the manufacturer with multiple housing choices for the turbine, and sometimes the compressor cover as well.

This lets the balance between performance, response, and efficiency be tailored to the application. The turbine and impeller wheel sizes also dictate the amount of air or exhaust that can flow through the system, and the relative efficiency at which they operate. In general, the larger the turbine wheel and compressor wheel the larger the flow capacity. Measurements and shapes can vary, as well as curvature and number of blades on the wheels.

A turbocharger's performance is closely tied to its size. Large turbochargers take more heat and pressure to spin the turbine, creating lag at low speed. Small turbochargers spin quickly, but may not have the same performance at high acceleration.

To efficiently combine the benefits of large and small wheels, advanced schemes are used such as twin- turbochargers, twin-scroll turbochargers, or variable-geometry turbochargers.

1.2.2 COMPRESSOR

The compressor increases the mass of intake air entering the combustion chamber. The compressor is made up of an impeller, a diffuser and a volute housing. The operating range of a compressor is described by the "compressor map". The flow range of a turbocharger compressor can be increased by allowing air to bleed from a ring of holes or a circular groove around the compressor at a point slightly downstream of the compressor inlet (but far nearer to the inlet than to the outlet).

The ported shroud is a performance enhancement that allows the compressor to operate at significantly lower flows. It achieves this by forcing a simulation of impeller stall to occur continuously. Allowing some air to escape at this location inhibits the onset of surge and widens the operating range. While peak efficiencies may decrease, high efficiency may be achieved over a greater range of engine speeds. Increases in compressor efficiency result in slightly cooler (more dense) intake air, which improves power.

This is a passive structure that is constantly open (in contrast to compressor exhaust blow off valves, which are mechanically or electronically controlled). The ability of the compressor to provide high boost at low rpm may also be increased marginally (because near choke conditions the compressor draws air inward through the bleed path). Ported shrouds are used by many turbocharger manufacturers.

1.2.3 CENTRE HOUSING / HUB ROTATING ASSEMBLY

The center hub rotating assembly (CHRA) houses the shaft that connects the compressor impeller and turbine. It also must contain a bearing system to suspend the shaft, allowing it to rotate at very high speed with minimal friction.

For instance, in automotive applications the CHRA typically uses a thrust bearing or ball bearing lubricated by a constant supply of pressurized engine oil. The CHRA may also be considered "water-cooled" by having an entry and exit point for engine coolant.

Water-cooled models use engine coolant to keep lubricating oil cooler, avoiding possible oil coking (destructive distillation of engine oil) from the extreme heat in the turbine. The development of air-foil bearings removed this risk. Ball bearings designed to support high speeds and temperatures are sometimes used instead of fluid bearings to support the turbine shaft.

This helps the turbocharger accelerate more quickly and reduces turbo lag. Some variable nozzle turbochargers use a rotary electric actuator, which uses a direct stepper motor to open and close the vanes, rather than pneumatic controllers that operate based on air pressure.

Variable-geometry turbochargers (VGTs), occasionally known as variable-nozzle turbines (VNTs), are a type of turbochargers, usually designed to allow the effective aspect ratio of the turbocharger to be altered as conditions change. This is done because the optimum aspect ratio at low engine speeds is very different from that at high engine speeds.

If the aspect ratio is too large, the turbo will fail to create boost at low speeds; if the aspect ratio is too small, the turbo will choke the engine at high speeds, leading to high exhaust manifold pressures, high pumping losses, and ultimately lower power output. By altering the geometry of the turbine housing as the engine accelerates, the turbo's aspect ratio can be maintained at its optimum. Because of this, VGTs have a minimal amount of lag, a low boost threshold, and high efficiency at higher engine speeds.

The rotating-vane VGT was first developed under Garrett and patented in 1953. One of the first production cars to use these turbochargers was the 1988 Honda Legend; it used a water-cooled VGT installed on its 2.0-litre V6 engine. The limited-production 1989 Shelby CSX-VNT, with only 500 examples produced, was equipped with a 2.2-litre Chrysler K engine with a Garrett turbo called the VNT-25 (because it used the same compressor and shaft as the fixed-geometry Garrett T-25).

In 1991, Fiat incorporated a VGT into the Croma's direct-injected turbodiesel. The Peugeot 405 T16, launched in 1992, used a Garrett VAT25 variable-geometry turbocharger on its 2.0-litre 16-valve engine. The 2007 Porsche 911 Turbo has twin variable-geometry turbochargers on its 3.6-litre horizontally-opposed six-cylinder gasoline engine.

The 2015 Koenigsegg One:1 (named after its power-to-weight ratio of 1:1) uses twin variable-geometry turbochargers on its 5.0-litre V8 engine, allowing it to produce 1361 horsepower. The two most common implementations of VGTs are as follows:

For light-duty engines (passenger cars, race cars, and light commercial vehicles), the turbine's vanes rotate in unison, relative to its hub, to vary its pitch and cross-sectional area. For heavy-duty engines, the vanes do not rotate, but instead, their effective width is changed. This is usually done by moving the turbine along its axis, partially retracting the vanes within the housing. Alternatively, a partition within the housing may slide back and forth. The area between the edges of the vanes changes, leading to a variable-aspect-ratio system with fewer moving parts. VGTs may be controlled by a membrane vacuum actuator, electric servo, 3-phase electric actuation, hydraulic actuator, or pneumatic actuator using air brake pressure. Unlike fixed-geometry turbines, VGTs do not require a wastegate.

VGTs tend to be much more common on diesel engines, as lower exhaust temperatures mean they are less prone to failure. Early gasoline-engine VGTs required significant pre-charge cooling to extend the turbocharger life to reasonable levels, but advances in technology have improved their resistance to

high-temperature gasoline exhaust, and they have started to appear increasingly in gasoline-engined cars.

Typically, VGTs are only found in OEM applications due to the level of coordination required to keep the vanes in the most optimal position for whatever state the engine is in. However, there are aftermarket VGT control units available, and some high-end aftermarket engine management systems can control VGTs as well.

In trucks, VGTs are also used to control the ratio of exhaust recirculated back to the engine inlet (they can be controlled to selectively increase the exhaust manifold pressure until it exceeds the inlet manifold pressure, which promotes exhaust gas recirculation). Although excessive engine backpressure is detrimental to overall fuel efficiency, ensuring a sufficient EGR rate even during transient events (such as gear changes) can be sufficient to reduce nitrogen oxide emissions down to that required by emissions legislation (e.g., Euro 5 for Europe and EPA 10 for the USA).

Another use for sliding-vane turbochargers is as a downstream exhaust brake, so that an extra exhaust throttle valve is not needed. The mechanism can also be deliberately modified to reduce the turbine efficiency in a pre-defined position. This mode can be selected to sustain a raised exhaust temperature to promote "light-off" and "regeneration" of a diesel particulate filter (this involves heating the carbon particles stuck in the filter until they oxidize away in a semi-self-sustaining reaction - rather like the self-cleaning process some ovens offer). Actuation of a VGT for EGR flow control, or to implement braking or regeneration modes in general, requires hydraulic actuators or electric servos.

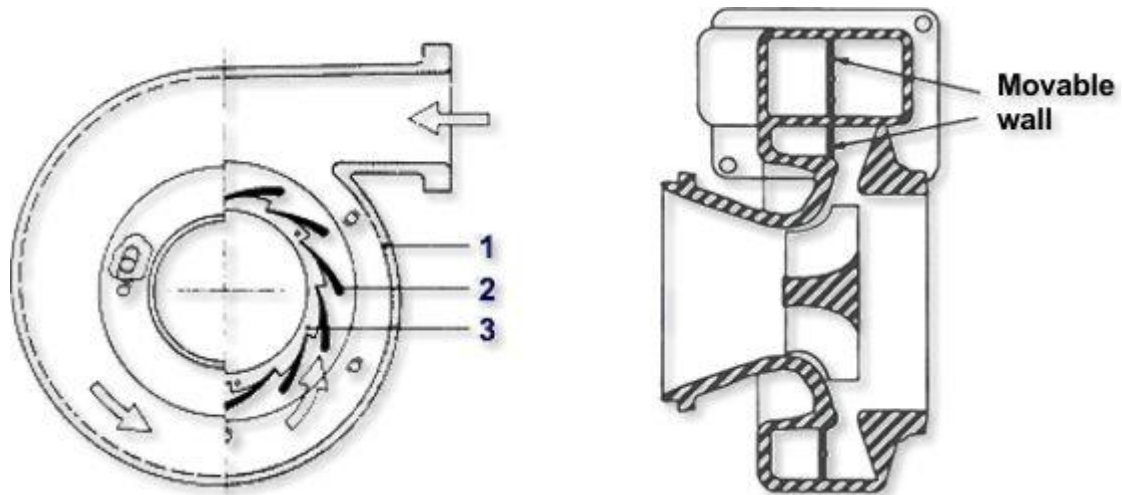


Figure 1.5 Pivoting vane (left) and moving wall (right) variable geometry turbochargers

1. Turbine housing;
2. Variable angle vanes;
3. Adjusting ring

There are a number of different acronyms that are commonly used when referring to turbochargers with variable geometry turbines. In most cases these are or have been trademarks that a particular manufacturer has used with reference to their product. In more common usage, a particular acronym can be used in a more general sense and not necessarily be a reference to a particular manufacturer's product. Some of these acronyms include:

- VGT—Variable Geometry Turbocharger (Cummins/Holset),
- VNT—Variable Nozzle Turbine (Honeywell/Garrett),
- VTG—Variable Turbine Geometry (BorgWarner and ABB)
- VG—Variable Geometry turbocharger (MHI)
- VGS—Variable Geometry System turbocharger (IHI)
- VTA—Variable Turbine Area (MAN Diesel & Turbo)

In many designs, a variable geometry turbine does not include a bypass so the turbine must be capable of handling all of the exhaust flow from the engine while

avoiding overboost and overspeeding the turbocharger. For a given engine power rating, this would imply a larger turbine swallowing capacity than that required by a wastegated fixed geometry turbine and comparable with that used for a fixed geometry turbocharger with no bypass.

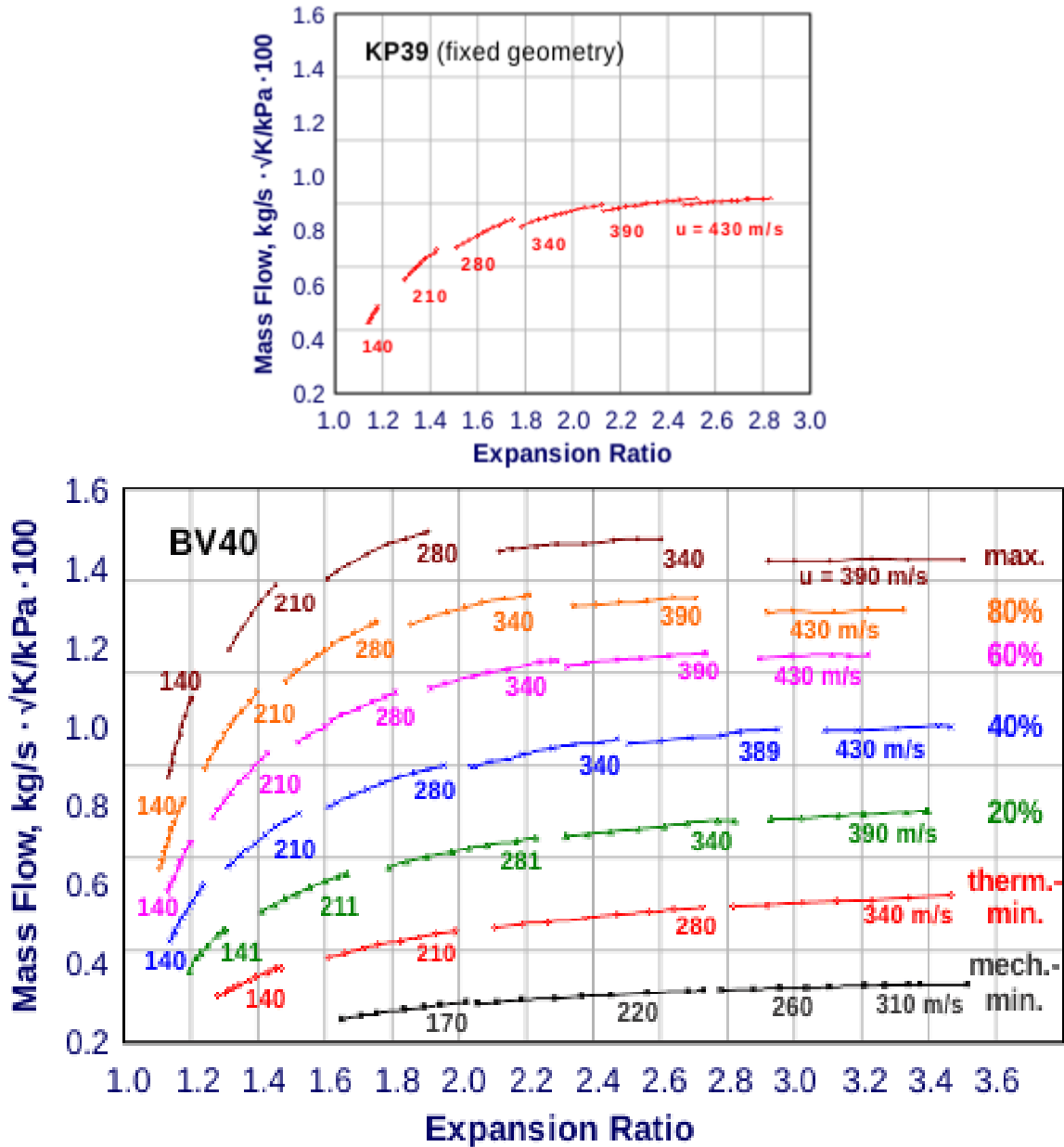


Fig1.6 Comparison of fixed geometry (BorgWarner KP39) and variable geometry (BorgWarner BV40) mass flow vs. pressure ratio

The peak efficiency of a variable geometry turbine occurs at about 60% nozzle opening. It is usually comparable to or a few percent lower than that for a fixed geometry turbine. However, efficiency drops off rather quickly as nozzle opening is reduced or increased from a mid-vane opening position, Figure 1.7.

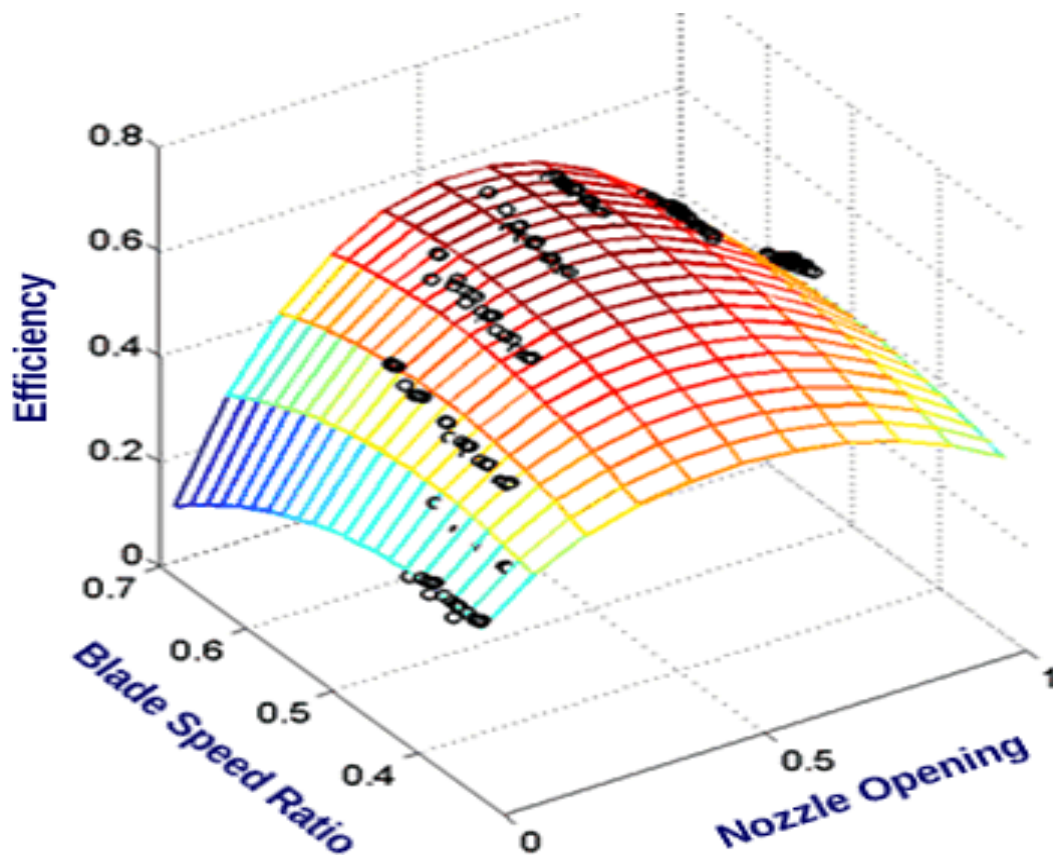


Fig1.7 Effect of variable geometry turbine nozzle opening and blade speed ratio on turbine efficiency

Additional technologies commonly used in turbocharger installations

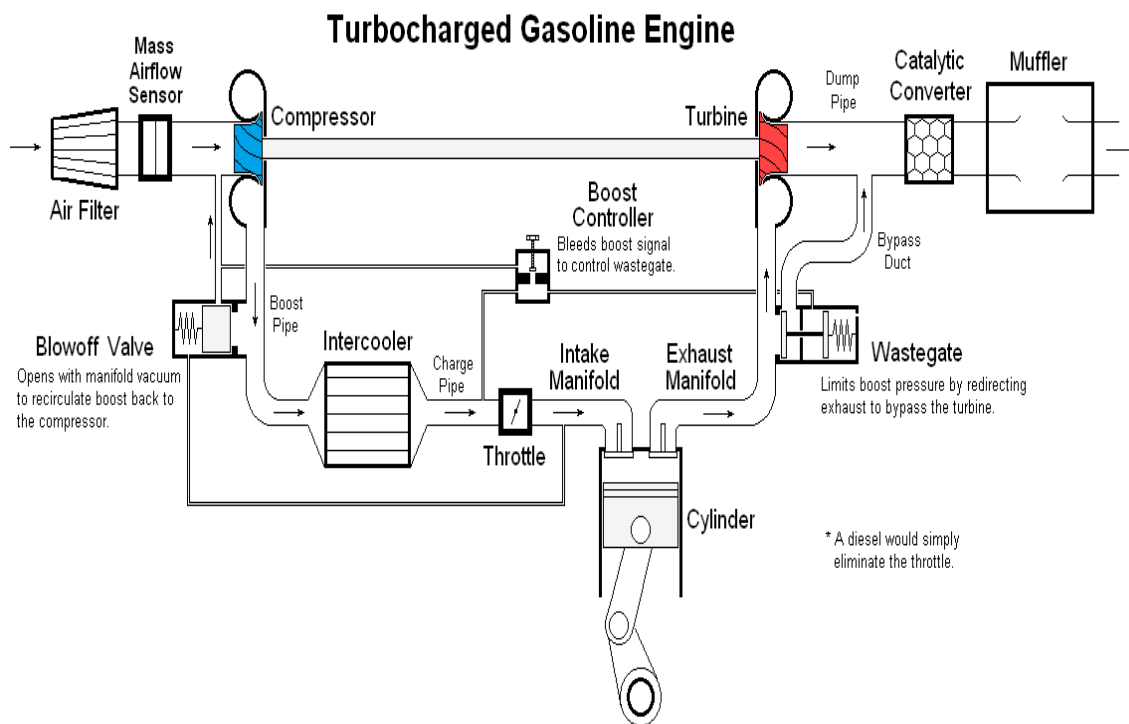


Fig 1.8 Illustration of typical component layout in a production turbocharged petrol engine.

1.2.4 Intercooling

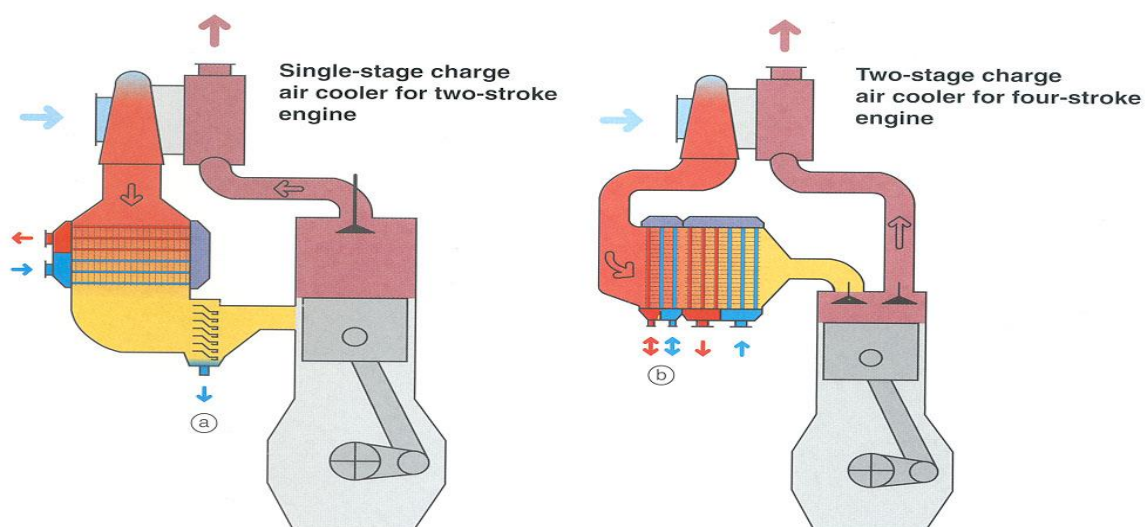


Fig 1.9 Illustration of inter-cooler location.

When the pressure of the engine's intake air is increased, its temperature also increases. This occurrence can be explained through Gay-Lussac's law, stating that the pressure of a given amount of gas held at constant volume is directly proportional to the Kelvin temperature. With more pressure being added to the engine through the turbocharger, overall temperatures of the engine will also rise. In addition, heat soak from the hot exhaust gases spinning the turbine will also heat the intake air. The warmer the intake air, the less dense, and the less oxygen available for the combustion event, which reduces volumetric efficiency. Not only does excessive intake-air temperature reduce efficiency, it also leads to engine knock, or detonation, which is destructive to engines.

To compensate for the increase in temperature, turbocharger units often make use of an intercooler between successive stages of boost to cool down the intake air. A charge air cooler is an air cooler between the boost stage(s) and the appliance that consumes the boosted air.

Top-mount (TMIC) vs. front-mount intercoolers (FMIC)

There are two areas on which intercoolers are commonly mounted. It can be either mounted on top, parallel to the engine, or mounted near the lower front of the vehicle. Top-mount intercoolers setups will result in a decrease in turbo lag, due in part by the location of the intercooler being much closer to the turbocharger outlet and throttle body. This closer proximity reduces the time it takes for air to travel through the system, producing power sooner, compared to that of a front-mount intercooler which has more distance for the air to travel to reach the outlet and throttle.

Front-mount intercoolers can have the potential to give better cooling compared to that of a top-mount. The area in which a top-mounted intercooler is located, is near one of the hottest areas of a car, right above the engine. This is why most manufacturers include large hood scoops to help feed air to the intercooler while the car is moving, but while idle, the hood scoop provides little to no benefit. Even while moving, when the atmospheric temperatures begin to rise, top-mount intercoolers tend to underperform compared to front-mount intercoolers. With

more distance to travel, the air circulated through a front-mount intercooler may have more time to cool.

Methanol/water Injection

Methanol/water injection has been around since the 1920s but was not utilized until World War II. Adding the mixture to intake of the turbocharged engines decreased operating temperatures and increased horse power. Turbocharged engines today run high boost and high engine temperatures to match. When injecting the mixture into the intake stream, the air is cooled as the liquids evaporate. Inside the combustion chamber it slows the flame, acting similar to higher octane fuel. Methanol/water mixture allows for higher compression because of the less detonation-prone and, thus, safer combustion inside the engine.

Fuel-air mixture ratio

In addition to the use of intercoolers, it is common practice to add extra fuel to the intake air (known as "running an engine rich") for the sole purpose of cooling. The amount of extra fuel varies, but typically reduces the air-fuel ratio to between 11 and 13, instead of the stoichiometric 14.7 (in petrol engines). The extra fuel is not burned (as there is insufficient oxygen to complete the chemical reaction), instead it undergoes a phase change from atomized (liquid) to gas. This phase change absorbs heat, and the added mass of the extra fuel reduces the average thermal energy of the charge and exhaust gas. Even when a catalytic converter is used, the practice of running an engine rich increases exhaust emissions.

Wastegate

A wastegate regulates the exhaust gas flow that enters the exhaust-side driving turbine and therefore the air intake into the manifold and the degree of boosting. It can be controlled by a boost pressure assisted, generally vacuum hose attachment point diaphragm (for vacuum and positive pressure to return commonly oil contaminated waste to the emissions system) to force the spring-loaded diaphragm to stay closed until the overboost point is sensed by the ecu or a solenoid operated by the engine's electronic control unit or a boost controller.

Anti-surge/dump/blow off valves



Fig 1.10A recirculating type anti-surge valve

Turbocharged engines operating at wide open throttle and high rpm require a large volume of air to flow between the turbocharger and the inlet of the engine. When the throttle is closed, compressed air flows to the throttle valve without an exit (i.e., the air has nowhere to go).

In this situation, the surge can raise the pressure of the air to a level that can cause damage. This is because if the pressure rises high enough, a compressor stall occurs—stored pressurized air decompresses backward across the impeller and out the inlet. The reverse flow back across the turbocharger makes the turbine shaft reduce in speed more quickly than it would naturally, possibly damaging the turbocharger. To prevent this from happening, a valve is fitted between the turbocharger and inlet, which vents off the excess air pressure. These are known as an anti-surge, diverter, bypass, turbo-relief valve, blow-off valve (BOV), or dump valve. It is a pressure relief valve, and is normally operated by the vacuum from the intake manifold.

The primary use of this valve is to maintain the spinning of the turbocharger at a high speed. The air is usually recycled back into the turbocharger inlet (diverter or bypass valves), but can also be vented to the atmosphere (blow off valve). Recycling back into the turbocharger inlet is required on an engine that uses a mass-airflow fuel injection system, because dumping the excessive air overboard downstream of the mass airflow sensor causes an excessively rich fuel mixture—because the mass-airflow sensor has already accounted for the extra air that is no longer being used. Valves that recycle the air also shorten the time needed to re-spool the turbocharger after sudden engine deceleration, since load on the turbocharger when the valve is active is much lower than if the air charge vents to atmosphere.

Free floating

A free floating turbocharger is the simplest type of turbocharger. This configuration has no wastegate and cannot control its own boost levels. They are typically designed to attain maximum boost at full throttle. Free floating turbochargers produce more horsepower because they have less backpressure, but are not driveable in performance applications without an external wastegate.

CHAPTER 2

LITERATURE SURVEY

Naumann, H. G. 1982 ⁽¹⁾.

Helmut G. Nauman in his journal paper titled 'Steam turbine blade design options: How to specify or upgrade' as discussed about the factors, geometrical and manufacturing differences of blade fastenings, lashing and shrouds. The qualitative method of identifying stress distributions and stress concentrations in root cross section is presented. The information is meant to be helpful in conjunction with blade specifications, design reviews, inspection and troubleshooting.

Ibaraki, S., Matsuo, et al 2004. ⁽²⁾

Seiichi Ibaraki, Testsuya Matsuo, Keiichi Shiraishi and Koichiro Imakiire from Mitsubishi Heavy Industries in their paper 'Design optimization of Turbocharger compressor of high pressure turbocharger diesel engine', describes the optimization of the compressor performance for high pressure turbocharger diesel engine. The objective is to develop optimized compressors that realize a wider operating range, high efficiency and relatively robust performance with respect to changes in engine operating conditions in high pressure region. The authors developed a new compressor impeller and has been applied in the Mitsubishi MET42SH Turbocharger for the Mitsubishi 18KU30B high power diesel engine and is operating successfully

LV, W., MA, C. C., ZHANG, Z. et al 2009.⁽³⁾

Supercharging the diesel engine used in a diesel-electric submarine has provided a reasonable performance compromise. The engine has to achieve a high power, often for relatively short periods, but this has to be carried out under widely varying inlet and exhaust conditions. Turbocharging of the size of engine used in a submarine has become almost universally adopted, due to the high efficiency achievable leading to high specific powers and good fuel consumptions. However, a turbocharged engine is extremely sensitive to inlet and exhaust pressure variations, unlike a supercharged engine, and the advantages of a turbocharger are difficult to achieve in this application. Although turbocharging a submarine engine has been shown to give an improved specific fuel consumption the full potential of the system could only be realised by incorporating a variable-area turbine nozzle. A performance prediction method is described to enable the engine system performance to be predicted during the fluctuating changes due to oceanic waves. A control strategy for the variable-area turbine nozzle is proposed and evaluated, indicating significant improvements in maximum allowable power when compared to both fixed nozzle area turbocharging and supercharging.

Tamaki, H., Unno, et al. (2010).⁽⁴⁾

Tamaki Hideaki, Unno Masaru and Hirata Yutaka in their paper 'Aerodynamic Design Of Centrifugal Compressor AT14 Turbocharger' explained about IHI developed new turbocharger, AT14 mounting a high pressure ratio centrifugal compressor, for 500 KW class diesel engines. Newly designed compressor were realized with the expected performance, stage pressure ratio, and efficiency. This paper outlines the aerodynamic design of the centrifugal compressor for AT14.

Bayomi, N. N .el at 2012. ⁽⁵⁾

The present paper introduces a turbocharger system that operates in two different modes according to turbocharging requirements. In the first mode, the turbocharger is operating with power assistance at lower engine speeds where the power of the exhaust gases is insufficient. Thereafter, the second mode is switched leading the compressor and the turbine of the turbocharger to rotate separately for best performance. Analysis is presented to find out the parameters affecting the operation of the turbocharger and their values to achieve enhanced turbocharger performance with high efficient impellers. The parameters studied are based on data of the turbocharger operating conditions and the operational requirements of the engine. The analysis considers the turbocharger system, its turbine and its compressor. The operational charts demonstrate the simulated results for two operating modes. This study is helpful as a guide to determine the turbocharger dimensioning and blade profile assignment without using any given blade dimensional value.

Abdelmadjid, C., Mohamed, et al . (2013).⁽⁶⁾

ChehhatAbdelmadjida, AneurMohamedb, BoumeddaneBoussad in their paper 'CFD Analysis of the Volute Geometry Effect on the Turbulent Air Flow through the Turbocharger Compressor' explained about the numerical analysis has been carried out extensively to explore impeller-diffuser-volute fluid interaction as well as to predict the flow and turbulence characteristics of the centrifugal compressor by varying the volute geometry without changing the number of impeller blades. It is found from the analysis that volute geometry presents a considerable effect on the pressure and temperature at the compressor outlet.

.Lüddecke, B., et. al 2014 ⁽⁷⁾

The trend to use advanced simulation tools for engine performance prediction is continuing and even emphasized due to shortening of development cycles. The highly accurate prediction of steady and transient engine behaviour becomes increasingly important. Complete drive cycle simulations (e.g. NEDC) help to assess turbocharged engine performance at very early stages of complex engine and vehicle development projects.

The turbocharger has recently developed away from an auxiliary part towards an integral component of the internal combustion engine. Hence, the accuracy of turbine and compressor maps becomes more and more relevant to achieve reliable simulation results and predictions. High quality turbocharger performance data are necessary over a wide range of operation conditions as input for engine simulation programs.

Especially modelling the turbine stage efficiency for engine-like operating conditions (pulsed flow) still is under research. In this context, many researchers raised the question about unsteady effects within the turbine stage and whether the stage, the volute and/or the wheel behave quasi-steadily or have to be considered as unsteady devices.

In the paper at hand, a contactless shaft torque detection technique - that has been integrated into an automotive turbocharger - is presented. It is possible to measure the turbine shaft torque with high accuracy and time resolution. A turbocharger equipped with the detection system has been adapted to a modern four cylinder gasoline engine with direct injection. Engine cycle resolved torque data has been gathered in order to assess the crank angle resolved, on-engine performance of the turbine stage. The available measurements represent an excellent basis for advancements in the modelling and simulation of turbocharger turbine stages with engine simulation tools. Furthermore, the results give a clear indication about the significance and magnitude of unsteady effects within the turbine stage under pulsed flow conditions.

Kumar, R. R., & Pandey, K. M. (2017).⁽⁸⁾

Ravi Ranjankumar in his work 'Static structural and modal analysis of gas turbine blade' as generated the specify power at rotating blade at specific RPM, blade profile and material has been decided by static structural analysis. He analyzed three different blade profiles and resulted that blade of Inconel 625 having 72.5° bent profile is the best combination.

.Chiavola, O., Palmieri, F.,. (2017).⁽⁹⁾

Monitoring of engine operating condition is essential to comply with severe limitations of harmful exhaust emissions and fuel consumption. Several strategies have been proposed, in which different types of sensors are used for the direct/indirect combustion sensing and to provide a feedback signal to optimize the process.

It has been demonstrated that in a turbocharged engine a relationship exists between the rotational speed of the turbocharger and the thermo-fluid dynamic condition of the gases at the exhaust valve opening. Such a relation allows to establish a link between the engine operating conditions in terms of speed, load and injection settings and the turbocharger speed.

This work presents a methodology devoted to extract from an accelerometer signal, the mean turbocharger rotational speed with the final aim of realizing a non intrusive control of combustion process, in which the variation of combustion development as regards nominal condition is detected via the estimation of the turbocharger speed

Romagnoli, A., Manivannan, et al. (2017). (10)

The conventional powertrain has seen a continuous wave of energy optimization, focusing heavily on boosting and engine downsizing. This trend is pushing OEMs to consider turbocharging as a premium solution for exhaust energy recovery. Turbocharger is an established, economically viable solution which recovers waste energy from the exhaust gasses, and in the process providing higher pressure and mass of air to the engine.

However, a turbocharger has to be carefully matched to the engine. The process of matching a turbocharger to an engine is implemented in the early stages of design, through air system simulations. In these simulations, a turbocharger component is represented largely by performance maps and it serves as a boundary condition to the engine. The thermodynamic parameters of a turbocharger are calculated through the performance maps which are usually generated experimentally in gas test stands and used as look-up table in the engine models. Thus, the operational of the engine is dictated by the air flow thermodynamic parameters (pressure, temperature and mass flow) from the turbocharger compressor; this in turn will determine the thermodynamic parameters for the exhaust gas entering the turbocharger turbine. The importance and its sensitivity dictate that any heat transfer affecting the experiments to acquire the performance maps will cause errors in the characterization of a turbocharger. This will consequently lead to inaccurate predictions from the engine model if the heat transfer effects are not properly accounted for. The current paper provides a comprehensive review on how the industry and academics are addressing the heat transfer issue through advancing researches. The review begins by defining the main issues related with heat transfer in turbochargers and the state-of-the-art research looking into it. The paper also provides some inputs and recommendations on the research areas which should be further investigated in the years to come.

Ding, Z., Zhuge, (2017)⁽¹¹⁾

With the widespread application of pulse turbochargers in internal combustion engines, steady or quasi-steady turbine models are no longer qualified for on-engine turbine performance prediction. Pulsatile flow condition caused by the reciprocating nature of the engine results in strong unsteadiness across the turbocharger turbine, which makes the turbine performance departing from that under steady or quasi-steady conditions. Modelling turbocharger turbine through a one-dimensional (1D) method is an important approach to simulate the unsteady performance of the turbine.

In this paper, a 1D performance model of turbocharger turbines is presented. The model solves the turbine volute flow with 1D viscous equations, with volute curvature and circumferentially continuously flow exiting at volute outlet considered. The circumferential flow non-uniformity at volute outlet is preserved. The turbine rotor is modeled with multiple meanline models. The model was used to simulate the performance of a mixed-flow turbine and validated by the experimental data. Results show that the performance predictions are in good agreement with the experimental data. Flow parameters at internal points of the turbine predicted by the 1D model were compared with three-dimensional unsteady simulation results and reasonable agreement was observed, which demonstrates the ability of the 1D model in capturing the pulse propagation.

Smolík, L., Hajžman, et al (2017).⁽¹²⁾

Turbochargers are modern and very interesting dynamical systems used in various engines in order to increase their power. They are operated at hundreds of thousands revolutions per minute and tend to be fatigue and stability prone. For this reason, a turbocharger rotor has to be designed carefully with respect to its dynamic properties. The following article deals with effects of radial bearing clearances on the dynamical response of the turbocharger rotor. The influence of a bearing clearance on stiffness and damping of a single-film journal bearing is well known and documented. Turbochargers, however, are often supported by floating ring bearings. Such bearings have two bearing clearances—between a journal and a floating ring and between a floating ring and a housing—which are determined by different temperatures of oil films. Turbocharger analysed in the article is modelled by means of flexible multibody dynamics approaches. Bearings' behaviour is described using Reynolds equation, which is solved numerically. It is shown, but not mathematically proved, how the outer clearance and the ratio between the inner and the outer clearance affect amplitudes of sub-synchronous components in rotor's response.

Bahiuddin, I., et al (2017). ⁽¹³⁾

The flow input of a variable geometry turbochargerturbine is highly unsteady due to rapid and periodic pressure dynamics in engine combustion chambers. Several VGT control methods have been developed to recover more energy from the highly pulsating exhaust gas flow. To develop a control system for the highly pulsating flow condition, an accurate and valid unsteady model is required. This study focuses on the derivation of governing the unsteady control-oriented model (COM) for a turbine of an actively controlled turbocharger (ACT). The COM has the capability to predict the turbocharger behaviour regarding the instantaneous turbine actual and isentropic powers in different effective throat areas. The COM is a modified version of a conventional mean value model (MVM) with an additional feature to calculate the turbine angular velocity and torque for determining the actual power. The simulation results were further compared with experimental data in two general scenarios. The first scenario was simulations on fixed geometry positions. The second simulation scenario considered the nozzle movement after receiving a signal from the controller in different cases. The comparison between simulation and experimental results showed similarities in the recovered power behaviours the turbine inlet area increases or vice versa. The model also has proved its reliability to replicate general behaviour as in the example of ACT cases presented in this paper. However, the model is incapable to replicate the detailed and complicated phenomena, such as choking effect and hysteresis effect.

Zhao, B., Sun, H., et al. (2017). ⁽¹⁴⁾

In a turbocharger system, curved pipes are usually used to connect compressors with other parts due to limited packaging space. It is well known that an elbow can generate flow distortion to and interact with the compressor inducer and therefore deteriorate compressor stage performance. The compressor efficiency change may vary with relative positions of inlet elbow and volute. The compressor's stable flow range is

also possible to vary due to the shift of surge and/or choke points. In this paper, eight relative circumferential positions between the inlet elbow and the volute were studied by 3D numerical simulations with experimental validations. The numerical results confirm that adjusting the inlet bend from one circumferential orientation to others does cause an obvious deviation in the compressor aerodynamic efficiency. The result also indicates that the total pressure deficit and the vortices at the compressor inlet are the main contributors to the compressor operating range. With the numerical findings in this paper which was validated by experimental measurements, it is suggested that unfavorable orientations of an elbow relative to volute should be avoided in an intake system.

Chiavola, O., Palmieret a (2018).⁽¹⁵⁾

The optimum management of the engine system has a crucial role in order to achieve high efficiency and reduced pollutant emissions. Advanced methods have been proposed, in which several types of sensors are used to directly/indirectly sense the combustion and to provide a feedback signal to optimize the engine management.

In turbocharged engines, it has been demonstrated that a relationship exists between the rotational speed of the turbocharger and the thermo-fluid dynamic condition of the gases at the exhaust valve opening. Such a relation allows to establish a link between the engine operating conditions in terms of speed, load and injection settings and the turbocharger speed.

A research activity was performed aimed at developing a methodology in which the signal from an accelerometer mounted on the compressor housing was used to extract information about the turbocharger speed value. The activity was organized in two subsequent steps, each one focused on one specific objective:

- estimation of the mean turbocharger rotational speed
- evaluation of the turbocharger speed fluctuations.

Tests were performed on a small displacement two-cylinder diesel engine mainly used in urban vehicles that was equipped with a turbocharger. The results obtained during the first step of activity demonstrated the opportunity of further investigations in order to compute the turbocharger speed fluctuation from the accelerometer signal processing. This paper is devoted to present the results of the second step of the research activity, with the final aim of realizing a non intrusive control of combustion process, in which the variation of combustion development as regards nominal condition is detected via the estimation of the turbocharger speed.

Jiaqiang, E., Zhao, X et al (2019). ⁽¹⁶⁾

Compared with the diesel engine with variable nozzle turbocharger, the performance and economy characteristics of diesel engine without variable nozzle turbocharger are experimentally investigated under various operating conditions in this paper. The diesel engine with variable nozzle turbocharger is employed to evaluate the effects of the opening degree on supercharging pressure, air flow, brake specific fuel consumption, smoke intensity and exhaust temperature of diesel engine. And the external and universal characteristics of diesel engines are also studied. The result shows that the variable nozzle turbocharger is beneficial to improve the performance and economy characteristics of diesel engine at the speed range of 900–1300 r/min. The experiments were carried out on the urban bus in Hezhou Road located in Guangxi Province (China) with engine of the YC6J200-42 series. The variable nozzle turbocharger can significantly optimize the performance and economy characteristics of whole vehicle, especially at low and medium speeds with lower smoke and nitrogen oxide emissions. Owing to the research data, the opening degree of variable nozzle turbocharger should be adjusted as much as possible to reduce the exhaust back pressure and pumping loss to improve the fuel economy of the engine.

Le Roux, W. G., et al. (2019) ⁽¹⁷⁾

A recuperated solar-dish Brayton cycle with an off-the-shelf turbocharger as micro-turbine is investigated for potential low-cost power generation. Integrated phase-change thermal storage in the solar receiver can be used to improve the power stability and performance of the cycle; however, the phase-change temperature affects the solar conversion efficiency. In this paper, three different off-the-shelf turbochargers and various recuperator geometries are considered so that the maximum thermal efficiency of the cycle can be found for a fixed receiver geometry at different solar receiver temperatures. Metallic phase-change material of high conductivity is proposed as thermal storage material which is placed around a coiled tube in an open-cavity tubular solar receiver. An analytical model is presented to determine the thermal efficiency of the cycle for different solar receiver temperatures. Results show that maximum thermal efficiencies of 20.2–34.2% can be achieved at receiver temperatures of between 900 K and 1200 K, and that solar conversion efficiencies of 13.5–21% (11–17% when dish reflectivity and intercept factor are both assumed 90%) can be achieved. High solar conversion efficiencies require a large solar input power which would require a more expensive solar dish. A map is therefore provided for each turbocharger which shows the expected solar input power for the shaft power generated at different solar receiver temperatures. Overall, the results show that an open-cavity tubular solar receiver with metallic phase-change thermal storage material can be used together with an off-the-shelf turbocharger for power generation in a solar-dish Brayton cycle.

Li, C., Wang, Y., et al. (2019). ⁽¹⁸⁾

Because of the late intake valve closure (LIVC), Miller cycle is kind of low temperature cycle which means it has the ability to refrain the knocking and produce higher thermal efficiency effectively in engines. As kind of clean energy and whose combustion products are perfectly environmental-friendly, ethanol has been considering as an ideal fuel substitution for a

long time. Therefore in order to reduce NO_x and other particulates emissions from engine, this paper presented the technical route which applied Miller cycle and ethanol to a turbocharged diesel engine. The simulation results shown that, Miller cycle did bring considerable improvements on reducing NO_x emission in a certain extent. Comparing with the conventional Diesel cycle NO_x emission value has been reduced in the range of 8.5–12.9% by applying Miller cycle. After applying turbocharger into Miller cycle engine model, NO_x emission was slightly raised mostly back to the same figure as Diesel cycle produced. Moreover, taking ethanol as fuel also produced large reduction on NO_x emission comparing with the conventional engine model which taking diesel as fuel, and the range of reduction was 5.2–8.5% which could be considered as a considerable improvement. However, when turbocharger added under the same situation the figure of the range of reduction was 4.53–5.16% which is slightly lower than without turbocharger. As for particulate emission in the engine, the situation which Miller cycle and turbocharger caused was opposite to the result of NO_x emission that both Miller cycle and turbocharged Miller cycle caused a larger amount of particulate emission probably due to the higher burning temperature.

Koutsovasilis, P. (2019).⁽¹⁹⁾

The analysis of turbocharger rotordynamics has been conducted so far focusing solely on the effect of radial bearings on the non-linear oscillations of the rotor-bearing system. It is well known that the oil-film concentrated in the rotor's journal bearings is the root cause of the system's occurring nonlinear vibrations. Nevertheless, the rotor-assembly requires to be supported in the axial direction as well in order to compensate the various thrust load effects occurring during operation. This paper investigates the influence of hydrodynamic thrust bearings on the nonlinear oscillations and bifurcations of the rotor system in terms of the thrust- and radial bearing interaction during run-ups. For that purpose the conventional rotordynamics environment is extended by integrating a nonlinear hydrodynamics thrust

bearing model suited for transient run-up simulations. Focus is set on the impact of two major parameters that drive the virtual prototype process of new rotor-assemblies: the shaft diameter and the thrust bearing's position along the shaft. It is shown that for a given set of boundaries the thrust bearing's position along the shaft can have either positive, neutral or negative influence on shaft motion. Furthermore, certain combinations of shaft diameter and thrust bearing positions could occur that may have a negative impact on the thrust bearing itself, for example by means of the associated load capacity. In this regard, it is demonstrated that simulating the thrust and radial bearing interaction during run-ups is mandatory not only for shaft motion purposes, but for designing a robust thrust bearing as well. Finally, with the help of correlation coefficients and response surface methods, trends are identified that set guidelines while designing a new turbocharger center section.

Sandoval, O. R., Fonda, M. . (2019). ⁽²⁰⁾

The use of turbochargers is linked to strategies such as engine downsizing or downspeeding, once the use of this device compensates performance losses observed with the reduction of the displaced volume by compressing the air to be admitted. Steady-state tests of turbochargers are common in literature although not consistent with real behavior associated with a vehicular transient operation. To approximate the experimental tests using gas standard test benches to these real conditions, this paper aims to identify transient behavior of a turbocharger in a vehicular application. Experimental data is collected in two tests: steady-state on a dynamometer and transient on a real highway cycle. Added to the experimental tests, a computational one-dimensional model is developed. The steady-state engine data is used in the model inputs and results of a real transient cycle simulation are validated with the experimental transient data. A standard driving cycle is used to analyze the turbocharger speed behavior when both gear shifting strategy and vehicle load are changed. The computational method presented errors below 5% for the engine and turbocharger speeds,

resulting in a powerful tool to perform experimental test profiles and to evaluate operational turbocharger parameters.

Lee, J., Park, C., (2019). ⁽²¹⁾

This study systematically investigated the application of a turbocharger system to a hydrogen spark ignition engine to extend operating limitations under high loads. The exhaust system of a commercial 2.4-L natural aspiration spark ignition engine was modified by adopting a turbocharger system. Engine test speeds were 2000–6000 rpm at intervals of 1000 rpm. The intake pressure was fixed for each experimental case, however, the quantity of hydrogen and spark advance timings were varied before the back-fire occurred. High load conditions under natural aspiration and turbocharging conditions were compared. The results indicated that distinctly higher boosts with the turbocharging system helped extend high load conditions, however, the high exhaust pressure obstructed the increasingly high load conditions under high speeds.

El-Shahat, A., Hunter,. (2019). ⁽²²⁾

This paper proposes technical guidelines, modelling, and control of an ultra-high-speed-switched reluctance motor- generator for automotive turbo-charged assistance and energy recovery. Creation of an ideal model using electromagnetic finite element analysis and conducting a low cost/low scale experiment is proposed. The first objective focuses on the transient simulation process. The second objective focuses on an investigation of the proposed control criteria. The modelling and analysis of a “Switched Reluctance Motor” (SRM) is an initial task for the selection of the coupled mover. Two controllers are selected for the experiment which consists of a generally low-cost solution and an optimized development board for prototyping optimization. The low-cost control solution is implemented with an Arduino Uno and an assortment of relays configured into an asymmetrical half bridge. The second controller is the “Digilent Zed Board Zynq-7000 ARM/FPGA SoC Development Board” (Zed board).

ANSYS 2D, 3D modelling, data simulation for the stator and rotor are implemented. Current, voltage, and flux for all phases waveforms are included. Rotor dynamic simulation, machine transient simulations, and some other characteristics are depicted through 3D figures.

Reihani, A., Hoard, Et al (2020).⁽²³⁾

In Low-Pressure Exhaust Gas Recirculation (LP-EGR), clean exhaust gas is extracted downstream of the after treatment, and reintroduced upstream of the turbocharger compressor. A major pathway for engine fuel economy improvement, by employing LP-EGR, is the enhancement of compressor and turbine efficiencies by increased flow rates which moves the operating points towards higher efficiencies. However, what is often overlooked in the literature is the influence of LP-EGR/air mixing flow field on the compressor performance. Here, we systematically study this effect on a turbocharger unit for a diesel engine on a hot gas stand using response surface methodology. In addition, the mixing flow field of LP-EGR and air upstream of the compressor was scanned using a 3-dimensional directional probe. A reconfigurable T-junction mixer geometry was used, enabling the study of major mixing parameters such as mixing length, and EGR introduction angle.

The mixing flow field showed a strong dependence on EGR-to-air momentum ratio, significantly affecting the EGR uniformity and axial velocity uniformity. Furthermore, multiscale stream-wise vortices were generated in the mixing section, with an intensity that increased with momentum ratio, and decreased with mixing length. In addition, by eccentric LP-EGR introduction a bulk swirl was generated in the mixing section similar to the flow field obtained using an intake guide vane.

A decrease in compressor efficiency with LP-EGR introduction, compared to baseline compressor map, was observed. The efficiency degradation was larger at higher EGR momentum ratios and flow rates. In the range of mixing lengths limited by engine packaging, up to length-to-diameter ratio

(L/D) = 2.5, the flow perturbations were not damped, and a decline in both compressor pressure ratio and efficiency was observed. Efficiency degradation mechanism is found to be the formation of strong vortices in the mixing zone upstream of the compressor, which are advected to the compressor impeller inlet and perturb the local incidence angle. In contrast, the EGR and axial velocity non-uniformities did not show a negative impact on the compressor.

This study identifies the major flow parameters that cause significant degradation of compressor performance, and proposes a figure of merit for design of efficient LP-EGR mixers to benefit from the fuel economy advantages of LP-EGR architecture in diesel and gasoline direct injection engines.

Andrearczyk, A., et al. (2020)..(24)

This study investigates the operating characteristics of a turbocharger compressor having components manufactured by multiJet printing technology. Currently, studies are being conducted worldwide that aim to develop parts of innovative fluid-flow machines through additive manufacturing techniques. This manufacturing technique has a lower production time and cost compared to conventional prototyping methods used for components with complex shapes. In this article, we focused on the application of the above-mentioned method for improving the design and optimization process of the main parts of fluid-flow machines. This article also presents a numerical model and analysis of a compressor wheel. Experimental tests were conducted at high rotational speeds (up to 100,000 rpm) with the reference material (aluminum compressor wheel) and a polymer wheel. The results obtained were compared with the results of numerical calculations. A modified automotive turbocharger was subjected to experiments on a test stand. This paper also describes the different operating nature of the tested machine compared to the standard version as observed during rundown tests. These tests were necessary in order

to obtain the precise characteristics of the compressor, which was vital for performing a vibrodiagnostic analysis.

Dyk, Š., Smolík, L., et al (2020). ⁽²⁵⁾

A floating-ring bearing (FRB) is composed of a journal, a floating ring and a housing which are separated by two thin oil films. This system is inherently nonlinear and if it is lightly loaded or operated at high speeds, it is prone to the fluid-induced instability. The threshold speed for the instability of a journal bearing with one oil film can be estimated using linearized forces acting in the film. However, the linear analysis of FRB might be problematic because results of such an analysis are usually difficult to interpret. Nevertheless, the linear analysis can provide some fundamental insights into system behaviour. This work aims to evaluate in detail the use of linear theory in the stability analysis of rotating systems supported on FRBs. Several approaches for the linearization of the forces acting in FRB are proposed and analysed. The results are visualized in the form of a holistic Campbell diagram which together depicts natural frequencies, whirl frequencies, modal damping and precession of mode shapes.

Dyk, Š., Smolík, L., & Rendl, J. (2020). ⁽²⁶⁾

This paper presents a novel non-invasive technique to estimate the turbocharger shaft whirl motion. The aim of this article is to present a system for monitoring the shaft motion of a turbocharger, which will be used in turbocharger destructive testing. To achieve this, a camera and a light source were installed in a turbocharger test bench with a controlled lubrication circuit.

An image recording methodology and a process algorithm have been developed, in order to estimate the shaft motion. This processing consists on differentiating specific zones of the image, in order to obtain their coordinates. Two reference points have been configured on the compressor

side, which help to calculate the relative position of the shaft, avoiding the errors due to structural vibrations. Maximum eccentricity of the turbocharger has been determined and it has been compared with shaft motion when it is spinning in different conditions. A luminosity study has been also done, in order to improve the process and to obtain locus of shaft position in a picture exposition time period.

The technique has been applied to diagnosis of a lubrication failure test and the main results will be presented in this article: like shaft motion figures; thermodynamic variables and pictures of the shaft while it is spinning at abnormal lubrication conditions. The measuring components used in this technique have the ability to withstand the catastrophic failure of the turbocharger in this type of test.

Zhu, S., Zhang, K., & Deng, K. (2020).⁽²⁷⁾

This paper aims at presenting an extensive review of waste heat recovery (WHR) from the marine engine with highly efficient bottoming power cycles which include the steam Rankine cycle, organic Rankine cycle, Kalina cycle and CO₂-based power cycles. After detailed introductions and comparisons of the bottoming power cycles, the design and selection of system components are reviewed. An in-depth survey of the WHR systems operating under off-design conditions is then conducted, followed by a summary of technoeconomic evaluation. Finally, challenges and opportunities of integrating the WHR systems with other emission reduction technologies are discussed.

According to the literature, trade-offs between working fluid characteristics, cycle configuration, size, cost and WHR potential should be made in designing an optimal bottoming power cycle, and fuel savings ranging from 4% to 15% can be expected. The payback time of installing a bottoming WHR system lies typically in the range from 3 to 8 years, depending on the fuel price, ship type, heat and power demands and component costs. The high-pressure exhaust gas recirculation technology is superior to other

NO_xreduction technologies due to its high potential of recovering waste heat from the high-temperature recirculated gas. Ship's operational profiles, engine tuning and slow steaming as well as other emission reduction technologies are recommended to be fully considered for future research on WHR systems.

Sridhar, G., et al (2005).⁽²⁸⁾

This paper summarizes the findings involved in the development of producer gas fuelled reciprocating engines over a time frame of six years. The high octane rating, ultra clean, and low-energy density producer gas derived from biomass has been examined. Development efforts are aimed at a fundamental level, wherein the parametric effects of the compression ratio and ignition timing on the power output are studied. These findings are subsequently applied in the adaptation of commercially available gas engines at two different power levels and make. Design of a producer gas carburettor also formed a part of this developmental activity. The successful operations with producer gas fuel have opened possibilities for adapting a commercially available gas engine for large-scale power generation application, albeit with a loss of power to an extent of 20–30 per cent. This loss in power is compensated to a much larger extent by the way toxic emissions are reduced; these technologies generate smaller amounts of toxic gases (low NO_x and almost zero SO_x), being zero for greenhouse gas (GHG).

Ravindra babu yarasu, 2009. ⁽³⁰⁾

Producer gas derived from biomass is one of the most environment friendly substitute to the fossil fuels. Usage of producer gas for power generation has effect of zero net addition of CO₂ in atmosphere. The engines working on producer gas have potential to decrease the dependence on conventional fuels for power generation. However, the combustion process is governed by complex interactions between chemistry and fluid dynamics, some of which are not completely understood. Improved knowledge of combustion is, therefore, of vital importance for both direct use in the design of engines, and for the evolution of reliable simulation tools for engine development. The present work is related to the turbulent combustion of producer gas in closed vessels and engine cylinders. The main objective of the work was multi-dimensional simulation of turbulent combustion in the bowl-in-piston engine operating on producer gas fuel and to observe the flame and flow field interaction. First, the combustion model was validated in constant volume combustion chamber with experimental results.

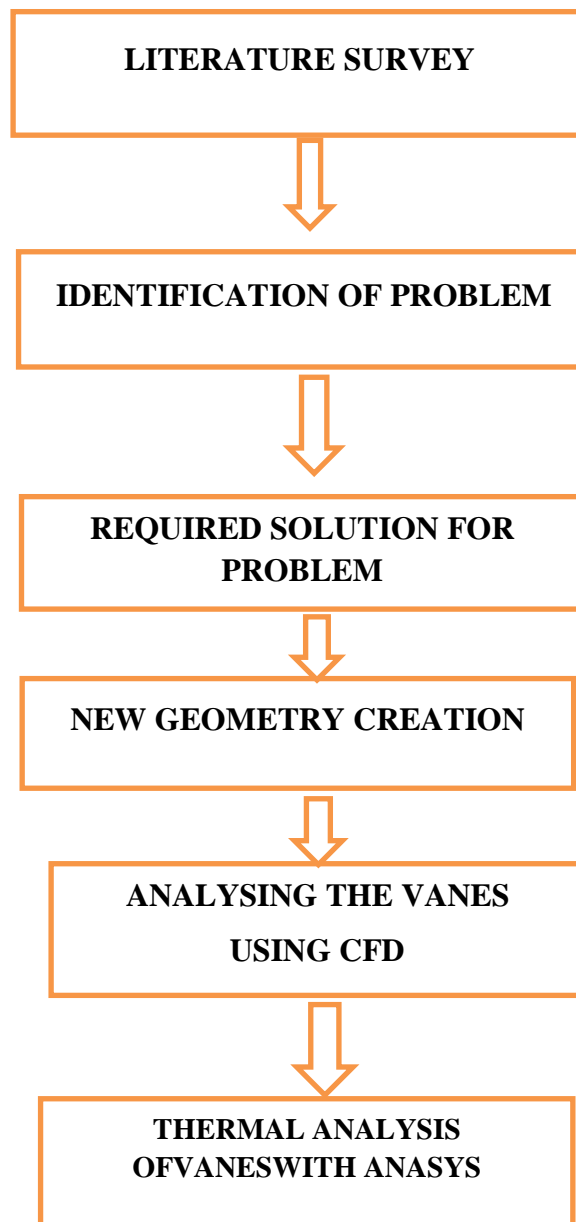
CHAPTER 3

OBJECTIVE & METHODOLOGY

3.1 OBJECTIVE

- The aim of the project is to improve the thermal performance predict the flow property and pressure distribution of turbocharger compressor with different angles.

3.2 METHODOLOGY



CHAPTER-4

SIMULATION WORK

SOLIDWORKS

4.1. INTRODUCTION TO SOLIDWORKS:

SolidWorks (stylized as SOLIDWORKS), is a solid modeling computer-aided design (CAD) and computer-aided engineering (CAE) software program that runs on Microsoft Windows. The SolidWorks is produced by the DASSAULT SYSTEMÈMES— a subsidiary of DassaultSystèmes, S. A. based in Velizy, France— since 1997.

SolidWorks is currently used by over 2 million engineers and designers at more than 165,000 companies worldwide. In 2011–12, the fiscal revenue for SolidWorks was reported \$483 million.

4.2. COMMONLY USED TOOLS FOR MODELLING IN SOLIDWORKS:

1. Extrude
2. Extrude cut
3. Revolve
4. Revolve cut
5. Sweep
6. Swept cut
7. Fillet
8. Chamfer
9. Mirror

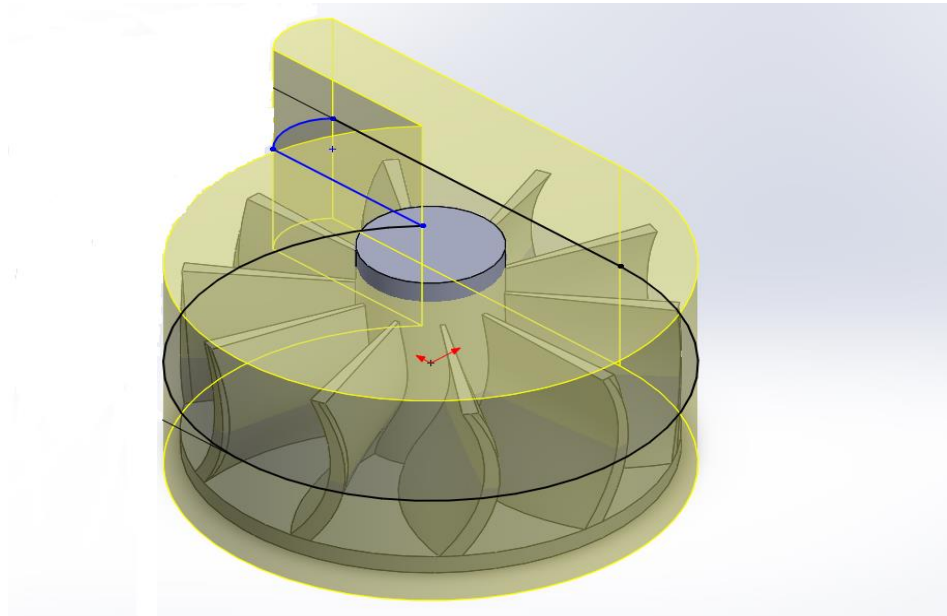


Fig.4.1 Design and modeling of compressor

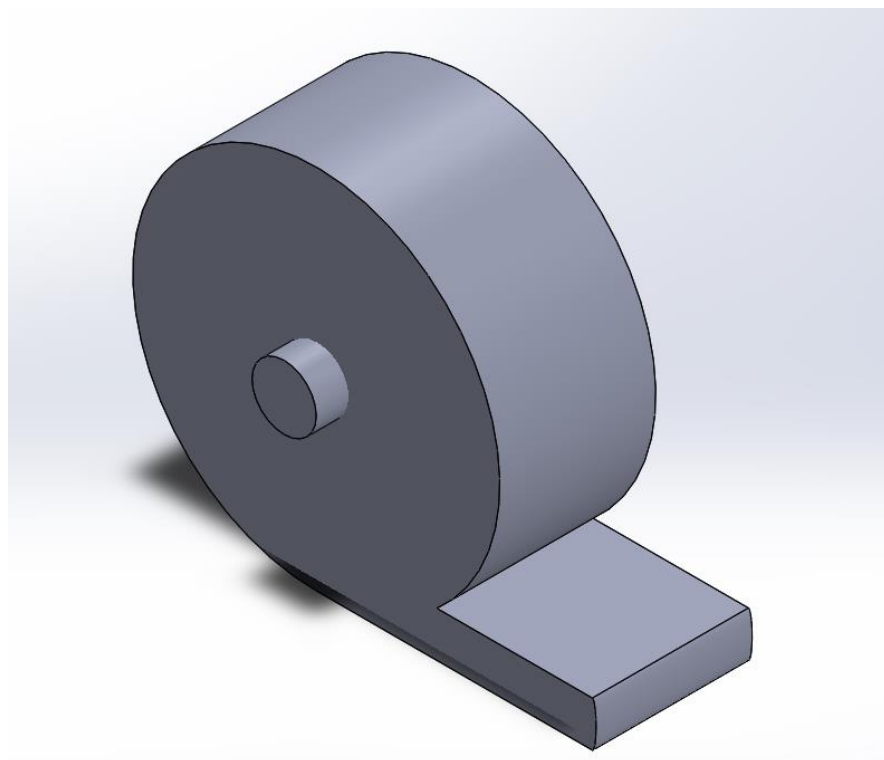


Fig.4.2 Isometric view of compressor

VELOCITY CALCULATION FOR COMPRESSOR

4.3. FOR BLADE ANGLE 15°

$$\begin{aligned}\text{Radius of the propeller point} &= 190\text{mm} \\ \text{Station distance} &= 0.70\text{mm} \\ \text{Station distance from the origin} &= 0.70 \times 190 \\ &= 133 \\ \text{The speed of the propeller} &= 1500\text{rpm} \\ \text{In revolution per second} &= 25\text{rp} \\ \text{Distance moved for every} &= 2 \times \pi \times 133 \\ \text{revolution} & \\ &= 835.60 \text{ mm/s} \\ 835.60 \times 25 &= 20.89 \text{ m/s} \\ \tan\left(\frac{S}{20.89}\right) &= 15^\circ \\ \frac{S}{20.89} &= \tan^{-1} 15 \\ S &= 86.18 \times 20.89 \\ S &= 1800\text{m/s}\end{aligned}$$

4.4. FOR BLADE ANGLE 18°

$$\begin{aligned}\tan\left(\frac{S}{20.89}\right) &= 18^\circ \\ \frac{S}{20.89} &= \tan^{-1} 18 \\ S &= 86.82 \times 20.89 \\ S &= 1813.6\text{m/s}\end{aligned}$$

4.5. FOR BLADE ANGLE 20°

$$\tan\left(\frac{S}{20.89}\right) = 20^\circ$$

$$\frac{S}{20.89} = \tan^{-1} 20$$

$$S = 87.13 \times 20.89$$

$$S = 1820.3 \text{ m/s}$$

Table.4.1 Speed of the compressor for respective angle

BLADE ANGLE (θ) (°)	SPEED (S) m/s
15°	1800
18°	1813.6
20°	1820.3

CHAPTER-5

ANALYSIS OF TURBOCHARGER COMPRESSOR

This analysis is carried out to predict the flow property and pressure distribution of turbocharger compressor with different angles.

5.1. FOR BLADE ANGLE 15°

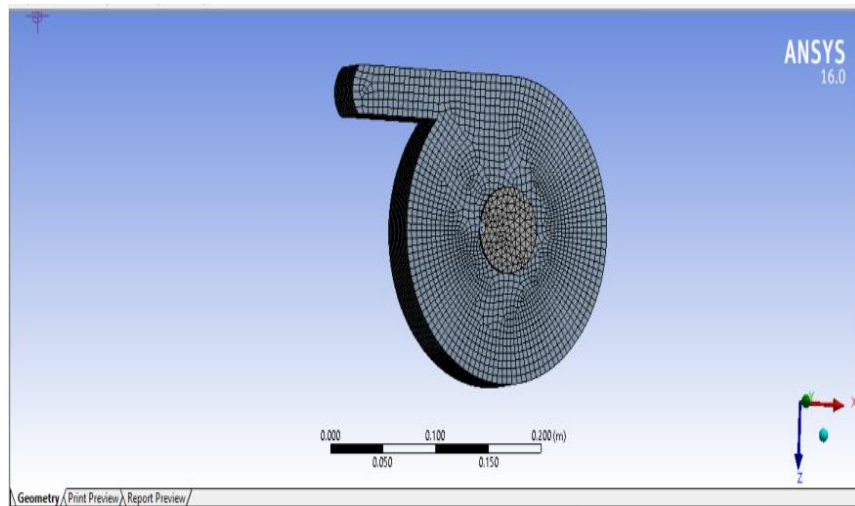


Fig.5.1 Mesh model of compressor

Fig5.1 created in ansys using hyper mesh software for blade angle 15°

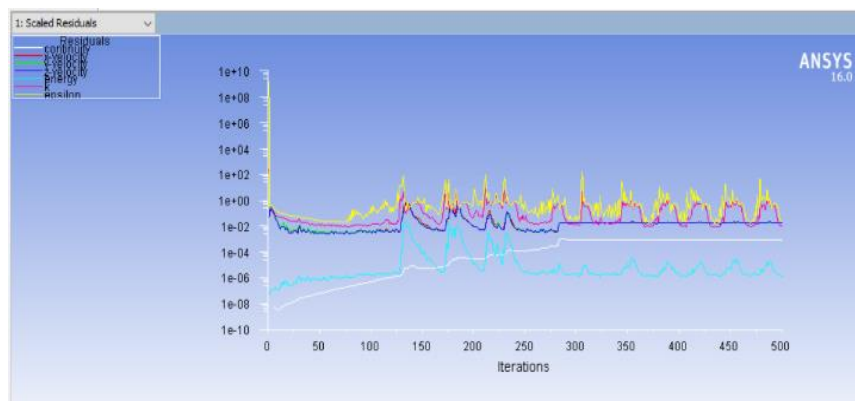


Fig.5.2 Iterations

Iterations were carried out for 500 Iterations

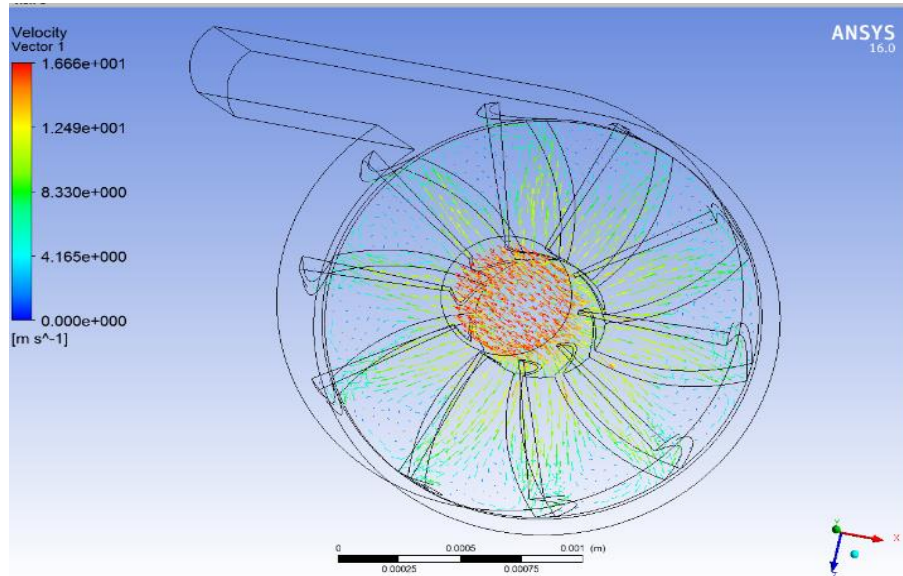


Fig.5.3 Velocity distribution

Fig 5.3 shows that velocity is higher at centre of the turbine and lower at the vanes

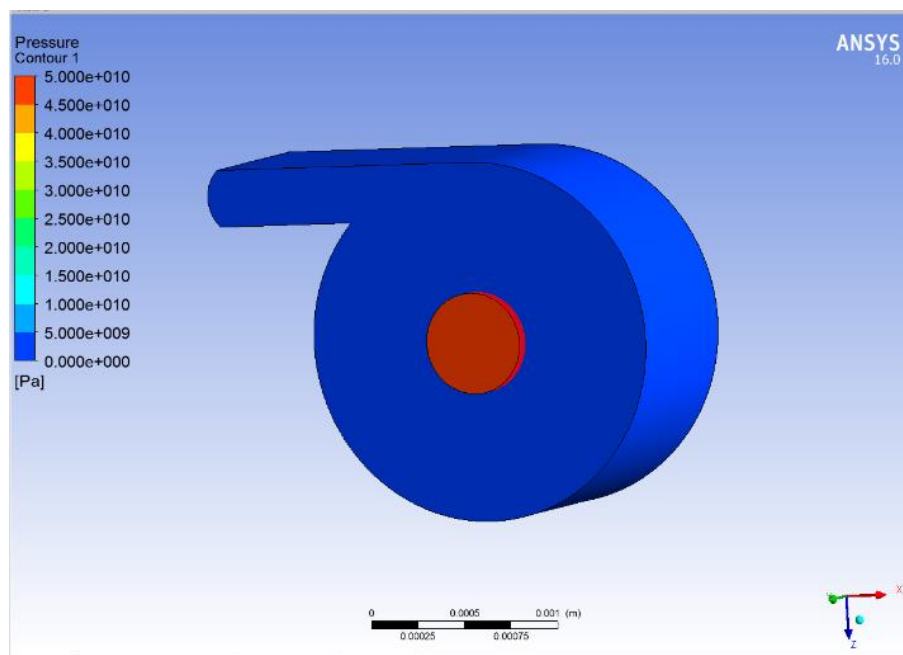


Fig.5.4 Pressure distribution at out casing

Fig 5.4 shows that pressure is higher at the centre of the casing and lowers at the out casing

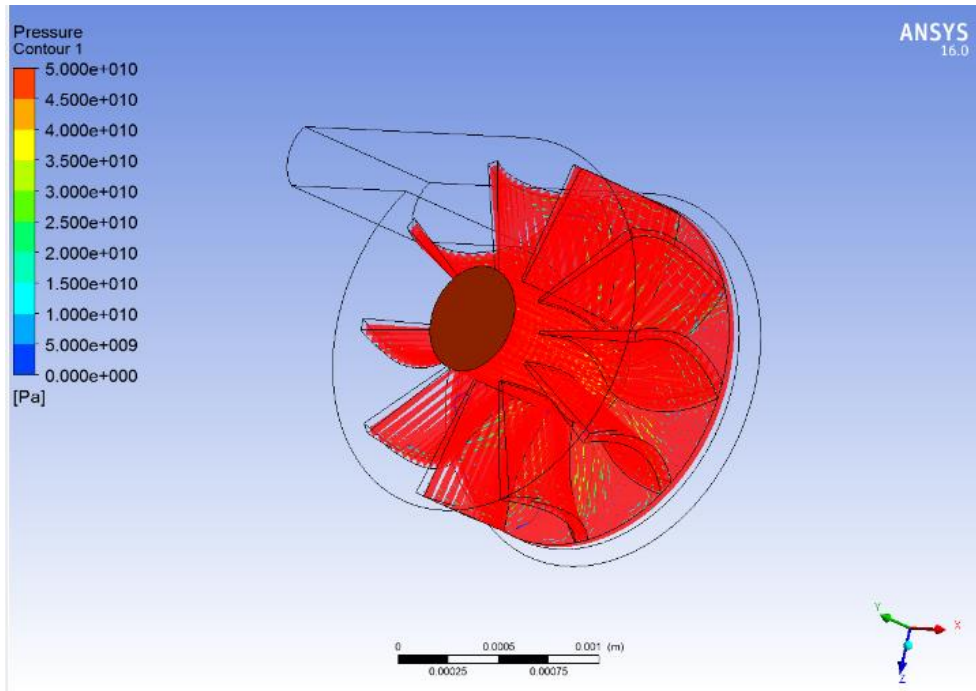


Fig.5.5 Pressure distribution at blades

Fig 5.5 Pressure is equally distributed at blades

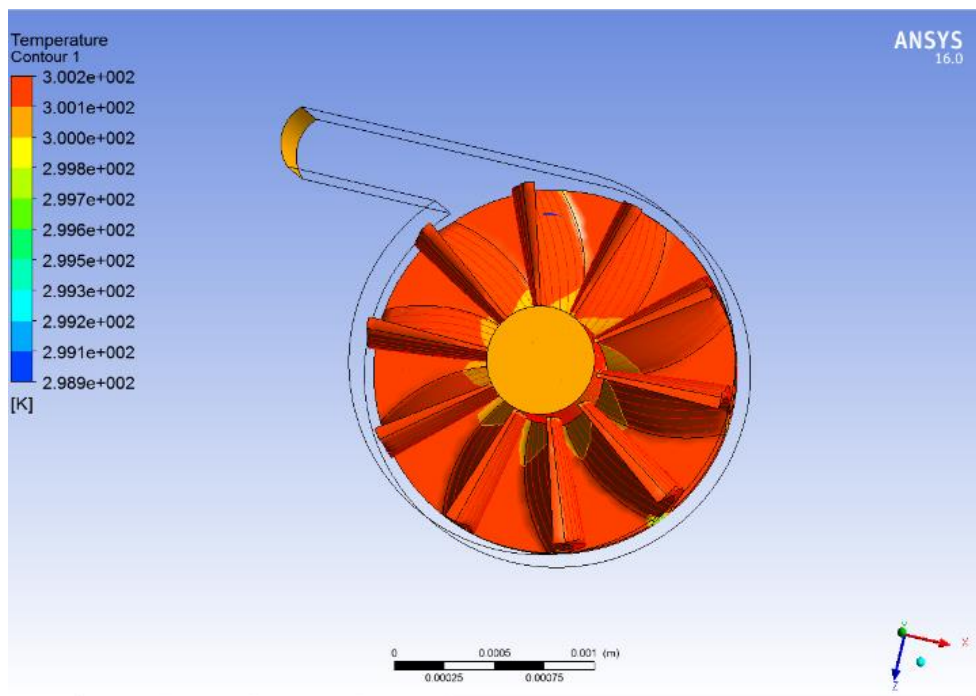


Fig.5.6 Temperature distribution

Fig 5.6 Temperature distributions is high at blades and medium on blades

5.2. FOR BLADE ANGLE 18°

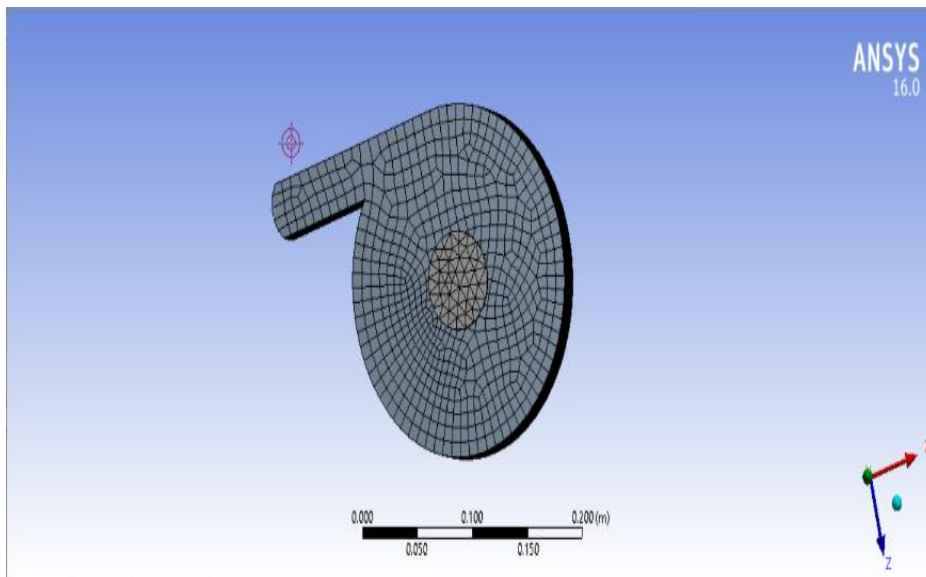


Fig.5.7 Mesh model of compressor

Fig.5.7 created in ansys using hyper mesh software for blade angle 18°

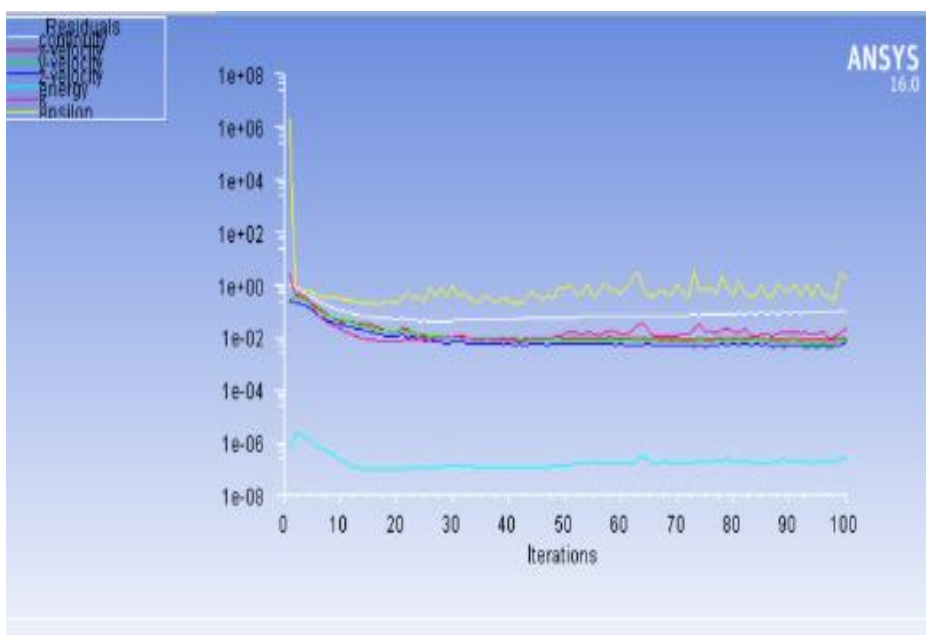


Fig.5.8 Iterations

Iterations were carried out for 100 Iterations

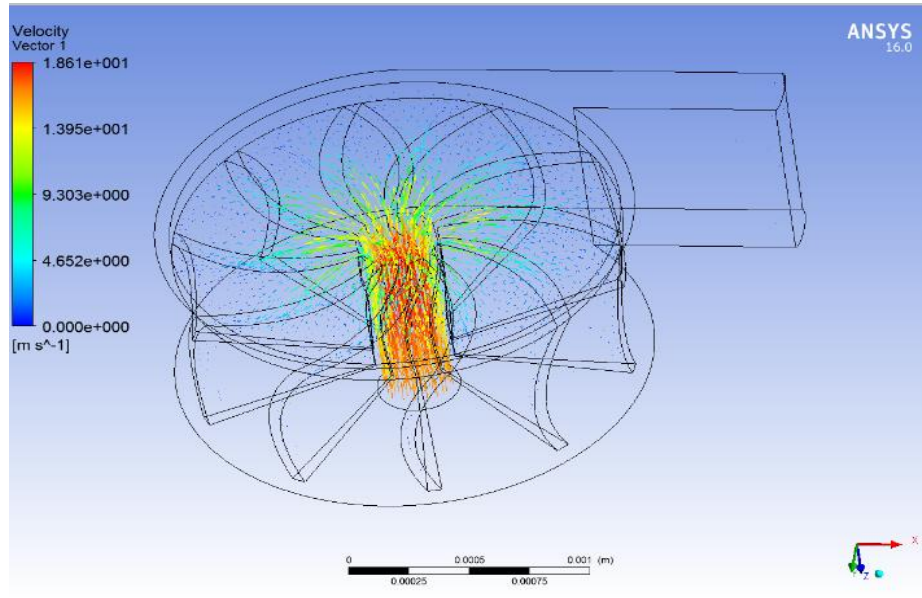


Fig.5.9 Velocity distribution

Fig 5.9 Velocity distribution was high at centre of the shaft and its gradually deceases

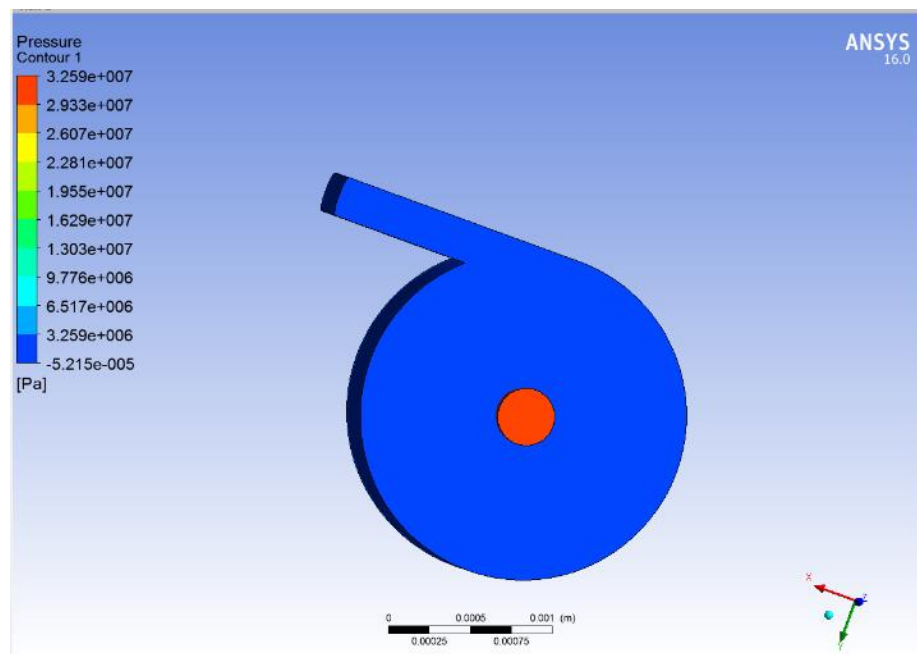


Fig.5.10 Pressure distribution at out casing

Fig 5.10 shows that pressure is higher at the centre of the casing and lowers at the out casing

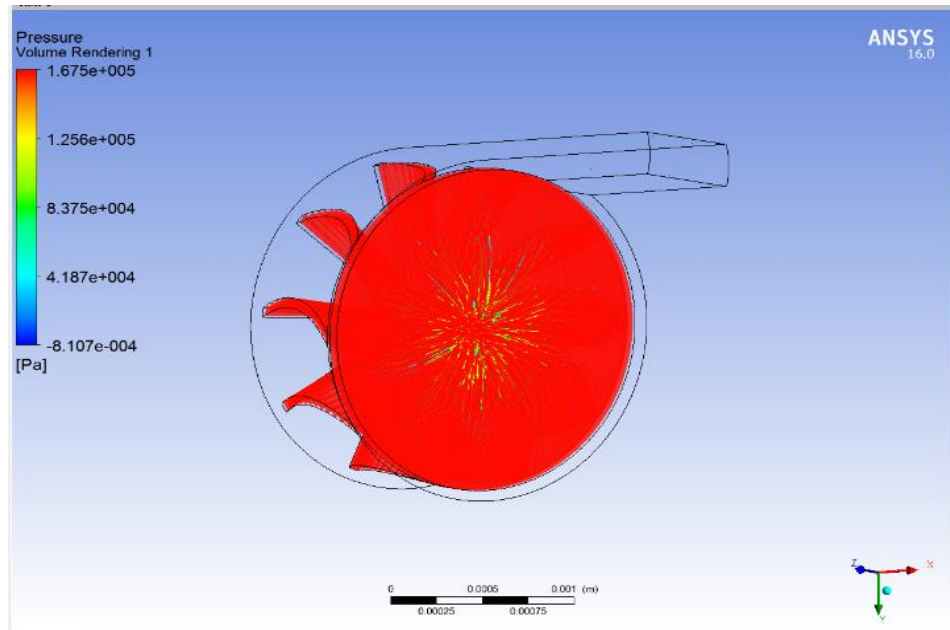


Fig.5.11 Pressure distribution at blades

Fig 5.11 Pressure is equally distributed at blades

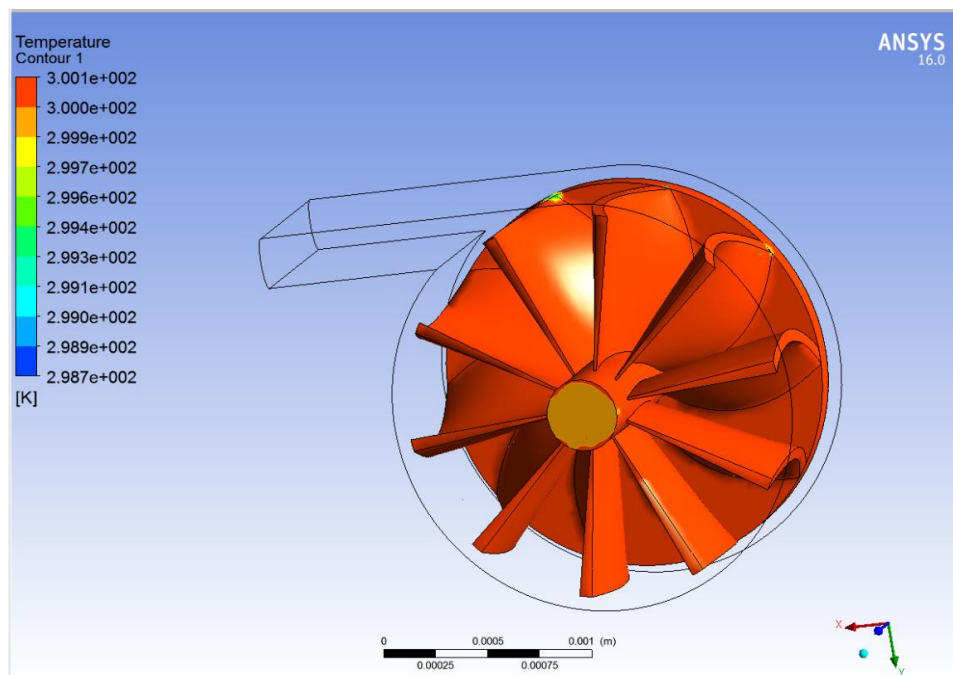


Fig.5.12 Temperature distribution

Fig 5.12 Temperature distributions is high at blades and medium on blades

5.3. FOR BLADE ANGLE 20°

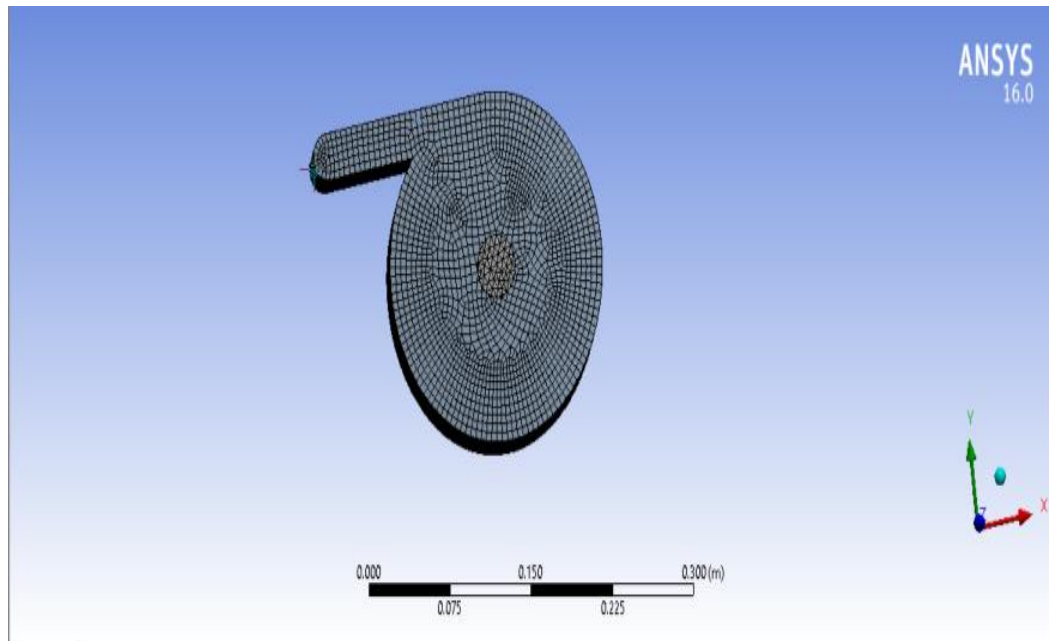


Fig.5.13 Meshed model of compressor

Fig5.13 created in ansys using hyper mesh software for blade angle 20°

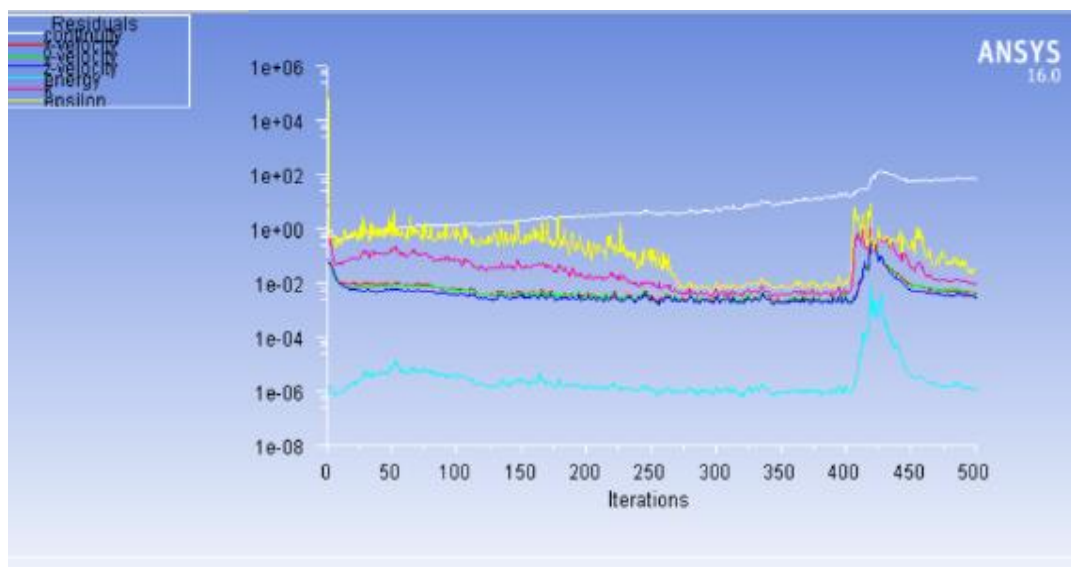


Fig.5.14 Iterations

Iterations were carried out for 500 Iterations

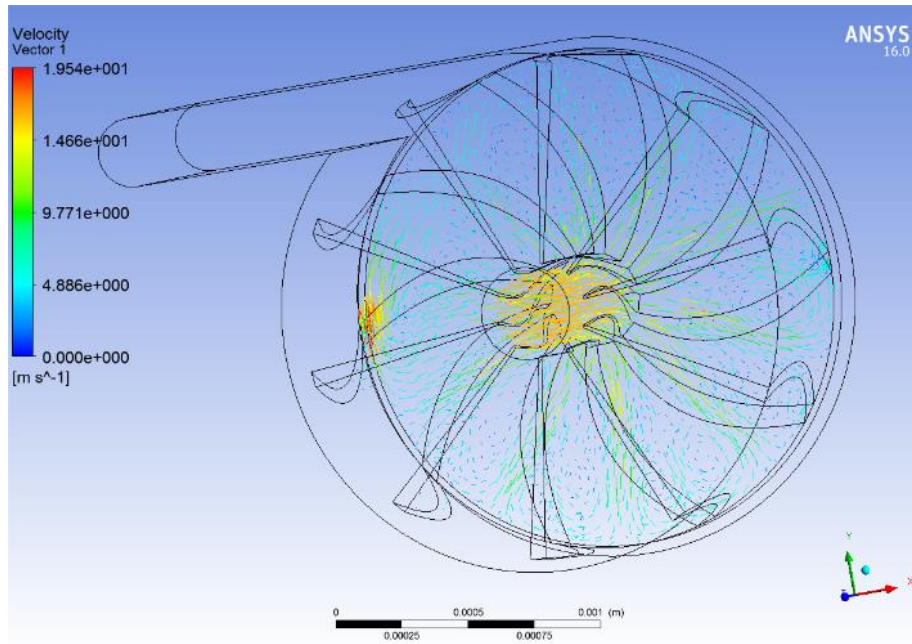


Fig.5.15 Velocity distribution

Fig 5.15 shows that velocity is higher at centre of the turbine and lower at the vanes

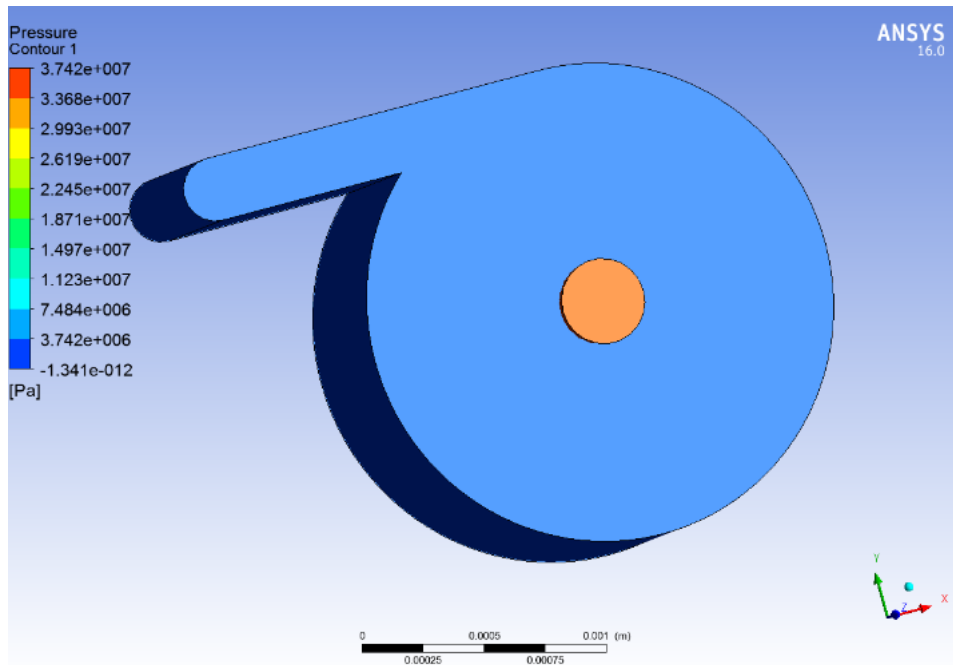


Fig.5.16 Pressure distribution at out casing

Fig 5.16 shows that pressure is higher at the centre of the casing and lowers at the out casing

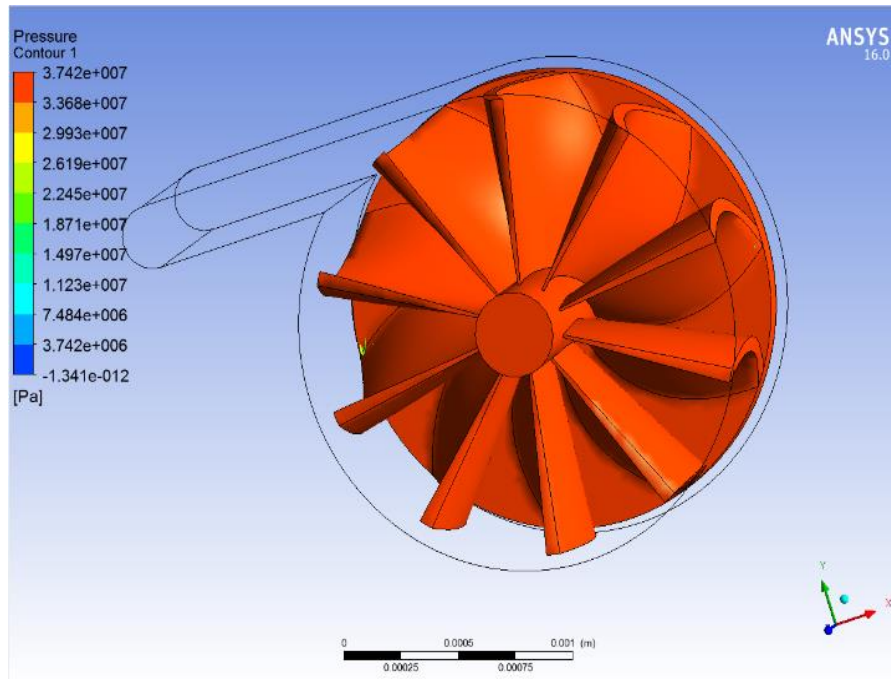


Fig.5.17 Pressure distribution at blade

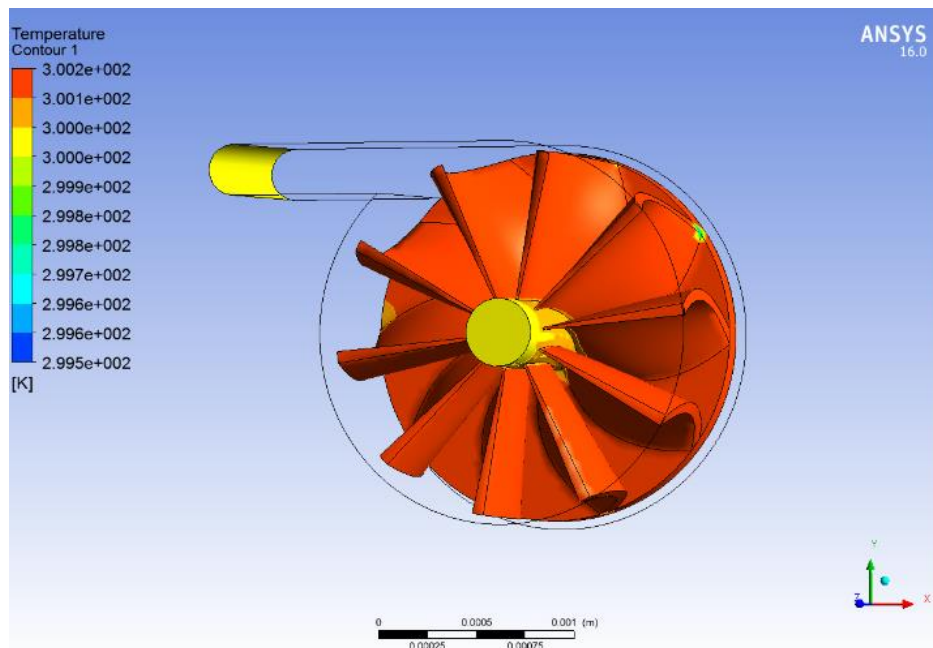


Fig.5.18 Temperature distribution

Fig 5.18 Temperature distributions is high at blades and medium on blades

CHAPTER 6

RESULTS AND DISCUSSION

6.1. COMPARISON OF ANALYSIS RESULTS

The comparison of different blade angles on basis of velocity, pressure and temperature has been done in the following tables.

Table.6.1 Comparison of velocity

Blade angle (°)	Velocity (m/s)
15	16.66
18	18.61
20	19.54

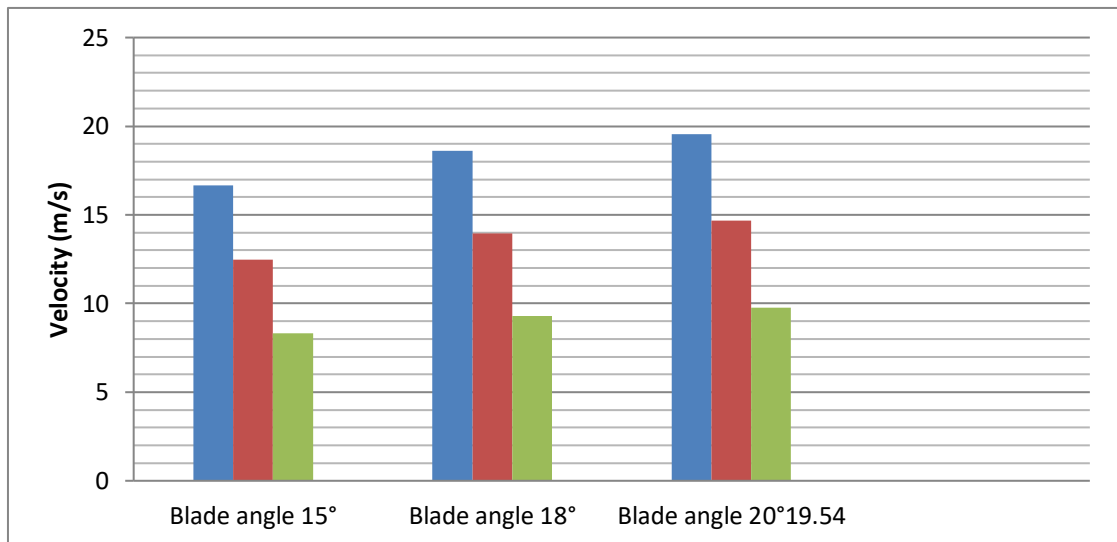


Chart.6.1 Velocity comparison

Table.6.2 Comparison of Pressure distribution

Blade angle (°)	Pressure (pa)
15	5×10^{10}
18	1.675×10^5
20	3.742×10^7

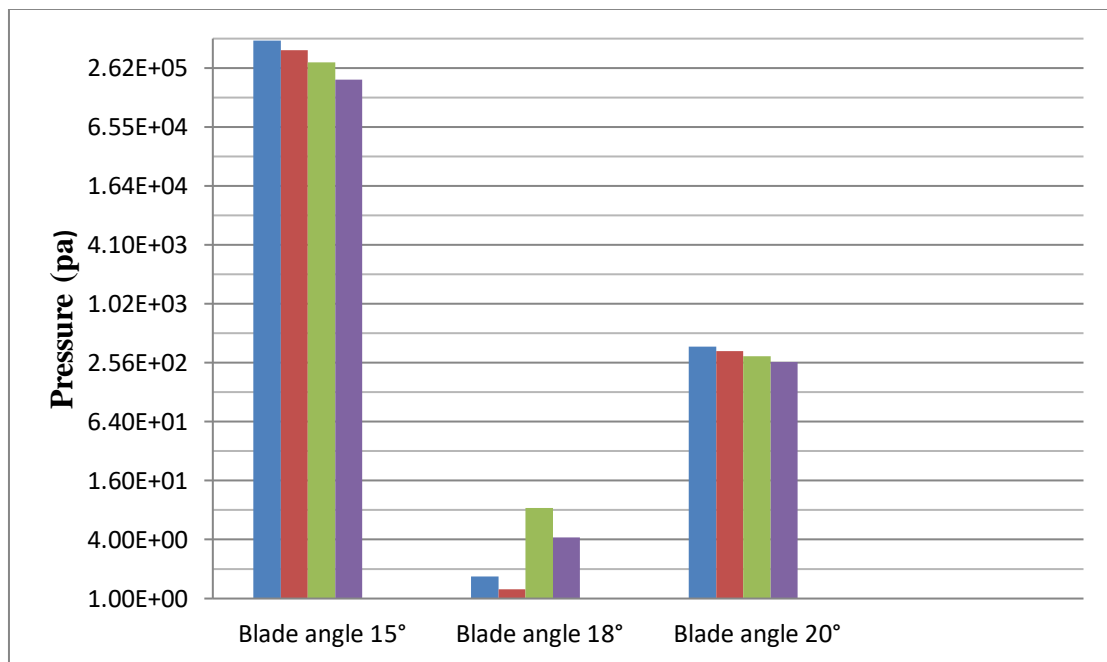


Chart.6.2 Pressure distribution comparison

Table.6.3 Comparison of Temperature distributon

Blade angle (°)	Temperature (K)
15	3.002×10^2
18	3.001×10^2
20	3.002×10^2

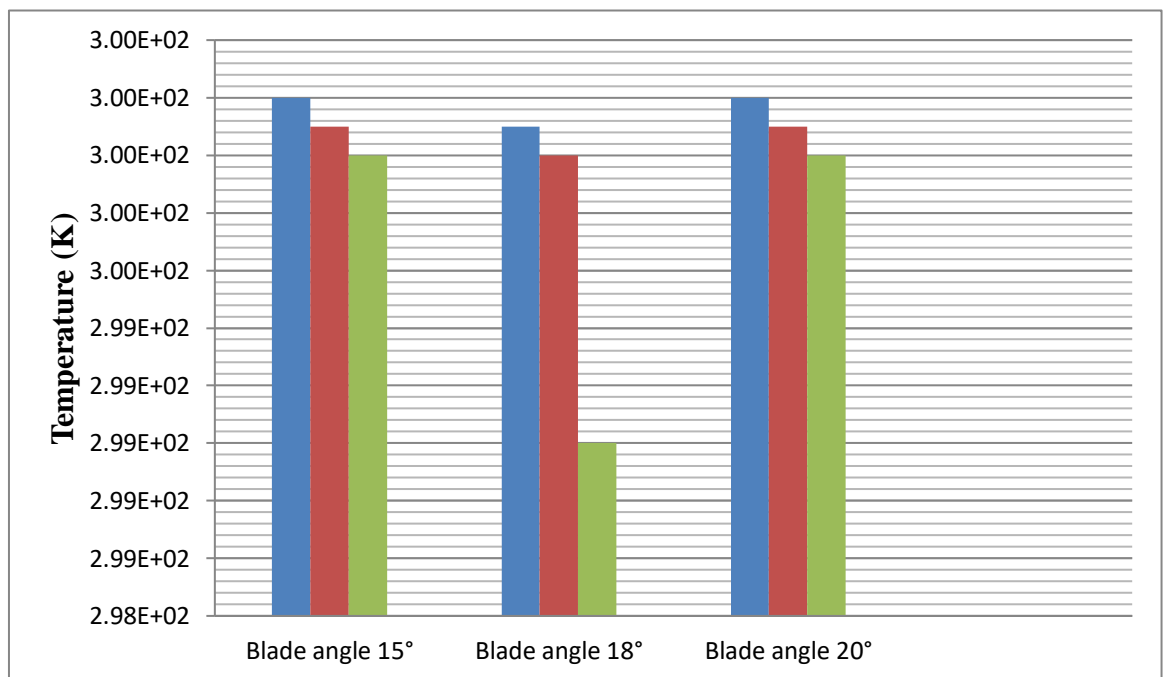


Chart.6.3 Comparison of Temperature distribution

CHAPTER 7

CONCLUSION

In this work, a turbocharger compressor is modelled using a CFD software ANSYS – FLUENT. This paper presents a numerical performance prediction of pre defined angles under inlet steady flow condition.

The computed pressure ratio is in reasonable agreement with experimental data.

We find that no remarkable differences are obtained from rather specified blade shape with nominal constant incidence angle.

The pressure ratio of the turbocharger compressor is likely to increase in future as well. To develop a turbocharger compressor with pressure of approximately 5×10^{10} pa ,

It is necessary to develop new design method for achieving greater efficiency that will prevent reduction in material strength due to an increase in the internal flow temperature as well as analysis techniques to support this development.

REFERENCES

1. J. Galindo, H. Climent, C. Guardiola, A. Tiseira, J. Portalier, “Assessment of a sequentially turbocharged diesel engine on real-life driving cycles”, *Int. J. Veh. Des.* 49 (1/2/3).
2. J. Galindo, H. Climent, C. Guardiola, J. Domenech, —Strategies for improving the mode transition in a sequential parallel turbocharged automotive diesel engine”, *Int. J. Automot. Technol.* 10 (2) (2009) 141–149.
3. Bayomi, N. N., & Abd El-Maksoud, R. M. (2012). Two operating modes for turbocharger system. *Energy conversion and management*, 58, 59-65
4. Saxena, S. C., Henry, R. F., & Podolski, W. F. (1985). Particulate removal from high-temperature, high-pressure combustion gases. *Progress in energy and combustion science*, 11(3), 193-251.
5. F. Pflüger, —Regulated two-stage turbocharging – KKK’s new charging system for commercial diesel engines”, in: IMechE, C554/035/98, Sixth International Conference on Turbocharging and Air Management Systems, 1998.
6. LV, W., MA, C. C., ZHANG, Z. Q., & SHI, X. (2009). Experimental Research on Pneumatic Torque of Adjustable Turbine Nozzle Guide Vane [J]. *Vehicle Engine*, 2.
7. Lüddecke, B., Filsinger, D., & Bargende, M. (2014, October). Engine crank angle resolved turbocharger turbine performance measurements by contactless shaft torque detection. In *11th International Conference on Turbochargers and Turbo-Charging of the IMechE* (pp. 301-320).
8. Lüddecke, B., Filsinger, D., & Bargende, M. (2014, October). Engine crank angle resolved turbocharger turbine performance measurements by

- contactless shaft torque detection. In *11th International Conference on Turbochargers and Turbo-Charging of the IMechE* (pp. 301-320).
9. Chiavola, O., Palmieri, F., &Recco, E. (2017). Turbocharger speed estimation via vibration measurements for combustion sensing. *Energy Procedia*, 126, 842-849
 10. Romagnoli, A., Manivannan, A., Rajoo, S., Chiong, M. S., Feneley, A., Pesiridis, A., & Martinez-Botas, R. F. (2017). A review of heat transfer in turbochargers. *Renewable and Sustainable Energy Reviews*, 79, 1442-1460
 11. Ding, Z., Zhuge, W., Zhang, Y., Chen, H., Martinez-Botas, R., & Yang, M. (2017). A one-dimensional unsteady performance model for turbocharger turbines. *Energy*, 132, 341-355.
 12. Smolík, L., Hajžman, M., &Byrtus, M. (2017). Investigation of bearing clearance effects in dynamics of turbochargers. *International Journal of Mechanical Sciences*, 127, 62-72.
 13. Bahiuddin, I., Mazlan, S. A., &Imaduddin, F. (2017). A new control-oriented transient model of variable geometry turbocharger. *Energy*, 125, 297-312.
 14. Zhao, B., Sun, H., Wang, L., & Song, M. (2017). Impact of inlet distortion on turbocharger compressor stage performance. *Applied Thermal Engineering*, 124, 393-402.
 15. Chiavola, O., Palmieri, F., &Recco, E. (2018). Vibration analysis to estimate turbocharger speed fluctuation in diesel engines. *Energy Procedia*, 148, 876-883.
 16. Jiaqiang, E., Zhao, X., Qiu, L., Wei, K., Zhang, Z., Deng, Y., ...& Liu, G. (2019). Experimental investigation on performance and economy characteristics of a diesel engine with variable nozzle turbocharger and its application in urban bus. *Energy Conversion and Management*, 193, 149-161.
 17. Le Roux, W. G., &Sciacovelli, A. (2019). Recuperated solar-dish Brayton cycle using turbocharger and short-term thermal storage. *Solar Energy*, 194, 569-580.

18. Li, C., Wang, Y., Jia, B., & Roskilly, A. P. (2019). Application of Miller cycle with turbocharger and ethanol to reduce NO_x and particulates emissions from diesel engine—A numerical approach with model validations. *Applied Thermal Engineering*, *150*, 904-911.
19. Koutsovasilis, P. (2019). Automotive turbocharger rotordynamics: Interaction of thrust and radial bearings in shaft motion simulation. *Journal of Sound and Vibration*, *455*, 413-429.
20. Sandoval, O. R., Fonda, M. V., Roso, V. R., da Costa, R. B. R., Valle, R. M., & Baêta, J. G. C. (2019). Computational technique for turbocharger transient characterization using real driving conditions data. *Energy*, *186*, 115822.
21. Lee, J., Park, C., Kim, Y., Choi, Y., Bae, J., & Lim, B. (2019). Effect of turbocharger on performance and thermal efficiency of hydrogen-fueled spark ignition engine. *International journal of hydrogen energy*, *44*(8), 4350-4360.
22. El-Shahat, A., Hunter, A., Rahman, M., & Wu, Y. (2019). Ultra-High Speed Switched Reluctance Motor-Generator for Turbocharger Applications. *Energy Procedia*, *162*, 359-368.
23. Reihani, A., Hoard, J., Klinkert, S., Kuan, C. K., Styles, D., & McConville, G. (2020). Experimental response surface study of the effects of low-pressure exhaust gas recirculation mixing on turbocharger compressor performance. *Applied Energy*, *261*, 114349.
24. Andrearczyk, A., Baginski, P., & Klonowicz, P. (2020). Numerical and experimental investigations of a turbocharger with a compressor wheel made of additively manufactured plastic. *International Journal of Mechanical Sciences*, 105613.
25. Dyk, Š., Smolík, L., & Rendl, J. (2020). Predictive capability of various linearization approaches for floating-ring bearings in nonlinear dynamics of turbochargers. *Mechanism and Machine Theory*, *149*, 103843.
26. Dyk, Š., Smolík, L., & Rendl, J. (2020). Predictive capability of various linearization approaches for floating-ring bearings in nonlinear dynamics of turbochargers. *Mechanism and Machine Theory*, *149*, 103843.

27. Zhu, S., Zhang, K., & Deng, K. (2020). A review of waste heat recovery from the marine engine with highly efficient bottoming power cycles. *Renewable and Sustainable Energy Reviews*, 120, 109611.
28. G Sridhar, H V Sridhar, S Dasappa, P J Paul, N K S Rajan, H S Mukunda, "Development of producer gas engines", Proceedings of the Institution of Mechanical Engineers", Part D: Journal of Automobile Engineering Vol. 219, pp. 423-437; 2005
29. H V Sridhar, "Characterization and Matching of Turbochargers for Producer Gas Engine Applications-Experiments and Analysis", Ph.D. Thesis, Combustion, Gasification and Propulsion Laboratory, Dept. of Aerospace Engineering, IISc, Bangalore, 2008.
30. Ravindra babu yarasu, "Premixed turbulent combustion of Producer gas in closed vessel and Engine cylinder", Ph.D. Thesis, Combustion, Gasification and Propulsion Laboratory, Dept. of Aerospace Engineering, IISc, Bangalore, 2009.